6-10-2020

Sediment Transport and Geomorphological Evolution in the Transgressive Ship Shoal, Louisiana: Insights from Geophysical Observation, Modeling, and Machine Learning Studies

Haoran Liu

SEDIMENT TRANSPORT AND GEOMORPHOLOGICAL EVOLUTION IN THE TRANSGRESSIVE SHIP SHOAL, LOUISIANA: INSIGHTS FROM GEOPHYSICAL OBSERVATION, MODELING, AND MACHINE LEARNING STUDIES

A Dissertation

Submitted to the Graduate Faculty of the
Louisiana State University and
Agricultural and Mechanical College
in partial fulfillment of the
requirements for the degree of
Doctor of Philosophy

in

The Department of Oceanography and Coastal Sciences

by
Haoran Liu
B.S. China University of Geoscience (Wuhan), 2013
M.S China University of Geosciences, 2015
August 2020

ACKNOWLEDGMENTS

I would like to express my most profound appreciation to my Ph.D. major adviser, Dr. Kehui Xu, for his unwavering guidance and persistent help during my doctoral research in geophysics and marine geology. I would also like to extend my deepest gratitude to my dual MS major adviser, Dr. Bin Li, for helping me expand the research interest to geostatistics and machine learning. My other committee members, Drs. Carol Wilson and Zuo Xue provided invaluable suggestions and advice. I would also like to thank Dr. Green Christopher for serving as the Graduate School's Dean's Representative.

In chapters two and three, funding for this study was provided by the U.S. Department of the Interior, Bureau of Ocean Energy Management, Coastal Marine Institute, Washington DC, under Cooperative Agreement Number M16AC00018. Our work was built upon an earlier study funded by the Bureau of Ocean Energy Management Agreement Number M14AC00023. Christopher DuFore, Michael Mine, and Tershara Mathews served as the project officers of the Bureau of Ocean Energy Management. I am thankful to the Field Support Group of Coastal Studies Institute, particularly Captain Chris Cleaver, Bill Gibson, and Charlie Sibley, who provided logistical support in all data collection efforts.

In chapters three and four, I am thankful for the generous help from Dr. Zuo Xue's group for providing model grid and forcing files and helping build up model domain, my friend Dr. Bingqing Liu for sediment concentration validation, Robert Bales for wave validation, Kelli Moran and Guandong Li for collecting sediment samples, Dr. Carol Wilson's group and the editing help from Dr. Nancy Rabalais.

My Ph.D. program was funded by Economic Development Assistantship from the Graduate School of Louisiana State University. Many thanks to the technical support of Michael

Redmayne from Caris and Anthony Cavell from the Center for Geoinformatics of LSU in data acquisition and processing. I would like to extend my sincere thanks to Zehao Xue and Matthew Barley for geophysical data acquisition. Special thanks to my friends Drs. Jiaze Wang and Kendall Valentine for assisting with preparing my general exam and help to review my manuscripts. Lab mates, both past and current, including Jeff Obelcz, Courtney Elliton, Xiaoyu Sha, Patrick Robichaux, and others assisted when necessary and provided moral support. A special acknowledgment must be given to my officemate, and close friend, Robert Bales, for always being kind and helpful.

Finally, numerous people helped me to be a brave and independent scholar. I'd also like to extend my gratitude to my close friends Sarah Margolis, Xi Du, Yuanjun Hu, Zelong Zhang, Gaomin Wang, and Gaojian Xiao. Last but most important, thank you to my parents, sister, and two adorable nephews for always supporting my decision. To all the people I've loved before, thank you for being here.

TABLE OF CONTENTS

ABSTRACT

Ship Shoal has been a high-priority target sand resource for dredging activities to restore the eroding barrier islands in Louisiana, USA. Many studies have been performed in Ship Shoal in recent decades, but our knowledge of temporal and spatial variations of sediment transport and post-dredge morphology is still limited. The objectives of this dissertation are to explore the sediment infilling process, the spatial and temporal evolution of the morphology of dredge pits near and on Ship Shoal by using multiple methods. Scientific methods used in this study include (a) geophysical observation using bathymetry, side-scan and subbottom technique, (b) sediment transport hindcasts using Regional Ocean Modeling System, and (c) machine learning technique including random forest, classification tree, and logit lasso.

There are a total of four primary findings in this dissertation. (1) Caminada dredge pit located on the east of Ship Shoal displays a unique mixing and redistribution of cohesive mud with noncohesive sand. Initial sediment infilling in this pit appears to be dictated by micro-topography on the pit bottom created by the dredging cuts. Raccoon Island dredge pit located north of Ship Shoal is in a mixed environment in which sand was capped by mud before dredging, and it was filled with mud after dredging. The sediment infilling rate and pit wall slope changing rate in Raccoon Island pit is greater than these in the Caminada pit, likely due to turbid ambient sediment concentration and trough-like morphology. (2) A sediment transport model shows a minimal amount of suspended mud from the Atchafalaya River that can be delivered to Ship Shoal in a one-year time scale, but suspended mud from nearby estuaries and inner shelf could be episodically transported to Ship Shoal to fill in dredge pits. Two hurricanes and one tropical storm during 2017-2018 changed the direction of sediment transport flux near Ship Shoal and contributed to the pit infilling (less than 10% for this specific period). (3) Geophysical

and geomorphological features, including backscatter, roughness derived from bathymetry, rugosity derived from backscatter, and bathymetry, are identified as the most effective predictors of sediment texture in Caminada pit via multiple supervised machine learning methods. (4) High-quality sand from sandy shoals (such as Caminada pit) and mud-capped paleo-channels (such as Raccoon Island pit) can both be used as borrow areas for barrier system restoration in Louisiana coast. However, Caminada and Raccoon Island pits are not considered as renewable resources for future restoration due to the high content of mud infilling. Prospective observational and modeling studies are needed to keep monitoring the nonlinear pit infilling and post-filling-up processes like degassing and consolidation.

CHAPTER 1. INTRODUCTION

Barrier barriers protect the mainland coast and interior wetlands from meteorological and marine forcings and help to regulate estuarine conditions. It was reported that the barrier islands in southern coastal Louisiana have been experiencing the highest rates of land loss problem (Allison et al. 2014). A significant component of the State of Louisiana's effort to manage coastal land loss is to restore degraded barrier shorelines by dredging sand resources from borrow sites and delivering to the coastal sedimentary environments. High-quality sand for dredging is mostly limited to isolated shoals or infilled paleo-river channels in estuaries and shelf of coastal Louisiana (CEC, 2017). At present, one type of offshore sand resource on the Louisiana shelf is submarine sandy shoals, which include Ship Shoal, Tiger and Trinity Shoals, Sabine Bank and others (Dubois et al. 2009). Ship Shoal is located off the south-central Louisiana coast, which is a transgressive sand deposit located 15 km offshore of Isles Dernieres near the 10 m isobaths. Ship Shoal is comprised of well-sorted, clean quartz sand, where the median grain diameter on the crest of Ship Shoal ranges from 2.73 - 3.20 phi (0.1 - 0.15 mm) (Nairn et al. 2005). Ship Shoal has been a high-priority target sand resource to restore the Isles Dernieres barrier chain, Caminada-Moreau headland, and Timbalier island system, all of which are among the high -loss regions in Louisiana (e.g., Drucker et al. 2004; Penland et al. 2005; Khalil et al. 2007; Williams et al. 2012). Caminada (dredged in 2014; volume: 9.1×10^6 m^3) and Block 88 (dredged in 2019; volume: 3.1×10^6 m^3) dredge pits are two of the largest located on Ship Shoal. Understanding the sediment transport process and geomorphological evolution of seafloor in/near Ship Shoal is critical for the dredging activities and environmental monitoring in Ship Shoal.

An alternative type of offshore sandy resource for barrier island restoration in Louisiana is sandy paleo-channels. Unlike sandy shoals, excavating sand from paleo-channels in the Gulf of Mexico requires the removal of mud overburden formed by modern sediment transport processes. Raccoon Island pit was excavated in 2013 from a paleo-river valley north of Ship Shoal for the restoration of Raccoon Island of Louisiana. However, our knowledge of the similarities and differences of the sediment process near Caminada and Raccoon Island pits and their influences on the morphologic evolution is still limited. Caminada dredge pit in a submarine sandy shoal and Raccoon Island pit dredged from a sandy paleo-channel are selected as two main study sites to monitor long-term changes of geometry in dredge pits of two different resources. In this dissertation a total of three methods will be applied, including geophysical observation, sediment transport modeling, and machine learning, to study the sediment infilling process, the spatial and temporal evolution of the morphology of Caminada dredge pit in a sandy shoal environment, and the comparison with Raccoon Island pit in a paleo-channel environment near Ship Shoal.

There are six chapters in this dissertation. Chapter Two is focused on the sediment infilling and geomorphic change of Caminada pit on the eastern tip of Ship Shoal. This pit has a size of 2.5 km x 6.0 km, and the horizontal resolution of bathymetric data is 1 km x 1 km (Table 1.1.). Chapter Three explores the seafloor change of Raccoon Island pit and makes a comparison with Caminada pit. Raccoon Island pit has a smaller size of 1.0 km x 1.5 km and the same horizontal resolution of 1 km x 1 km. Chapter Four is focused on seafloor sediment types identification via multiple supervised machine learning methods in Caminada dredge pit (Table 1.1.). Chapter Five is to study possible sediment sources supplying the infilling of Caminada and Raccoon Island pits via ROMS modeling method. It has a study area size of roughly 200 km x

250 km, a horizontal model grid cell resolution of 250m, and a temporal scale of 20 s in the model domain. This model's temporal resolution is much higher than the monthly to yearly scales in chapters two and three. Chapter Six includes a summary of this dissertation and recommended future work.

Table 1.1. Study areas and topics of each chapter

Chapter number	Study areas	Topics	Methods	Study Area Size	Horizontal Resolution (m)	temporal scale
Two	Caminada Pit	Sediment infilling and geomorphology change	Geophysics	2.5 x 6.0 (km^2)	1	years
Three	Raccoon Island Pit	Seafloor change and comparison with Caminada	Geophysics	1.0 x 1.5 (km^2)	1	years
Four	Caminada Pit	Seafloor sediment types identification	Machine learning	2.5 x 6.0 (km^2)	1	years
Five	Ship shoal and Atchafalaya shelf/bay	Sediment source and transport	ROMS modeling	200 x 250 km^2	250	20s

CHAPTER 2. GEOMORPHOLOGIC RESPONSE AND PATCHY MUD INFILLING IN A SANDY DREDGE PIT IN SHIP SHOAL, COASTAL LOUISIANA SHELF, USA

2.1. Introduction

Barrier islands are sandy sedimentary environments separated from the mainland by estuary or lagoon environments, which protect the mainland coast and interior wetlands from meteorological and marine forcings (Otvos et al. 2018). Japan, Netherlands, China, Korea, United Kingdom, United States, and others are currently some of the leading countries using sand dredging from coastal areas to protect barrier island systems (Waye Barker et al. 2015). In recent years, the increasing demand for dredging sand from the Gulf of Mexico is driven by human activity to manage the coastal land loss (e.g., Day et al. 2007; Morton et al. 2008; Viles et al. 2014; Wiegman et al. 2018), which has been ongoing for a century or more (e.g., Alleway et al. 2015; Needles et al. 2015). The Louisiana coast has been facing extensive coastal land loss due to subsidence, shortage of sediment supply from the Mississippi River, occasional hurricane landfalls, frequent passages of winter storms, and human intervention such as levee construction, dam construction, and dredging navigation channels (Allison et al. 2014; Twilley et al. 2016; Xu et al. 2019). A major effort to manage coastal land loss is to restore degraded barrier shorelines by dredging sand resources from borrow areas and deliver to the coastal sedimentary environments (Khalil et al. 2010). Offshore/nearshore, estuarine/bays, and fluvial/riverine sediment resources available for critical restoration projects will also be limited in quality and quantity (Khalil et al. 2018), which makes the future utilization of sand resources more difficult and costly. Although billions of cubic meters of sand are needed for initial and recurring restoration (e.g., Stone, et al. 2004; Hanley et al. 2014; Jonah et al. 2015; Brown et al. 2015;

Rangel et al. 2015), high-quality sand is largely limited to isolated submarine shoals or infilled paleo-river channels on the inner shelf.

At present, the largest sand resources on the Louisiana shelf are submarine sandy shoals, such as Ship Shoal, Tiger and Trinity Shoals, and Sabine Bank, and some paleo-channels such as Peveto Channel, Raccoon Island, and Sandy Point (Dubois et al. 2009). Previous studies found most of these paleo-channels are now covered by muddy overburden from delta transgression and modern continental shelf sedimentation. Nairn et al. (2005) defined this kind of sediment deposit as 'mud-capped' sandy resources. Obelcz et al. (2018) studied the mud-capped dredge pits of Sandy Point (northwest of the modern Mississippi River Delta). They found the infilling rate (~200,000 m^3/year) was higher than dredge pits in the sandy substrate, sediment-starved settings. Wang et al. (2018) analyzed the physical oceanographic conditions (e.g., currents and waves) in Sandy Point dredge pit. They found that the dominant source infilling the pit was the suspended sediments from the Mississippi River plume in summer with little resuspension of seafloor sediment locally. Robichaux et al. (2020) reported nonlinear accumulation rate and continuing degassing and consolidation even after 100% sediment infilling at Peveto Channel dredge pit in the western Louisiana shelf. In terms of sandy shoals, Ship Shoal borrow area (SSBA) is considered the closest available sand resource for barrier shorelines in Louisiana and has been dredged for significant volumes of the high-quality beach and dune restoration sediment in Port Fourchon and Grand Isle of Louisiana (Fig. 2.1.). Dredge pits in Ship Shoal are on the inner continental shelf, and the dredging and transporting sediment from Ship Shoal to coastal barriers are expensive because of the great distance (Fig. 2.2.) (CEC, 2017). However, our understanding of long-term changes of geometry in sandy dredge pits and impacts from dredging is still relatively poor. In total, Ship Shoal is estimated to have 1.2 billion cubic meters

of potential high-quality quartz sand (Kobashi et al. 2007). However, a previous survey suggests the existence of transient mud bypassing on the seabed surface, which could fill borrow areas and affect physical/biological processes and sand quality for future coastal restoration (Stone et al. 2009; Liu et al. 2017; Xue et al. 2017; Xu et al. 2018; Liu et al. 2018; Liu et al. 2019). Nairn et al. (2005) predicted the infilling rate of a simulated pit in Block 88 of the SSBA and estimated that it would take ~ 5 years to fill a 365-m wide and 5.2-m deep pit. Kobashi et al. (2007) found that the sediment on the crest of Ship Shoal could change drastically from mud to fine sand during two months in the winter storms season, which suggested the deposition of fine-grained mud, following by winnowing and remobilization during winter storms. Stone et al. (2009) hypothesized that occasional sediment plume shifts from the Atchafalaya Bay to the southeast might result in the accumulation of a thin fluid-mud layer on some portions of the shoal. Liu et al. (2018, 2019) applied multiple machine learning classifiers to identify the sediment types and found mud was prone to deposit in the trough zones with lower backscatter values in a dredge pit of Ship Shoal. These findings indicate that mud may temporarily blanket the shoal but is later transported elsewhere. However, there is minimal knowledge about the process and forcing of the continental shelf and shoal mud deposition. Thus, dredge pits of SSBA provide a unique and artificial container to capture the mud-bypassing process in a sandy shoal depositional environment, which can be used to reveal the mechanism for mud infilling in the dredge pits.

Alterations to seafloor topography and pit marginal edge deformation from dredging practices in SSBA might potentially affect proximal oil and gas infrastructure (e.g., pipelines, platforms). Nairn et al. (2005) predicted that the pit in Ship Shoal will be filled up quickly about 3-6 years after initial dredging and predicted that the horizontal migration rate of the pit in both onshore and longshore directions could be 3 to 5 m/year. This prediction was used to inform

dredging companies' decisions regarding dredging setback distances from pipelines and potential cultural resources. To date, site-specific data required to make accurate predictions and empirical measurements to test and validate predictive models are somewhat limited. Our study will provide a better understanding of sandy-shoal dredge pits by filling data gaps and validating predictive models. Thus, the objective of this study is to address the issue of bypassing mud transport and geomorphologic response within the sandy dredging pit in a sandy environment on the continental shelf offshore Louisiana. Specifically, this study strives to (1) quantify the pit geomorphic evolution including infilling rate and pit wall slope in a dredge pit of SSBA; (2) characterize and observe the geomorphic control on mud distribution inside the dredging pit; (3) test Nairn et al. (2005)'s model and provide recommendations for future sand management of dredged areas; and (4) compare this sandy pit with other dredge pit sites in East and Gulf Coasts of USA.

2.2 Background

Ship Shoal is located off the south-central Louisiana coast (Fig. 2.1.), which is a transgressive sand deposit located 15 km offshore of Isles Dernieres near the 10 m isobaths. The shoal is approximately 50 km long, varies in width from 2 to 10 km, and is the easternmost member of a group of Holocene inner shelf shoals located southwest of the modern Mississippi River deltaic plain (Penland et al. 1986). Ship Shoal composes of well-sorted, clean quartz sand, where the median grain diameter on the crest of Ship Shoal ranges from 2.73 - 3.20 phi (0.1 - 0.15 mm) (Penland et al. 1986; Nairn et al. 2005). It has been a high-priority target sand resource to restore the Isles Dernieres barrier chain, Caminada-Moreau headland, and Timbalier Islands system, all of which are among the high-barrier-island-loss regions in Louisiana (e.g., Drucker et al. 2004; Penland et al. 2005; Khalil et al. 2007; Williams et al. 2012). In the past few years,

several pits were dredged in SSBA, including Caminada and Block 88 dredge pits. The area in SSBA analyzed in this study is Caminada dredge pit (hereafter abbreviated as Caminada) located 50 km west of Bayou Moreau in Lafourche Parish (Fig. 2.2.). The Caminada restoration project was the first such project to use sand resources from the Ship Shoal area for barrier island restoration and is the largest Louisiana monetary investment in restoration to date (Stone et al. 2004; Dartez et al. 2016; CEC, 2017). Sand dredging in Caminada pit included of two increments, I and II, during which a total volume of 9.07×10^6 m^3 of sand was excavated from December 2014 to October 2016 based on the calculation of data collected during pre- and post-construction surveys (CEC, 2017).

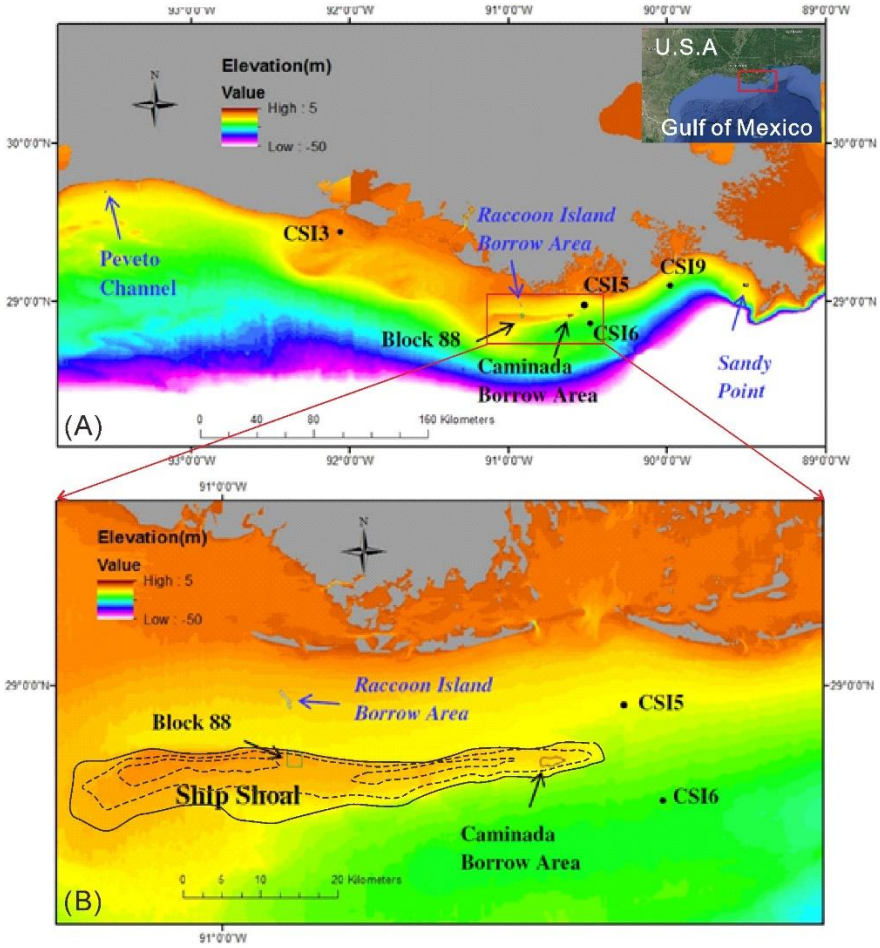

Figure 2.1. (A) Location of three mud-capped dredge pits and two sandy pits along the Louisiana shelf (After Xu et al. 2016). The elevation map was extracted from ETOP1 (NOAA), which were considered WGS 84 geographic as the horizontal datum and sea level as (caption cont'd).

the vertical datum. Mud-capped dredge pits are Peveto channel, Raccoon Island, and Sandy Point. Sandy dredge pits are Caminada and Block 88 dredge pits. (B) Two borrow areas in Ship Shoal are Caminada and Block 88. The black dashed lines are 2m isobaths intervals. CSI stations are referring to the wave-current surge information system from the Coastal Studies Institute.

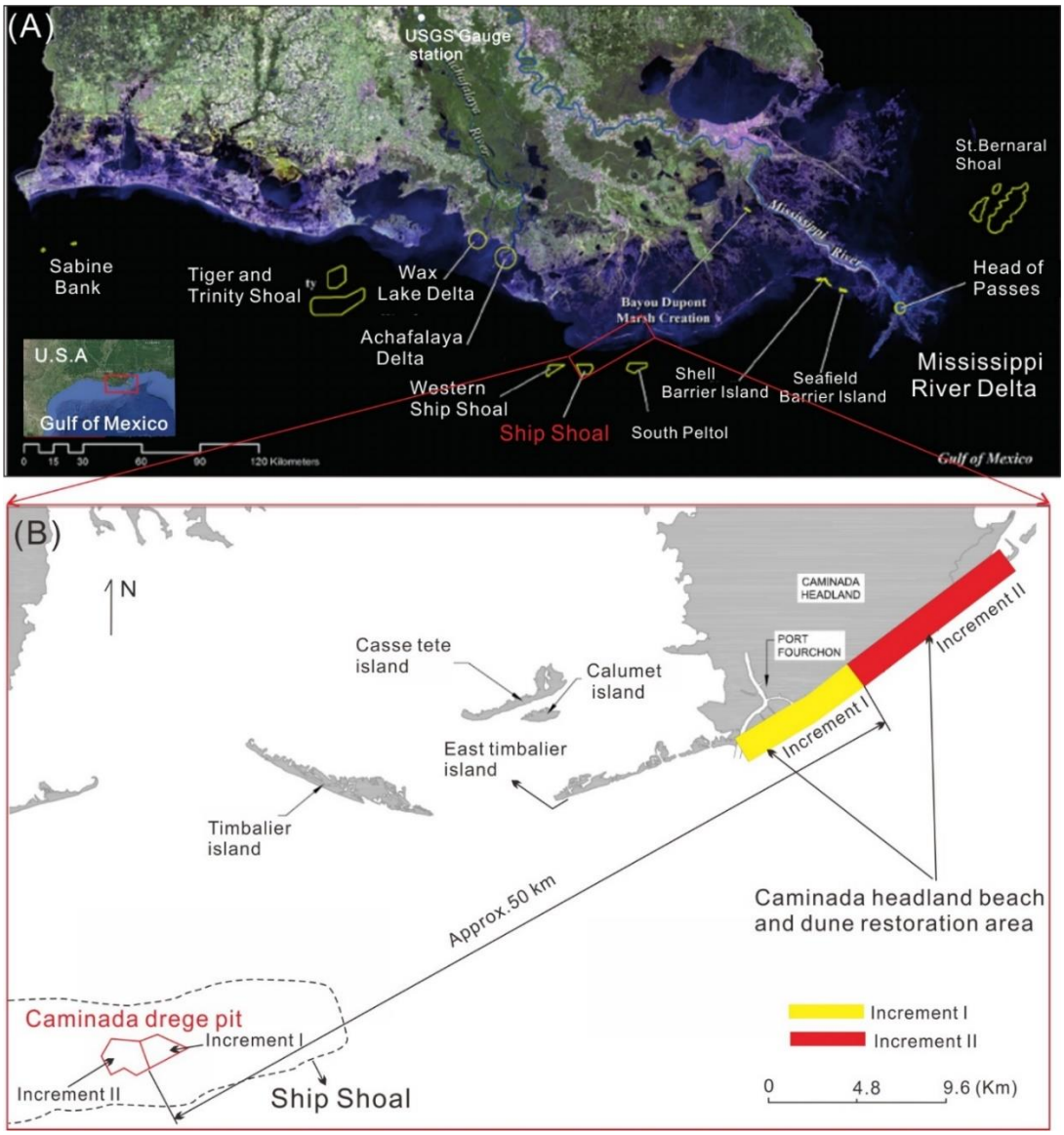

Figure 2.2. (A) Deltas, barrier islands, and major sand shoals in coastal Louisiana (After Khalil et al. 2018). (B) Caminada dredge pit in Ship Shoal and restoration areas in Caminada Headland, which include increment I and II of Caminada Headlands Restoration Project (After CEC, 2017).

2.3 Methods

Interferometric swath bathymetry and side-scan sonar imaging were used to quantify the seafloor morphology, topography, and evolution of Caminada pit. Bathymetric data from three

post-dredging surveys (2016, 2017, and 2018) were utilized and processed in CARIS HIPS and SIPS v.11.2. Bathymetric data were applied tides correction, sound velocity profiles, patch tests, and using filtering, then exported to ArcMap 10.2 for generating Digital Elevation Models (DEMs), Difference of Depth maps (DODs), gradient maps and calculating volumes. The vertical bathymetry control was referenced to, and verified by, NOAA Texas Gas Platform, Caillou Bay, LA (Station ID: 8763535). The gross volume gain primarily determines the infilling rate over time. The time intervals of 2016-2017 and 2017-2018 surveys were nine months and thirteen months, respectively. This study converted the unit of volumetric infilling rate to m^3/year.

The Atchafalaya River water discharge data were obtained from the U.S. Geological Survey (USGS) station at Simmesport, LA. Hourly wind data were downloaded from the National Oceanic and Atmospheric Administration (NOAA) Data Buoy Center at Grand Isle station, LA. Additional supporting wave and current data were collected to provide background information for our study area. An Acoustic Doppler Velocimeter (ADV) Ocean from Sontek was mounted on a tripod, which was about 1.5 km northwest of Caminada pit from 07/08/2018 to 09/14/2018. High-resolution 3D velocity data were collected about 0.5 m above seafloor using a sampling rate of 8Hz, a burst duration of 4.3 minutes, and a burst interval of 60 minutes. Burst-averaged horizontal velocities were calculated using the method of Wang et al. (2018). A wave gauge was used during the same period to collect data using a sampling rate of 10Hz, a burst duration of 20 minutes, and a burst interval of 60 minutes. Wave spectral analysis was performed using the toolbox developed by Karimpour and Chen (2017) with the corrections of wave attenuation with depth.

Modeling wave data were downloaded for Gulf of Mexico region from WAVEWATCH III Hindcast and Reanalysis Archives (https://polar.ncep.noaa.gov/waves/); spatial and temporal resolutions of wave data were 1/15° and 3 hours, respectively. Modeling surface current velocity data were downloaded from the archive of HYCOM + NCODA Gulf of Mexico Analysis (https://www.hycom.org/data/goml0pt04/expt-32pt5); spatial and temporal resolutions of velocity data were 1/25° and 24 hours, respectively. Wave and velocity data were then interpolated to Caminada pit for comparison with the observed tripod data to provide background information.

Slope calculations were performed using the DEM Surface Tools following the method of the Arc-Chord Ratio (Du Preez et al. 2015). Side-scan mosaics were also generated in HIPS and SIPS and then exported in ArcMap to identify the reflectivity change of seabed inside the dredge pit. Reference uncertainty for DEMs and DODs in the different bathymetric dataset was quantified by the fixed-point method of Schimel et al. (2015). Grain size analysis was performed to identify the type and distribution of surficial sediment in the dredge pits. A total of 65 samples were collected using a Ponar grab in the post-dredging survey of 2018. Grain size analysis was conducted using a Beckmann Coulter laser diffraction particle size analyzer (Model LS 13 320). To prepare samples for this analysis, ~1 g subsample from each sample was placed in a centrifuge tube, and 10–20 milliliters of 30% hydrogen peroxide was added to remove organic matter. More details of processing and analysis can be found in Xu et al. (2016).

2.4 Results

2.4.1 Physical conditions near Ship Shoal

Physical conditions near Ship Shoal are essential in driving sediment transport and developing coastal morphology. Atchafalaya river discharge reached near $2*10^4$ m^3/s in spring

2018 (Fig. 2.3.A). Wind speeds were higher than 4 m/s during two geophysical surveys (Fig. 2.3.B). The average wave height near Caminada dredge pit was about 0.5 m (Fig. 2.3.C), which was verified by tripod data in Fig. A1. (Appendix). The average current velocity was 0.18 m/s near Caminada from July 2017 to September 2018 in HYCOM model (Fig. 2.3.D). However, the average current velocity from ADV in Caminada pit was less than 0.1 m/s from August 2018 to September 2018 (Fig. A1). The current velocity reached the peak near 0.3 m/s in August 2017 for Hurricane Harvey and 0.5 m/s in October 2017 for Hurricane Nate (Fig. 2.3.D).

2.4.2 Caminada pit infilling

Repeat bathymetric maps in 2016, 2017, and 2018 showed similar overall morphology of the pit walls but shoaling depths inside the pit over time (Fig. 2.4.A, B & C). As of July 2017 (nine months after increment II), sediments in Caminada mostly deposited inside the pit. The pit depth was approximately 13.3 m below sea level, compared to the ~9 m depth of the surrounding seafloor. As of August 2018, the average depth was 12.8 m (Fig. 2.5.). DOD maps of three post-dredging surveys revealed that nearly no net new sediment deposited outside pit, but there existed new sediments filling the troughs and wall margin inside the pit (See dotted polygons in Figs. 2.4.D & 2.4.E). The southern wall was found to be shoaling (blue in Fig. 2.4.D) while the northern wall showed erosion (red color), which indicated sediment transported and filled in Caminada from the southeastern wall. Morphological evidence for the localized failure (wall erosion and collapse) of pit walls was observed in the northern wall (Fig. 2.4.).

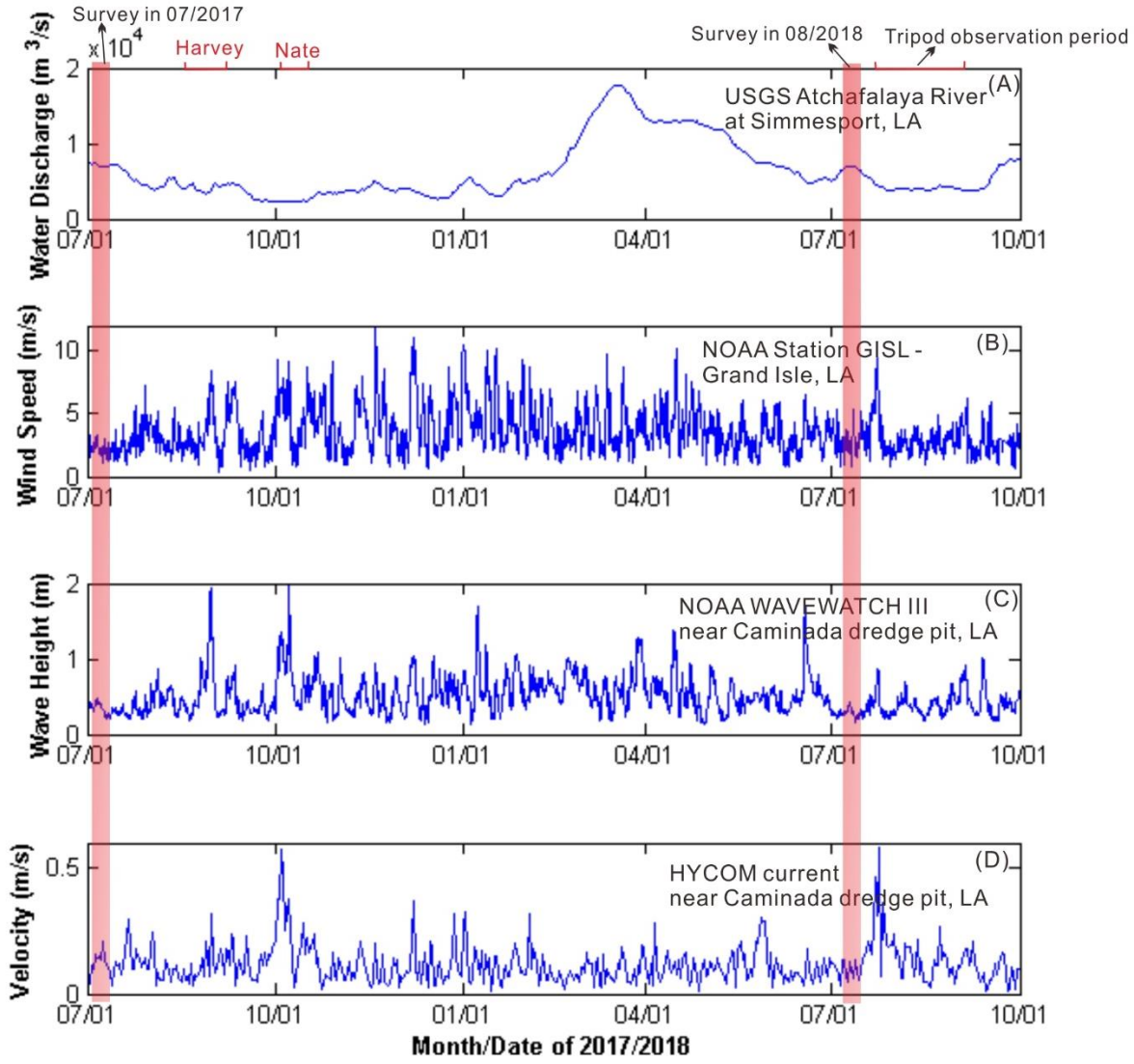

Figure 2.3 Time-series results outside of the Caminada pit from 07/01/2017 to 10/01/2018. (A) Daily river discharge at USGS station 07374525 Atchafalaya River in Simmesport, LA. (B) Daily wind speed from NOAA station GISL1-8761724 in Grand Isle, LA. (C) Daily wave heights from NOAA WAVEWATCH III near Caminada dredge pit; (D) Daily horizontal current velocity from HYCOM current near Caminada dredge pit. The two red bars indicate the period during two geophysical survey periods (07/2017 and 08/2018). Three red highlight lines are two hurricanes in 2017 and the period we deployed the tripod in Caminada pit.

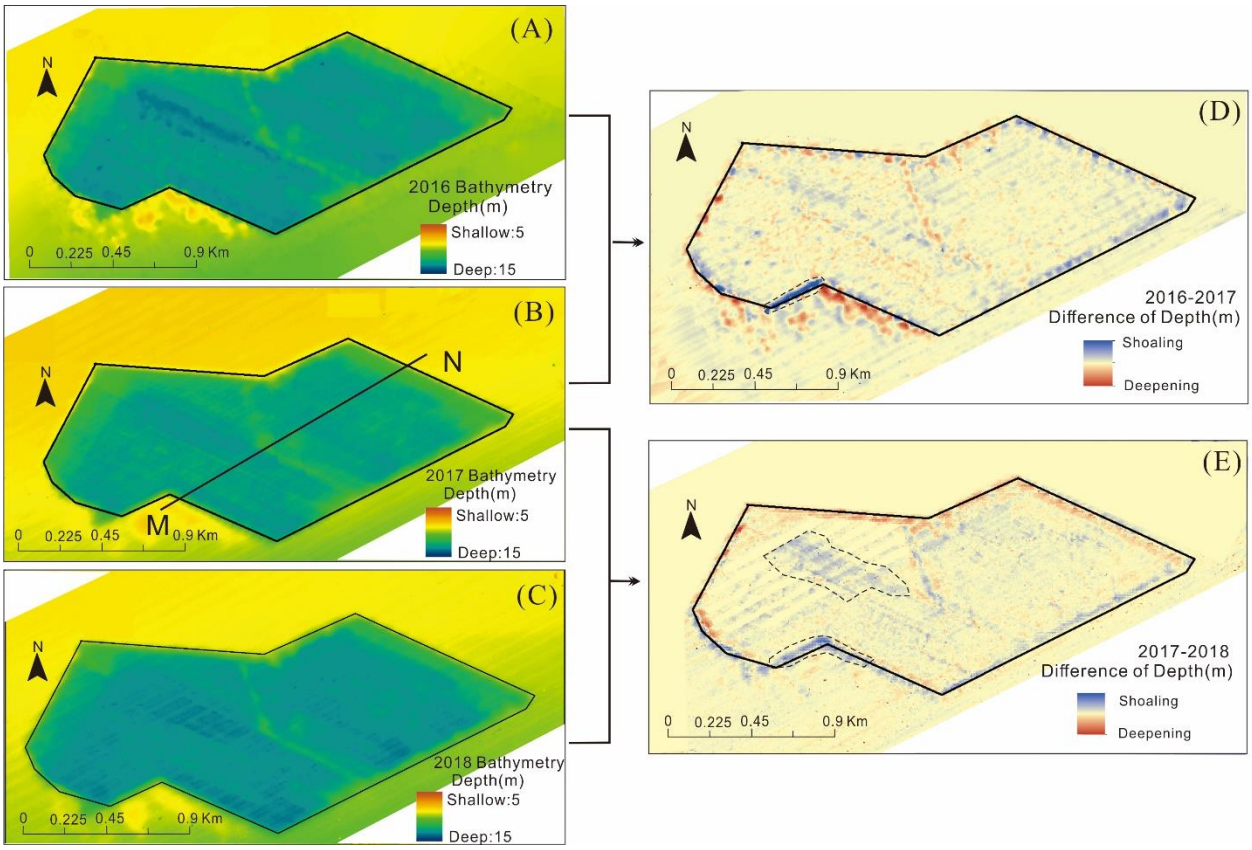

Figure 2.4. (A)(B)(C) Bathymetry map in three different surveys from 10/2016, 07/2017, and 08/2018. The black polygon is the same one and is the margin of the bathymetry map in 2016, which is considered as the reference polygon for comparison of repeated surveys. The depth value is positive with a unit of meter. The scale of the color bar is the same in panels (A)-(C). MN shows the location of transect in Fig. 2.5. (D) A difference of depth in meters between 2016 and 2017 surveys; (E) Difference of depth in meters between 2017 and 2018 surveys. The dashed lines in D and E highlight major zones of shoaling. Values within the 2σ range of uncertainty (0.1 m) are generally in beige and considered no significant depth change.

The estimation of the annual sand transport rate is essential to predict pit evolution for Caminada. The volume of infilling sediment calculated for the nine months in 2016–2017 is approximately like that of the 13 months in 2017–2018. It reveals that the sediment infilling rate in 2016-2017 was higher than that of 2017-2018. Post-dredging volumetric analysis of 2017-2018 indicates that Caminada is presently infilling at an average rate of approximately 27,480 m3/year (~ 0.15 m/year in terms of averaged thickness).

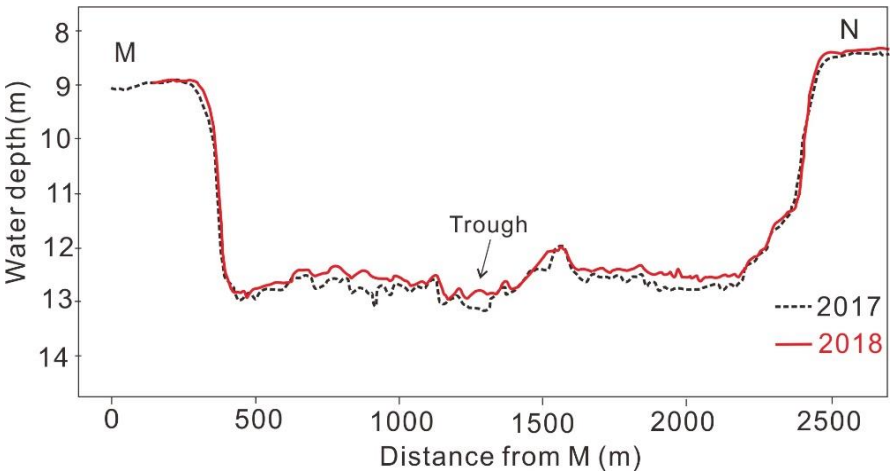

Figure 2.5. Bathymetric profiles of 2017 and 2018 along the transect MN (location in Fig. 2.4.B). The average sediment deposit is about 0.15 m/year.

2.4.3 Seafloor backscatter

A side-scan mosaic map in the 2017 survey showed three lineations that were associated with lower backscatter values (Fig. 2.6.A) and deeper depth (Fig. 2.4.B). Two lineations oriented northwest-southeast were in the central pit, and one elliptical lineation was located in the northeastern corner (Fig. 2.6.A). All of these are low-topography zones (hereafter referred to as troughs) inside Caminada pit, which are interpreted as a product of dredging activities. As of August 2018, the low-reflection troughs inside Caminada increased in size following the previous depositional pattern and direction (Fig. 2.6.B & 2.6.C).

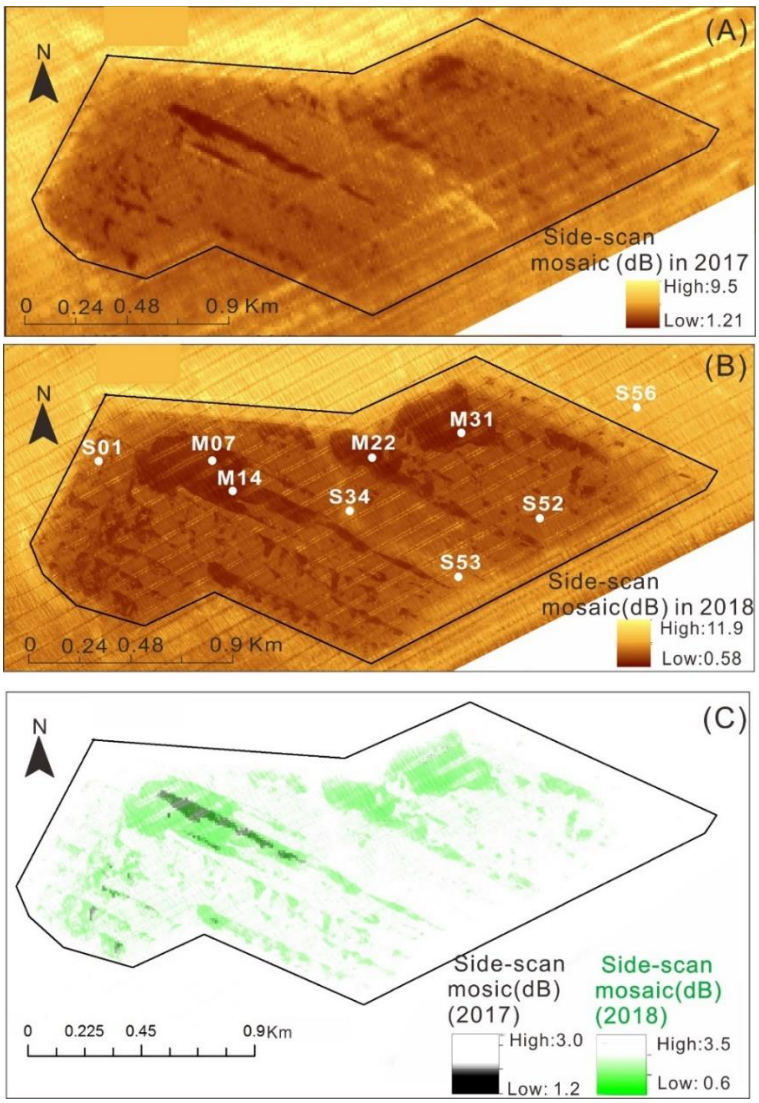

Figure 2.6. (A)(B) Side-scan maps of Caminada pit for two post-dredging surveys in 2017 and 2018. The side-scan mosaic shows the difference in backscatter values in the unit of Db (Decibel). Note the dark brown indicates the patchy mud with low backscatter value, while the bright yellow is associated with sandy sediment with high backscatter value. Note the scale of the color bars is different. The black contour is the margin of dredge pit in 2016. White dots show the location of surficial grab sediment samples collected in 2018 with an ID number for the grain size analysis (results are shown in Fig. 2.7.). (C) Overlaid side-scan mosaic map between years 2017 and 2018 (highlighting low backscatter values in black and green, respectively) show that muddy sediment deposited in the topographic lows within one year.

2.4.4 Median grain size

The grain size of a subtotal of 9 samples from inside and outside the Caminada pit is shown in Fig. 2.7. The grain size of relatively muddy samples inside the pit (M07, M14, M22, and M31) indicated the dominance of silt with a mean size of 15 μm. On average, sand and silt represented

23% and 74%, respectively, with silt being the dominant fraction for the four muddy samples (Fig. 2.7.A). However, the other four samples within the pit (S01, S34, S52, and S53) compose of a coarser sandy grain size of 100 µm (Fig. 2.7.B), which sand and silt represented 97% and 3%, respectively. Outside the pit, the surficial sediment (S56) was purely sandy with a mean grain size of 110 µm (Fig. 2.7.B).

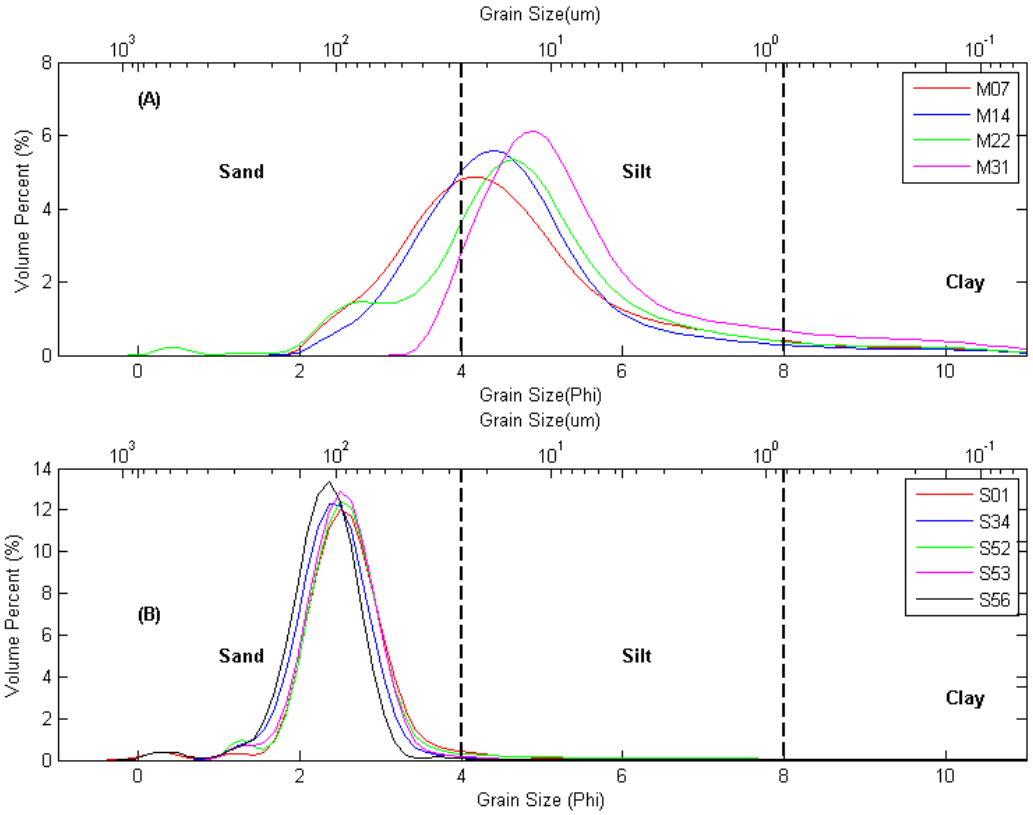

Figure 2.7. The grain size distribution of surficial sediment inside and outside of Caminada dredge pit (see Fig. 2.6. for grab sample locations). (A) The grain size of four muddy samples and (B) Grain size of the five sandy samples.

2.4.5 Caminada pit wall slope change

Between the 2017 and 2018 surveys, the seafloor of the Caminada pit became smoother and flatter with the sediment infilling topographically-low areas (Fig. 2.8.). Nearly all pit walls lost steepness in the first two years after dredging. Morphological evidence for localized failure was observed and primarily confined to the pit walls, particularly in the northern wall (Fig.

2.2.A). Total wall volume loss between the 2017 and 2018 surveys was approximately 3% (780-824 m^3) of infill volume in 2017-2018 (27,480 m^3/year). During both the years 2017 and 2018, the western walls were always steeper than the eastern walls (Figs. 2.8.A & 2.8.B). From 2017 to 2018, the pit wall slope decreased from 3.3-6.6 to 1.7-3.6 degrees (i.e., became gentler), which proves a 'relatively' stable condition for the dredging pit between these years. Previous bathymetric survey (Penland et al. 1986) found Ship Shoal migrated landward at a rate of 7 m/year (in the east) to 15 m/year (in the west). But the gradient change between the two surveys indicated Caminada did not experience much outward wall migration during the 2.5 years after dredging.

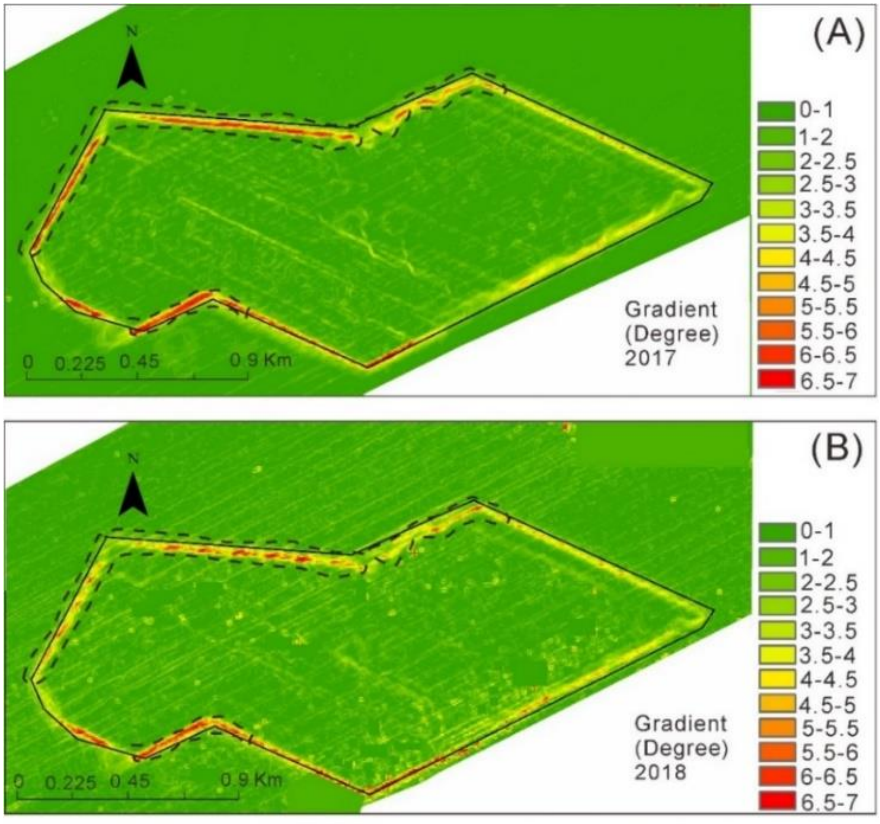

Figure 2.8. (A)(B) Gradient map of the Caminada dredge pit derived from 2017 and 2018 bathymetry. Green colors represent flatter surfaces, while red colors indicate steeper surfaces. Dashed polygons are the extents of northern and southern walls used for gradient analysis, which showed decreased slopes from 2017 (red) to 2018 (yellow).

2.5 Discussion

2.5.1 Sources of infilling sediments

The sandy Ship Shoal is under the combined influence of wind-driven currents, storm waves, tides, and the dynamic Atchafalaya and Mississippi river dispersal systems (Stone et al. 2009). Stone et al. (2004) found the sediments on the shoal were coarser at the eastern part than at the western shoal, which indicated the influence of the river discharges containing muddy sediment from the Atchafalaya River. Previous studies (e.g., Walker et al. 2005; Kobashi et al. 2007; Xu et al. 2011) also indicated that suspended sediment dispersal from Atchafalaya River (i.e., hypopycnal plume) often shifted in the direction from westward to southeastward during high river discharges and strong northwest winds. Ship Shoal is on the pathway of the shifted dispersal and is predominantly characterized as having a sandy bottom near the seabed. During conditions of high discharge and strong northwest winds, it could be covered with concentrated benthic suspension from Atchafalaya River, which dramatically alters its bottom sediment characteristics (Stone et al. 2009; Kobashi et al. 2009).

Additionally, the depth-averaged currents near Ship Shoal were estimated to be westward for the majority time in the long-term numerical model (Xu et al. 2011), which could carry muddy sediment from the Mississippi River plume toward Ship Shoal. Flows ultimately bring some suspended sediment to Ship Shoal when longshore current from the Mississippi River has a strong effect on sediment transport (Nairn et al. 2005). As shown in our results, DODs maps prove that nearly no new net sediment accumulated outside Caminada over the period analyzed (2016 to 2018), and bathymetric data show that Caminada pit of Ship Shoal served as an artificial trap to capture the transient mud inside the pit. Side-scan mosaic maps indicate new muddy sediment was transported into the troughs of Caminada pit from 2017 to 2018 (Fig. 2.6.).

Moreover, dating of beryllium-7 (^{7}Be) radioisotope activity ($T^{1/2} = 53$ days) in the muddy sediments collected using a multi-corer inside Caminada indicates at least a portion of the mud deposited within ~6 months before core collection (Xue, 2019). Xue (2019) found clays and fine silts deposited in Caminada pit were likely sourced from the Atchafalaya River plume during the study period in a long-term view based on satellite imagery of hypopycnal plumes. Walker and Hammack (2000), Kobashi et al. (2007) and Stone et al. (2009) also observed Atchafalaya hypopycnal surface plume could extend over Ship Shoal. Previous studies show the fine riverine sediment contributes to the deltaic wetlands such as Fourleague Bay (Restreppo et al. 2019), Breton Sound (Wang et al. 2019), and Barataria Bay (Wilson et al. 2008). As these winter storms or cold fronts pass, wind patterns shift from blowing from the southeast to blowing from the north with a decrease in barometric pressure (Stone et al. 2009). This postfrontal, north-originating wind could resuspend recently deposited sediments and distribute fine silts and clays on the continental shelf near Ship Shoal (Walker and Hammack, 2000; Kobashi et al. 2007; Xue, 2019).

The sediment infilling process in Caminada is also impacted by the erosion/deposition of the adjacent seabed sediment by waves and currents. The DODs map of 2016 and 2017 surveys showed deepening occurred in the southwestern corner outside the pit (red in Fig. 2.4.D), which was formerly a sediment mound spilled from a spider barge for dredging sediment delivery. Local wave and currents likely mobilized this sediment outside the pit and transported it in a northwestern direction to fill a proximal location within the pit that exhibited sediment shoaling (Blue zones in the dotted lines of Fig. 2.4.D, 2.4.E). Additionally, the erodible materials produced by local wall failure could contribute to the sediment infillings. The gradient of pit wall became gentler from 2017 to 2018 (Fig. 2.8.), which indicated the sandy sediment near the

pit margin could be transported into the pit, supplying some of the sand infills (Figs. 2.6.B & 2.7.).

Lastly, episodic extreme events such as hurricane and storms are likely another factor for sediment filling Caminada during the geophysical surveys (07/17-08/18). These high energy wind events (hurricanes and other tropical events) were strong enough to resuspend coarse silts and sands on the shelf and redeposit them as sediment layers that have been seen elsewhere across the Louisiana Shelf (Goni et al. 2007; Walker and Hammack, 2000; Xu et al. 2015). Kobashi et al. (2007) conclude that during the fair-weather conditions, a dense benthic mud layer on Ship Shoal originating from the Atchafalaya river is deposited, later resuspended and mixed during winter and spring storm passage. Xue (2019) found the timing of hurricanes or the tropical storms in 2017 correlated well with the occurrence of coarser grain size (coarse silt) inside Caminada pit, suggesting these coarser laminations are related to storm-induced deposition. It is well known that the sediment infilling process in pits will slow down through time. The episodic extreme events, such as hurricane and tropical storms, should be considered when calculating the sediment infilling rate. There were only two hurricanes during our study period. Hurricanes Nate and Harvey in 2017 did not pass Ship Shoal directly but were with a distance of ~ 200 km (Fig. A2). Hurricane Harvey changed to a tropical storm when it made landfall in Louisiana. These two hurricanes could bring sediments to Ship Shoal as one possible contribution to sediment filling in Caminada.

The sediment infilling process in Caminada is likely impacted and controlled by sediment availability, which is under the combined controls of the four aforementioned sediment supply mechanisms (suspended sediments from hypopycnal plumes of rivers, or concentrated benthic suspension seasonally deposited in the nearshore environment, the erosion of the adjacent seabed

sediment by waves and currents, sediments yielded by wall failure filling in the pit and hurricanes or tropical storms). However, bathymetry and backscatter maps of the past three surveys indicate new sediments deposited inside the Caminada contained mud primarily. Fig. 2.1.B shows that Caminada is in the east end of Ship Shoal, which is near the shoal crest with high topography of the seafloor. Comparing with mud sediments, sandy sediments likely need higher energy to be moved westward and upslope to Caminada pit.

2.5.2 Topography's control on mud distribution

Grain size analysis of samples collected inside and outside pit indicated sediment types had a close relationship with the side-scan backscatter value. The sediments (M07, M14, M22, and M31) collected from these three low-reflection troughs (Brown zone in Fig. 2.6.B) were proved to be patchy mud (Fig. 2.7.A). However, the sediments (S01, S34, S52, and S53) from dark yellow zone inside pit were sand or sand mixed with mud (Fig. 2.7.B), which revealed the high backscatter values (Fig. 2.6.B). Also, S56 was the pure sandy sediment collected from the outside pit, which corresponded with the bright yellow and highest backscatter value (Fig. 2.6.B).

The topography of seafloor inside Caminada pit has direct control over the patchy mud distribution. Figure 8A shows the troughs (blue-green color) inside Caminada of the 2017 bathymetric survey, which was the footprint of dredging activities. Suspended mud deposits (dark brown color in Fig. 2.9.B) appear to be prone to deposit within these low topography areas. In essence, the boundary of patchy mud distribution in the side-scan map of 2018 (white dash lines in Fig. 2.9.B) matches the troughs in the bathymetry survey in 2017 (Fig. 2.9.A). Two-dimensional transects from repeat bathymetric surveys indicate the troughs have not been filled

up yet (Fig. 2.5.). Based on that trend, it is expected that more mud sediment will deposit in the troughs in the coming years.

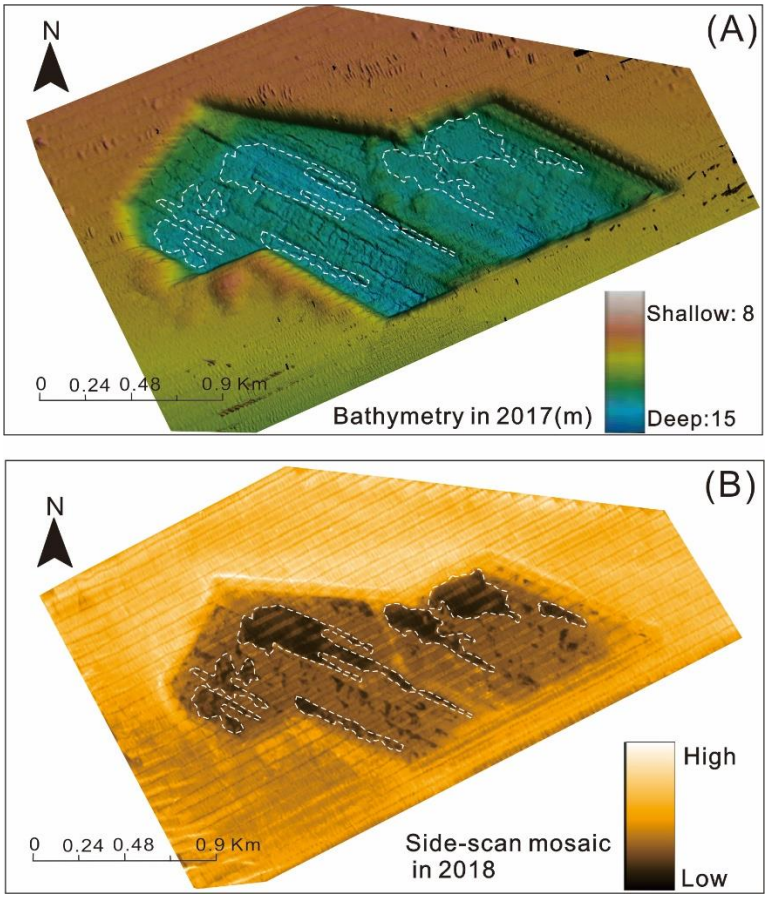

Figure 2.9. (A) 3-D geomorphology map of Caminada dredge pit in 2017 survey with the overlaid boundaries of distribution of patchy mud in 2018. The vertical exaggeration is 32 times. White dashed polygons are exacted from (B), which are boundaries of areas with low backscatter values. It indicates the new muddy sediments are prone to deposit in the troughs inside Caminada pit within one year. Dark blue color inside the pit indicates the topography-low zones, which refers to the patched zones. (B) Side-scan backscatter maps of Caminada for the post-dredging surveys in 2018.

2.5.3 Geomorphic model of SSBA sandy environment evolution

^{7}Be penetration depths observed in repeat multi-coring study in Caminada pit documented 2–15 cm of fresh deposition within ~100 days, equivalent to the seasonal sedimentation rates 7.3-55 cm/year (Xue et al. 2018). The lower estimate of the ^{7}Be infilling rate matched well with the infilling rate of 15 cm/year calculated by a repeat bathymetric survey in

2017-2018. Nairn et al. (2005) applied a 1D analytical model to study the evolution of a proposed dredge pit in Block 88 of Ship Shoal (see location in Fig. 2.1.B) 31 km west of Caminada pit. They included the empirical coefficients, settling velocity of mud, water depth of inside and outside the pit, background concentration outside, and tidal period but did not consider wave resuspension, episodic extreme hurricane and other tropical events (Equation 2.1). Caminada pit has a depositional environment generally like proposed Block 88 pit. We keep all the parameters the same but only changed h_0 and h_1 in Nairn's model to compare the infilling percentage in the first two years after dredging. Nairn's model of Block 88 infilling percentage (~ 75%) is much greater than what is observed in Caminada pit (~ 10%) (Fig. 2.10.).

$$\Delta Z_b = k_1 C_0 \omega_s T \frac{1}{\rho_{dry}} \left[1 - \left(\frac{h_0}{h_1} \right)^3 \right] \tag{2.1}$$

Where ΔZ_b is total sedimentation thickness per tide (m), which is used to calculate the infilling percentage in Figure 10. K1 is empirical coefficients. C_0 is background concentration outside the pit, which is generally determined by using the tide-mean and depth-averaged sediment concentration for the surrounding area (kg/m^3 or mg/l). ωs is settling velocity of mud (m/s). T is a tidal period (s). ρdry is dry bulk density (kg/m^3). h_0 is water depth outside the pit (m). h_1 is water depth inside the pit (m).

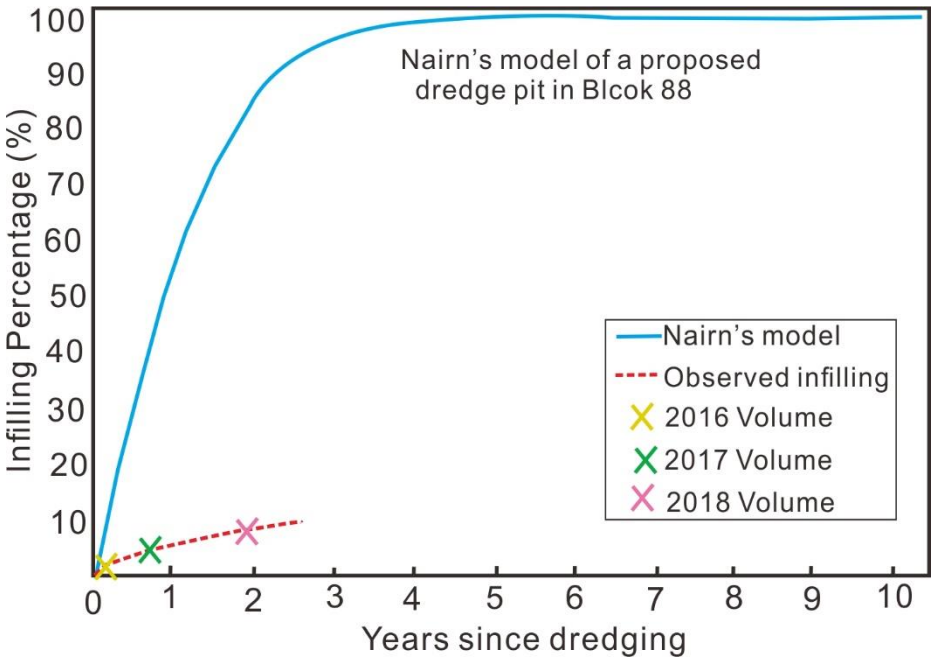

Figure 2.10. Observed infilling percentage in Caminada over time and its comparison with Nairn's model in a proposed Block 88 pit. Volumetric calculations for our surveys with uncertainty were made using the Cut-Fill tool in ArcMap

Based on our findings, a conceptual model is presented here to represent the sediment infilling process within sandy dredge pits based on observed Caminada pit evolution after sand excavation (Fig. 2.11.). The first and second phase occurs immediately when strong currents and waves continuously impact the pit: eroded sediments from slope/pit margin are transported into the dredge pit under the controls of short-timescale forcings such as currents, tides, and waves. Where dredge sediments are freshly deposited outside of the pit, they can be transported by the same short-timescale forcings into the pit along the pit slope/margin. After initial rapid failing and stabilization of the pit walls, far-field suspended muddy sediment from rivers, and sandy sediment from local erosion (Fig. 2.4.D) dominate infilling volumetrically (Fig. 2.11.A). As discussed previously, muddy sediment can be sourced from hypopycnal plumes of the Atchafalaya or Mississippi Rivers, or advection of concentrated benthic suspension that are seasonally deposited in the nearshore environment (Stone et al. 2009). These muddy sediments likely blanket the pit as a sheet-like layer (Fig. 2.11.B). Subsequently, sediments deposited inside

Caminada (both sand and mud) are re-suspended by local currents or storm winds that generate high bottom shear stress, strong bottom sediment suspension, and vertical mixing within the dredge pit (Fig. 2.11.C). The finest of these suspended sediments (mud) are then prone to deposit in the troughs inside the pit, as explained below (Fig. 2.11.D). Wall failure continues throughout all the phases, but the wall volume loss is less than 3% of total infill volume inside pit. Over time, freshly deposited sediments experience compaction and consolidation. These processes are cyclic and can restart once far-field muddy sediment or local sandy sediment is transported into the dredge pit.

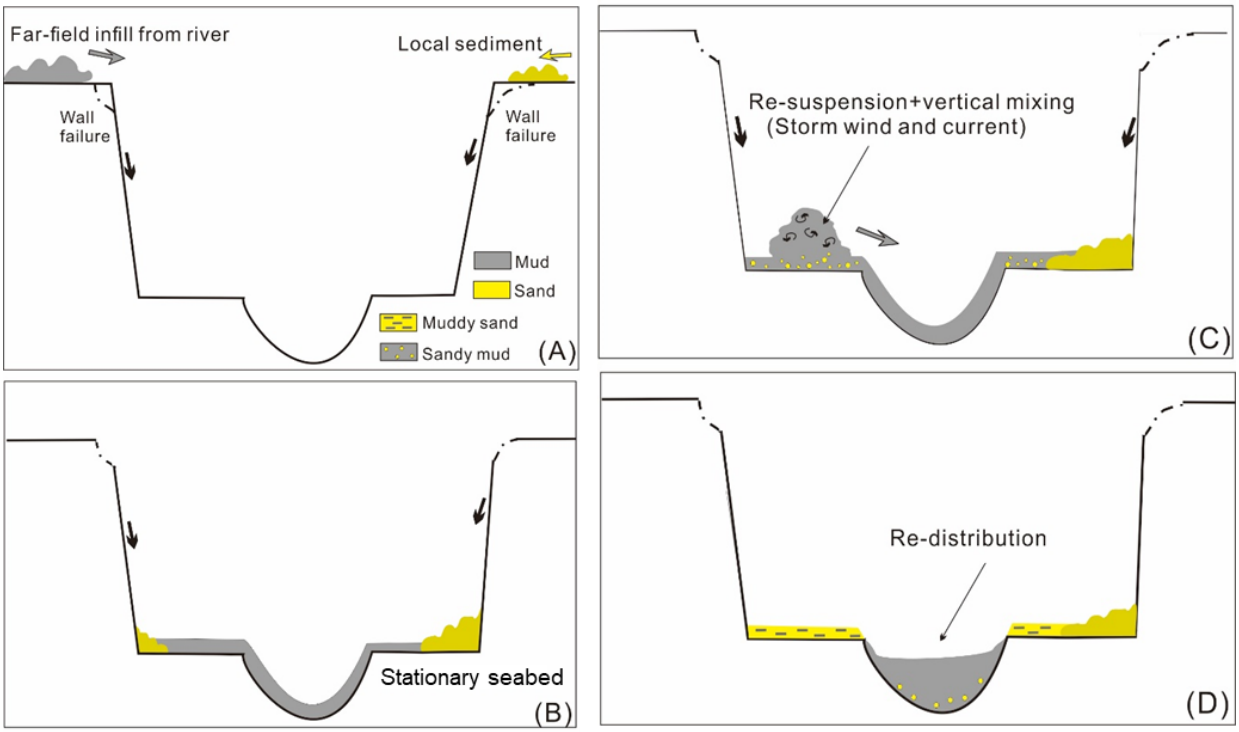

Figure 2.11. Schematic evolution model of SSBA Caminada dredge pit near a fine-grained sediment source. The graphs are dimensionless and not to the scale. (A) and (B) take place when the muddy sediment transport and fill into the pit. (C) The third phase of evolution, which local currents, waves, and storms drive the suspended sediment re-suspension and vertical mixing. (D) The last stage shows that mixed sediments re-distribution inside the pit. The troughs are prone to deposit finer and muddy sediments.

In this conceptual model, waves, currents, slope, sediment texture, and erodibility all can impact sediment transport and redistribution. For instance, based on the linear wave theory, the impact of the wave on the seabed can be quantified using the near-bed wave orbital velocity

(Wiberg and Sherwood, 2008). This theory predicts that the maximum horizontal component of orbital velocity U_b is directly proportional to wave height and depends inversely on water depth. We calculated the bottom wave orbital in the outside pit (9 m), pit bottom (13.3 m), and topographic lows (40 cm depth relative to the average pit bottom depth) from Wiberg and Sherwood (2008). Wave height (average of 0.5 m) and wave peak period (average of 5s) in Caminada were collected from the tripod sensors (Fig. A1). Wave orbital velocity outside pit was 0.0741 m/s, which was greater than 0.0413 m/s in pit bottom and 0.0393 m/s in topographic lows in pits.

The effect of wave on bottom shear stresses is calculated based on the theory from Grant and Madsen (1979). In this model, the maximum bottom shear stress is giving by:

$$\mathrm{Tw} = \rho \mathrm{Uw}^2 = \frac{1}{2}\rho * \mathrm{fw} * \mathrm{Ub}^2 \qquad (2.\ 2)$$

in which ρ is the water density, u_w is wave friction velocity, T_W is the maximum wave bed stress, f_w is the wave friction factor, and U_b is the near-bottom wave orbital velocity we calculate from Wiberg and Sherwood (2008). Wave shear stress is proportional to the square of orbital velocity if other parameters kept constant. Based on equation (2. 2), it is clear that deeper water depth in the pit bottom topographic lows would experience smaller bottom orbital velocities and shear stress when compared to pit bottom and the seafloor outside the pit. Although 40 cm is a small percent (3%) of total water depth of 13.3 m, it plays a role in the maximum wave bed stress because of the nonlinear change of Tw with water depth (Xu et al. 2016). Although no current data were collected in Caminada pit, Wang et al. (2018) collected valuable current data inside Sandy Point dredge pit in the eastern Louisiana shelf and reported a high turbidity layer and sluggish environment on the pit bottom. It is well known that (a) sediments tend to move downslope under the control of gravity in the coastal environment and that (b) newly-deposited

fine sediments are more mobile (and thus erodible) than coarser ones. Thus, we conclude that the slopes along the sides of small ridges on pit bottom, small wave orbital velocities, slower currents, sediment texture, and high erodibility of mud all promote the patchy mud deposition found in Caminada dredge pit.

2.5.4 Comparison and Implication

The dredging sand volume of Caminada pit is one of the largest in the U.S. eastern seaboard and Gulf Coast. The amount of sediment excavated from Caminada and the rate of subsequent infill can be compared with published results from other sandy and muddy dredge pits located in different geographic and geological settings (Table 2.1.). Byrnes et al. (2004a, 2004b) modeled the nearshore wave and sediment transport in post-dredging conditions and found sand mining at multiple sites (Corson Inlet and Mobile Quter Mound) in Alabama and New Jersey had a minimal environmental impact on sediment dynamics and wave height. Our results indicate Caminada pit is keeping a 27,480 $*10^3$ m^3/year sediment infilling rate, while dredge pits in the area of Mobile Quter mound (AL) have lower sediment infilling rates due to insufficient sediment supply from the major rivers feeding the pits and low longshore sediment transport rate (Byrnes et al. 2004b). Byrnes et al. suggested the proximity to sediment sources is an important variable for the infilling process. Compared with the muddy-capped dredge pits in Louisiana including Sandy Point and Peveto Channel borrow areas (15 years Obelcz et al. 2018; 13 years in Robichaux, 2020), Caminada pit has a relatively slower sediment infilling rate. All of these three muddy pits are close to major river sources, which again suggests the importance of proximity to fluvial sediment sources (Byrnes et al. 2004b)

Table 2.1. Multiple dredge pit areas and volumes in the East and Gulf Coasts

Resource Area	Depositional environment	Sand Volume (10^6 m^3)	Infilling rate (10^3 m^3/year)	Wave heights (m)	Current velocity (cm/s)	Hurricanes(year)
Corson Inlet, NJ[1]	Shelf/Sandy	8.8	164	0.3	13-31	simulating 50-yr hurricane and storm events
Mobile Quter Mound, AL[2]	Bay/Sandy	8.4	13.5	0.2-0.4	25-35	50-year storm simulations
Palm Beach, FL[3]	Beach/Sandy	0.938	276	6.1 (during hurricane)	NA	Hurricanes Frances (2004), Jeanne (2004), Katrina (2005)
Caminada, LA	Shoal/Sandy	9.07	27.48	0.5	0.18	Hurricanes Harvey (2017), Nate(2017)
Proposed pit in Block 88, LA[4]	Shoal/Sandy	~3.103	62.06	NA	NA	Not consider
Sandy Point, LA[5]	River/Muddy	3.74	200	0.1-0.2	0-5	Hurricanes from 2012-2015
Peveto channel, LA[6]	Paleo-channel/Muddy	2.059	377.3	NA	NA	Hurricanes from 2006-2016

Source:1. Byrnes et al. (2004a) modeled the wave transformation and included the simulating 50-yr hurricane and storm events in the model. 2. Byrnes et al. (2004b) considered the seasonal change of wave heights and 50-year storm simulations. 3. Kennedy et al. (2010) studied the infilling of dredge pits during 2004 and 2005 energetic hurricane seasons. 4. Nairn et al. (2005). The dredge pit of Block 88 in this table is a proposed one for modeling purposes in 2005. The real dredge pit in Block 88 was dredged in 2018 summer and with a total volume of 10.51 million m^3. 5. Obelcz et al. (2018) and Wang et al. (2018). 6. Robichaux et al. 2020.

However, these above sites are quite different from smaller pits such as in Boca Raton, Palm Beach, Fort Myers Beach, Panama City Beach, and John's Pass in Florida, which are predicted to be filled up within only a few years (Kennedy et al. 2009). This indicates that the excavation volume of dredge pits can also be an important factor controlling the filling time. Previous studies stated hurricane could be another important factor for sediment infilling dredge pits (Byrnes et al. 2004a, Kennedy et al. 2009). Kennedy et al. (2009) studied hurricane response

of nearshore borrow pit with smaller volumes such as in Boca Raton, Palm Beach, Fort Myers Beach, Panama City Beach and John's Pass in Florida. Two bathymetry surveys before and after hurricanes in 2005 indicated groups of pits captured volumes were the equivalent of up to four years of net longshore transport during hurricane seasons. These sandy dredge pits such as Corson Inlet (NJ), and Palm Beach (FL) had the highest sediment infilling rate with the relatively higher wave height or current velocity, which were likely the sediments brought by tropical cyclones and hurricanes (Kennedy et al. 2009). Although two hurricanes passed the Louisiana shelf in 2017-2018, the distance between hurricane landfalls and Caminada dredge pit was very far (>X km; Fig. A2). These hurricanes' impacts are likely to be small on Caminada dredge pit and are beyond the scope of this study.

Sources of infilling sediment in Caminada pit are mainly derived from (1) far-field river plume suspended sediments (e.g., from the Atchafalaya and Mississippi Rivers), (2) local sandy sediments under the impact of current and wave resuspension, (3) pit wall failure materials, and (4) hurricane or tropical storms. Caminada pit is in a unique depositional environment because of the interesting mixture of local sand with episodic mud bypassing the Ship Shoal. Caminada pit was dredged in the sand-dominated condition, where the infilling rate is significantly less than the prediction of Nairn et al. (2005). Because mud is useful for marsh restoration but is not considered a quality sediment resource for barrier island restoration, the infilling sediment of Caminada pit is not a renewable resource for the high-quality sand needed. Our findings indicate that it will take a long time to fill up Caminada pit. However, time-series geophysical, hydrodynamics and physical data should be collected so that we can better evaluate whether dredging activities in sandy dredge pits, such as in SSBA, are cost-effective and sustainable. Additionally, the quantity of sand available for restoration is drastically reduced due to setback

buffer distance required by regulatory agencies for subsea oil and gas infrastructures and cultural concerns over dredging in these shoals. Relatively small outer migrations (<1 m) of Caminada's walls indicate the current setback buffer distances of ~300 m from planned pipelines are sufficient. Our results will increase the government's decision-making ability regarding safety and protecting environmental and cultural resources and provide for better management of valuable sand resources in Caminada pit.

2.6 Conclusion

The sand volume of Caminada dredge pit in Ship Shoal is one of the largest in East and Gulf Coasts of the USA. The integration of repeat bathymetric and backscatter surveys in ~2 years following the dredging allowed for geomorphic analysis of pit evolution, which was characterized by patchy mud deposition inside Caminada dredge pit. Our conclusions are as follows:

(1) DOD maps of three post-dredging surveys indicated that nearly no new net sediments deposited outside pit but new sediment was deposited inside Caminada pit. Post-dredging volumetric analysis indicated that Caminada is presently infilling at an average rate of approximately 0.15 m/year, or 27,480 m^3/year.

(2) The topography of seafloor inside pit has a direct relationship with the patchy mud distribution. Side-scan mosaic maps showed topographic lows, or troughs, inside Caminada infilled with mud within two years after dredging. The seafloor inside Caminada pit became smoother and flatter with sediment infilling. Pit walls became gentler in two years after dredging, indicating slope failure also supplied some sediment (sand) to the pit. Relatively small outer migrations of Caminada's walls indicate the current setback buffer distances of ~300 m from planned pipelines are sufficient.

(3) The sediment infilling rate in Caminada dredge pit, like many dredge pits nationwide, is strongly impacted and controlled by sediment availability. In the case of Caminada pit, this is under the combined controls of the supply of far-field river plume suspended sediments, the erosion of the adjacent seabed sediment by waves and currents, the sediments filling in the pit produced by wall failure, as well as the sediments brought by the hurricane and tropical storms.

CHAPTER 3. SEDIMENT INFILLING AND GEOMORPHOLOGICAL CHANGE OF A MUD-CAPPED DREDGE PIT COMPARED TO A SANDY DREDGE PIT, SHIP SHOAL, LA

3.1 Introduction

Barrier islands are critical sedimentary environments because they serve as buffers to coastal areas during storms. It was reported that the barrier islands in southern coastal Louisiana have been experiencing the highest rates of land loss (Allison et al. 2014). Louisiana has suffered 90% of the total coastal wetland loss in the continental United States, and land loss between 1932 and 2010 was estimated to be 4877 km^2 (Couvillion et al. 2011). In recent years cumulative wetland loss in Louisiana has continued at a lesser but still significant rate of ~25 km^2/yr (Couvillion et al. 2017). A major component of the State of Louisiana's effort to manage coastal land loss is to restore degraded barrier shorelines by dredging sand resources from borrow sites for the replenishment of these coastal sedimentary environments (CEC,2017). With the implementation of barrier island restoration projects in Louisiana since the early 1990s, many of the nearshore sand sources have already been used, and beach-compatible sediment has become increasingly scarce and expensive (CEC,2017). Offshore sand environments provide an alternative resource.

The seabed of the continental shelf off the coast of Louisiana is mainly capped by a layer of mud, but a few sandy shoal environments exist (Stone et al. 2004). At present, one type of offshore sand resource on the Louisiana shelf is submarine sandy shoals, which include Ship Shoal, Tiger and Trinity Shoals, and Sabine Bank (Dubois et al. 2009). Caminada (volume: 9.1×10^6 m^3) and Block 88 (3.1×10^6 m^3) dredge pits are two of the largest dredge pits located on Ship Shoal, a sandy shoal located 15 km offshore of Isles Dernieres, central Louisiana. Liu et al. (2017) found muddy sediments were transported into sandy Caminada pit and deposited in

heterogeneous patches within two years after dredging. Xue et al. (2017) found at least a portion of the mud in the muddy sediments from Caminada dredge pit was derived from river plumes and deposited within ~6 months based on the presence of beryllium-7 (^{7}Be) radioisotope activity ($T^{1/2}$ = 53 days). Liu et al. (2019) applied multiple machine learning classifiers to identify the sediment types and found mud was prone to deposit in the trough zones with lower backscatter values in Caminada pit near Ship Shoal. Moran et al. (2019) collected the bathymetry and side-scan data in Block 88 pit. They found the steepest slopes were mainly at pit walls, and biogenic gas were found above low reflectivity sediment inside the pit.

An alternative type of offshore sandy resource for barrier island restoration in Louisiana is sandy paleo-channels. Unlike sandy shoals, excavating sand from paleo-channels in the Gulf of Mexico requires the removal of mud overburden formed by modern sediment transport processes (Nairn et al. 2005; Xu et al. 2016; Obelcz et al. 2016; Xu et al. 2018). Dredging in such an environment will create 'mud-capped dredge pits' (MCDPs), which are expected to evolve differently than their pure-sand counterparts. Peveto Channel, Raccoon Island, and Sandy Point dredge pits are three MCDPs located in western, middle and eastern Louisiana shelf, respectively, and they were dredged in 2003, 2013 and 2012, respectively (Xu et al. 2018). Obelcz et al. (2018) studied the mud-capped dredge pit of Sandy Point (northwest of the modern Mississippi River Delta). They found the infilling rate (~200,000 m^3/year) was higher than dredge pits in the sandy substrate, sediment-starved settings in East Coast of USA. Robichaux et al. (2020) reported nonlinear accumulation rate and continuing degassing and consolidation even after 100% sediment infilling at Peveto Channel dredge pit in the western Louisiana shelf.

Two areas of our study are Caminada and Raccoon Island pits. Previous geological and geophysical results of Caminada pit were published in Liu et al. (2020 and under review). New

results of Raccoon Island pit will be presented in this paper. Caminada pit was dredged in 2016 in a sandy submarine shoal environment on the inner Louisiana continental shelf that was used for the restoration of Caminada Headland. Raccoon Island pit was excavated in 2013 from a paleo-river valley north of Ship Shoal for the restoration of Raccoon Island of Louisiana. However, our knowledge of the similarities and differences of the sediment process and their influences on the morphologic evolution is still limited. Thus, the objective of this research is to study geomorphologic response within two contrasting dredge pits on the continental shelf offshore Louisiana: in a paleo-channel and a sandy shoal. Specifically, this study strives to: (1) quantify the pit geomorphic evolution including infilling rate and wall slope in Raccoon Island dredge pit; (2) characterize and observe the geomorphic control on mud distribution inside Caminada and Raccoon Island dredge pits; (3) compare the physical and geological processes impacting Caminada dredge pit and Raccoon Island pit. This study will also discuss the implications of dredging activities to morphology and benthic community, and provide recommendations for future coastal restoration, dredge site selections, sand resource management.

3.2. Geological setting

3.2.1 Racoon Island dredge pit in a paleo-channel

The Isle Dernieres barrier shoreline is a barrier island arc 22.0 miles long in Terrebonne Parish of Louisiana (Penland et al. 2005). The Isle Dernieres arc is part of the Lafourche deltaic complex formed as a result of the abandonment of the Caillou Headland approximately 500 years ago (Penland and Boyd, 1986). Raccoon Island is the western-most island in the Isles Dernieres chain, which is located approximately 50 miles south of Houma, Louisiana (Fig. 3.1). A long narrow dredge pit located north of Ship Shoal was excavated, and the sandy sediments inside the

paleo-channel were excavated and transported to Raccoon Island in 2013 (Fig. 3.1.B). Paleo-channels for Raccoon Island dredge pit were the stratigraphic remnants of ancient courses of the Mississippi River and its distributaries (Connor, 2017). Raccoon Island pit is located in a slight topographic low, very similar to a 'trough' (6.2 m deep and 100 m wide), between Ship Shoal and Isle Dernieres.

3.2.2 Caminada dredge pit in a sandy shoal

Ship Shoal is considered to be the final phase of Maringouin delta, which was active 7500- 5000 years BP (Penland et al. 1986). The morphology of Ship Shoal is the product of a process combining relative sea-level rise with regressive (delta building) sequences, and transgressive (delta abandoning) sequences of the Mississippi River (Penland et al. 1986). Short periods of rapid relative sea-level rise led to the transgressive submergence of shorelines, which today can be recognized at the 10 m to -20 m isobaths on the Louisiana continental shelf. Ship Shoal makes up the -10 m late Holocene shoreline trend and overlies a deltaic headland, which offset to the east. The Caminada Headland is the modern Gulf of Mexico shoreline that spans from Belle Pass on the west to Caminada Pass on the east, a distance of approximately 21.4 km (Fig. 3.1.A). Since 2014, the Caminada Headland Beach and Dune Restoration Projects (BA-45 & BA-143) were the first to use sand resources from the Ship Shoal area for barrier island restoration since 2014 (CEC, 2017). Ship Shoal is comprised of well-sorted, clean quartz sand, where the median grain diameter on the crest of Ship Shoal ranges from 2.73 - 3.20 phi (0.1 - 0.15mm) (Nairn et al. 2005). It is estimated to have 1.2 billion cubic meters of potential high-quality quartz sand (Kobashi et al. 2007). Ship Shoal has been a high-priority target sand resource to restore the Isles Dernieres barrier chain, Caminada-Moreau headland, and Timbalier Islands system, all of which are among the high-barrier-island-loss regions in Louisiana (e.g.,

Drucker et al. 2004; Penland et al. 2005; Khalil et al. 2007; Williams et al. 2012). Sand dredging in Caminada pit comprised of two increments, I and II, during which a total volume of $9.1x10^6$ m^3 of sand was excavated from December 2014 to October 2016 based on pre- and post-construction surveys (CEC, 2017).

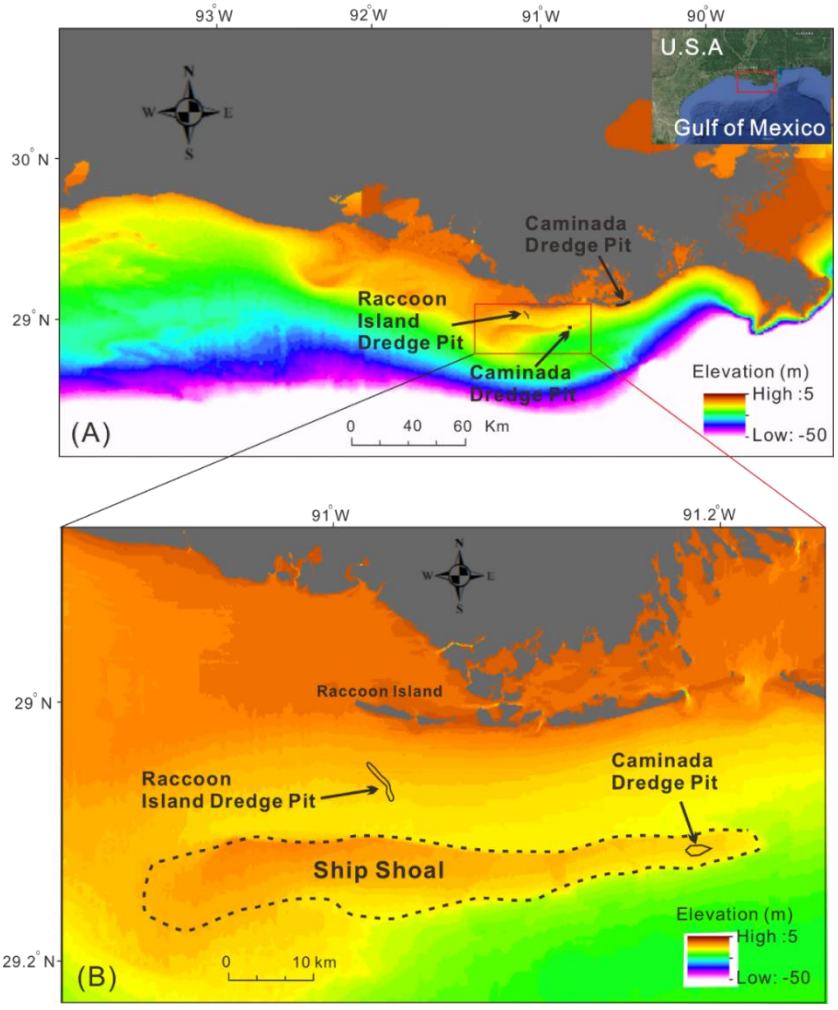

Figure 3.1. (A) and (B) Locations of Ship Shoal, and Raccoon Island and Caminada dredge pits on the south-central Louisiana continental shelf. The elevation map is extracted from ETOP1 (NOAA), which used WGS 84 as the horizontal datum and sea level as the vertical datum. The black dashed line in (B) is the 6m isobath for Ship Shoal.

3.3 Data and Methods

Interferometric swath bathymetry and side-scan sonar imaging were used to quantify the seafloor morphology, topography, and evolution of the Caminada pit and Raccoon Island pit.

Bathymetric data from three post-dredging surveys (2013, 2015, and 2018) were utilized and processed in CARIS HIPS and SIPS v.11.2. Bathymetric data were applied a tidal correction, sound velocity profiles, patch tests, and using filtering. These data were then exported to ArcMap 10.2 for generating Digital Elevation Models (DEMs), Difference of Depth maps (DODs), and gradient maps. The vertical bathymetry control was referenced to, and verified by, NOAA Texas Gas Platform, Caillou Bay, Louisiana (Station ID: 8763535). Slope calculations were performed using the DEM Surface Tools following the method of the Arc-Chord Ratio (Du Preez et al. 2015). Side-scan mosaics were also generated in HIPS and SIPS and then exported in ArcMap to identify the reflectivity change of seabed inside the dredge pit. Reference uncertainty for DEMs and DODs in the different bathymetric dataset was quantified by the fixed-point method of Schimel et al. (2015).

3.4 Results

3.4.1 Sediment infilling inside Raccoon Island pit

Repeat bathymetric maps in 2013 and 2015 showed different morphology of the pit walls and the depth of shoaling inside Raccoon Island pit over these two years. As of March 2013 (two months after dredging activities), the pit depth was approximately 13.5 m below sea level, compared to the ~8 m depth of the surrounding undisturbed seafloor (Fig. 3.2.A). As of June 2015, the average depth was 11.5 m (Fig. 3.2.B). DOD maps of these two post-dredging surveys revealed that nearly no new sediment deposited outside pit (less than 2σ range in uncertainty) but there existed ~2 m of new sediments filling the pit (Fig. 3.2.C). Morphological evidence for three pit-wall-failure zones was found in the western wall margin (See red dots in Fig. 3.2.C). The pit was filled up by our 2018 survey (Fig. 3.3.). We calculate the average infilling rate in Raccoon

Island pit from repeat bathymetric surveys were about 1.1 m/year (2013-2015) and at least 1.4 m/year (2015-2018).

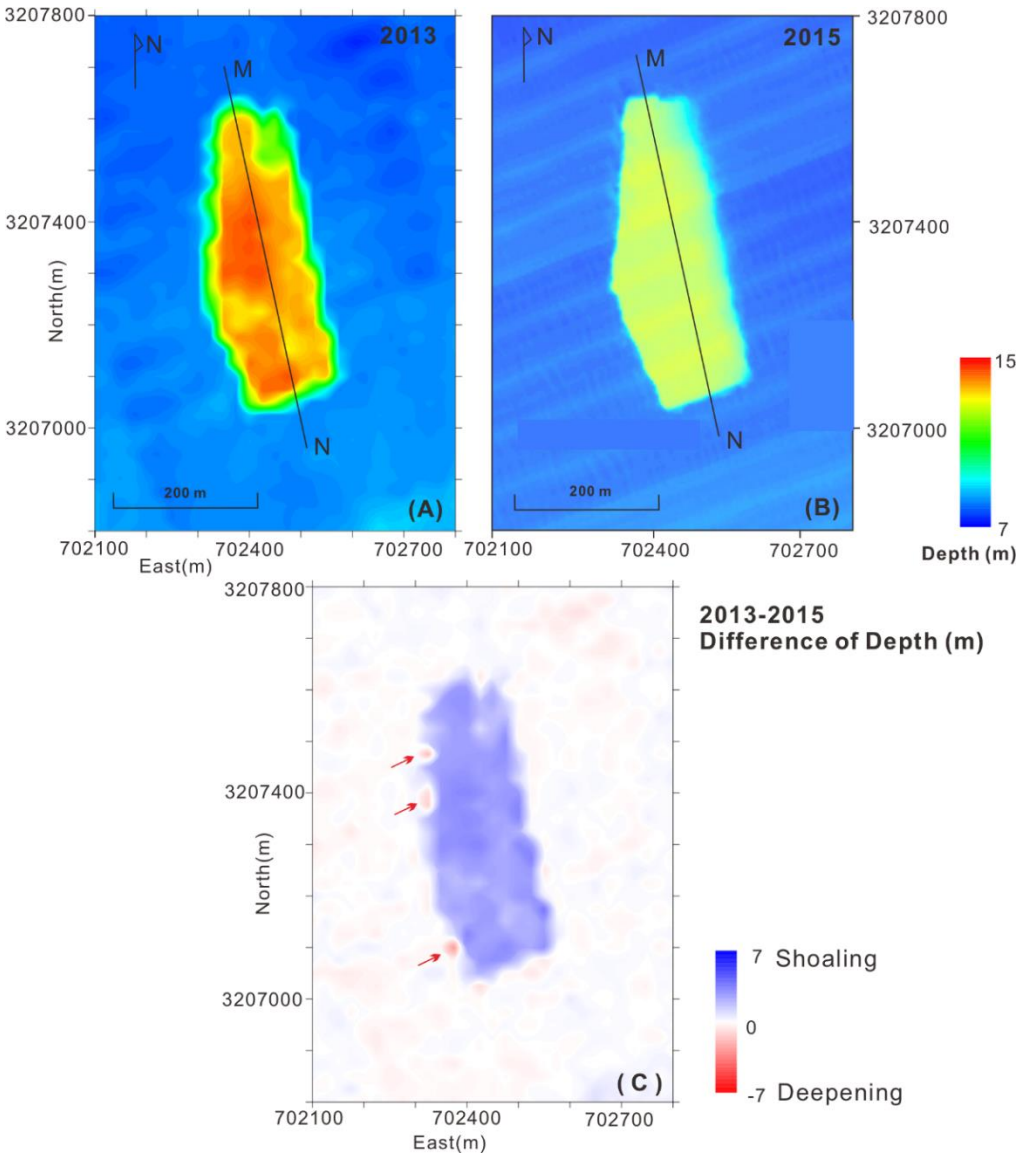

Figure 3.2. (A) and (B) Bathymetry map from two surveys (03/2013 and 06/2015) in Raccoon Island dredge pit. The depth value is positive with a unit of meter. MN shows the location of transect in Fig 3. (C) Difference of depth between 2013 and 2015 surveys. Values within the 2σ range of uncertainty (0.3 m) are generally in beige and considered no significant depth change. The coordinate system is UTM 15N zone.

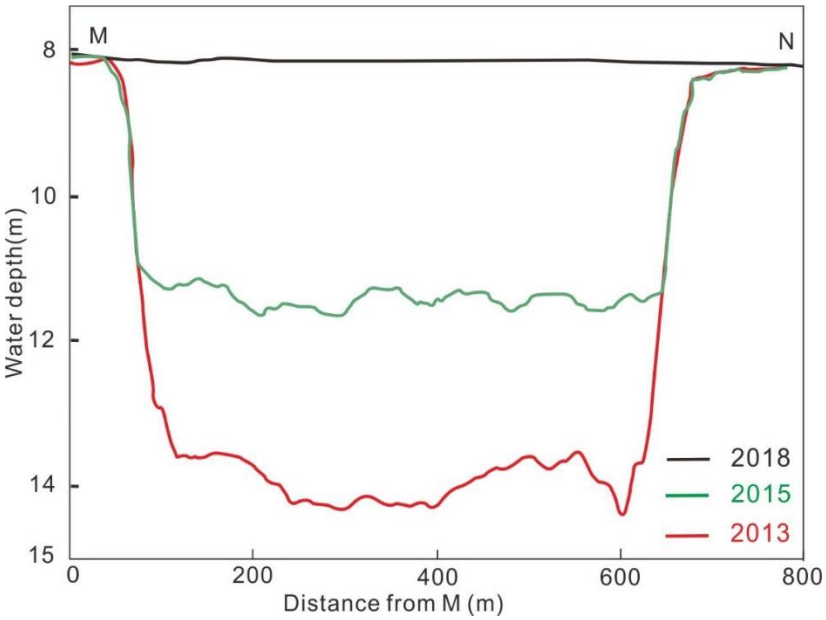

Figure 3.3. Bathymetric profiles of 2013, 2015, and 2018 along the transect MN (see location in Fig.2). The average sediment deposition rate increases from 1.1 m/year in 2013-2015 to ≥1.4 m/year between 2015-2018.

3.4.2 Geomorphology change

Between the 2013 and 2015 surveys, the seafloor of the Raccoon Island pit became smoother and flatter with sediment infilling the pit (Fig. 3.4.). All pit walls lost some steepness in the first two years after dredging. Morphological evidence for localized failure was mainly on the pit walls, particularly in the western wall (Fig. 3.2.C & 3.4.B). From 2013 to 2015, the pit wall slope decreased from 14.2-15 to 7.5-8.2 degrees (i.e., became gentler; Figs 3 & 4). Western wall in Raccoon Island pit was steeper than the eastern wall in 2013 and 2015 (Fig. 3.4.). The pit wall shows no obvious outward migrations from 2013 to 2015 (Fig. 3.3. & 3.4.).

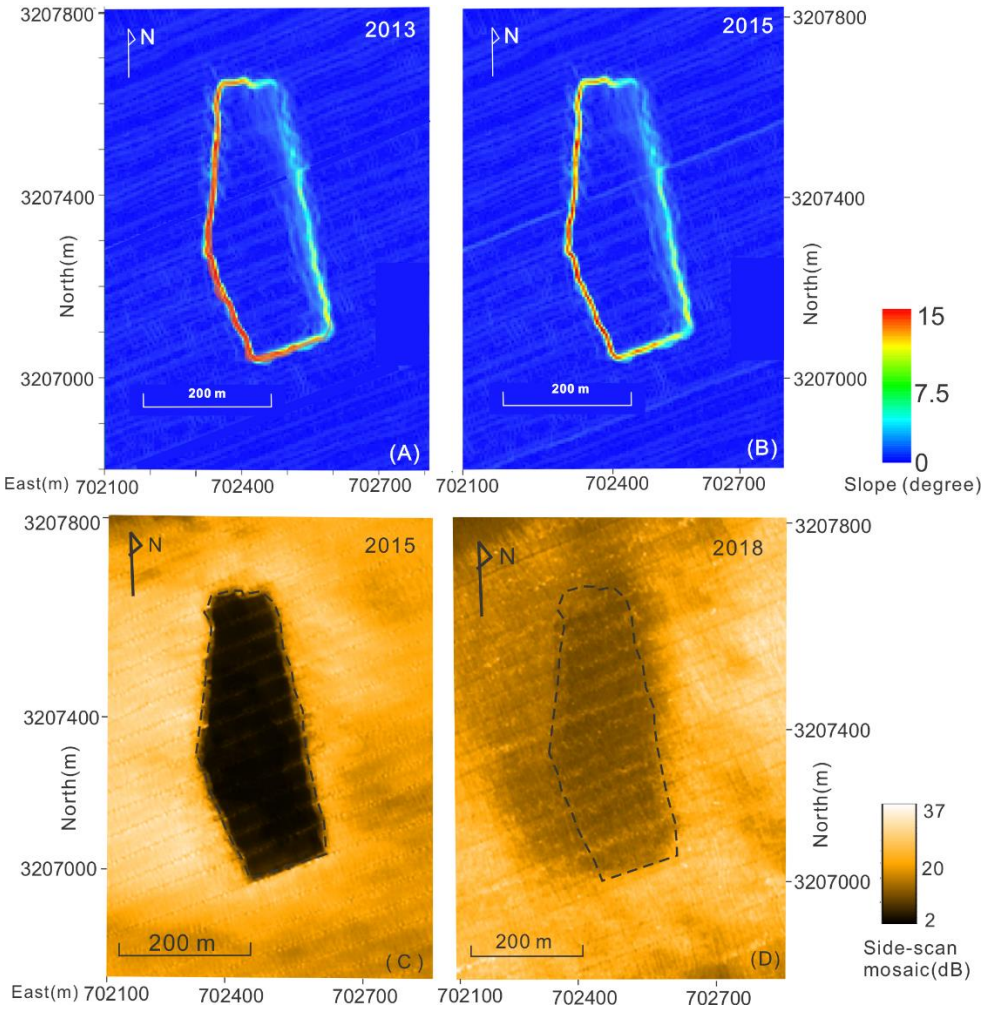

Figure 3.4. (A)(B) Gradient map of the Raccoon Island dredge pit derived from 2013 and 2015 bathymetry. Blue colors represent flatter surfaces, while red colors indicate steeper surfaces. (C)(D) Side-scan mosaic maps of Raccoon Island pit for two post-dredging surveys in 2015 and 2018. Side-scan mosaic reflected the difference in backscatter values in the unit of dB (Decibel). The dashed black line is the pit margin of the side-scan map in 2015, which is used as the reference borderline in other maps.

A side-scan mosaic map in the 2015 survey showed dark zones inside the pit with low backscatter values where bathymetry shows the depth is deep compared to outside the pit (Fig. 3.4.C). The 2018 survey map similarly showed lower backscatter value inside the pit but of lesser magnitude in 2015 (Fig. 3.4.D). There were also relatively low backscatter values observed in an area northwest and outside of the pit (Fig. 3.4.D). Sub-bottom seismic profiles show Raccoon Island dredge pit was dredged in a paleochannel, which can be seen bounded by

strong reflectors in Figure 5. Seismic profiles in 2015 and 2018 show a different reflection character for the sediment deposited in the pit. In particular, biogenic gas (degassing) was found in both infilling sediment and the water column in the 2015 and 2018 profiles (Fig. 3.5.B &3.5.C).

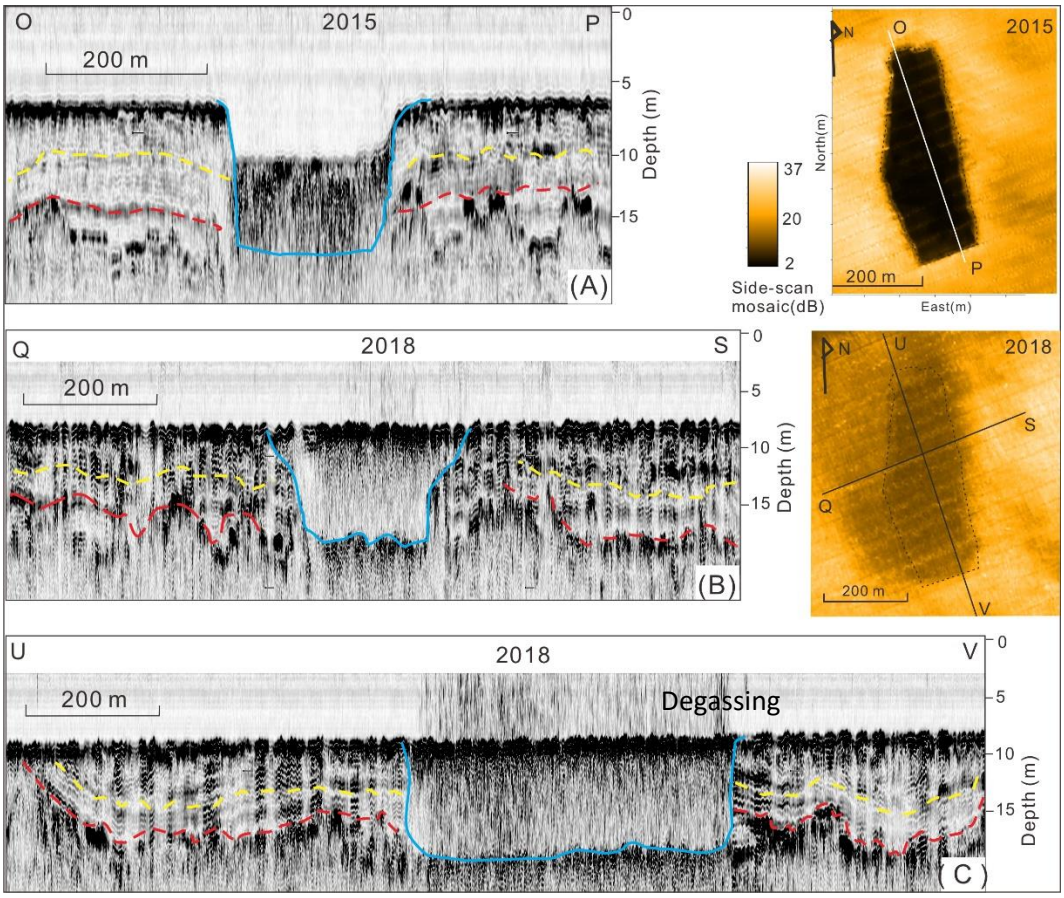

Figure 3.5. (A), (B) and (C). Sub-bottom seismic profiles collected across Raccoon Island dredge pit in 2015 and 2018. The blue lines delineate the bottom boundary of the pit. Two boundaries of paleo-channels are marked in red and yellow color. (A) and (C) are along the same surveying line but in different years and different lengths.

3.5. Discussions

3.5.1 Factors controlling sediment infilling in Raccoon Island pit

Raccoon Island pit is likely under the combined influence of the dynamic Atchafalaya and Mississippi river dispersal systems, wind-driven currents, pit wall failure, storm waves, and others. The suspended sediment load in the Mississippi and Atchafalaya Rivers is approximately

90% mud and 10% sand (Nittrouer, et al. 2008). Previous studies (e.g., Walker et al. 2005; Kobashi et al. 2009; Xu et al. 2011) found that suspended sediment from Atchafalaya River (i.e., buoyant hypopycnal plume) often shifts in the direction from westward to southeastward during high river discharges and strong northwest winds. An earlier study by Connor (2017) found the coring site outside Raccoon Island pit contained no ^{7}Be, indicating that river sediment does not normally accumulate on the seabed outside the pit (i.e., if it is deposited, it is removed quickly and transported elsewhere on the continental shelf). However, dating of ^{7}Be radioisotope activity in the muddy sediments collected inside Raccoon Island pit indicates a significant portion of the mud was derived from fluvial sources and deposited within ~6 months before core collection (Connor, 2017). It indicates that sediments from Mississippi and Atchafalaya Rivers are contributors of at least a fraction of the sediment delivered to and deposited in Raccoon Island dredge pit (Fig. 3.6.). Otherwise, previous studies show the fine riverine sediment contributes to the deltaic wetlands such as Breton Sound (Wang et al. 2019), and Barataria Bay (Wilson et al. 2008; Li et al. in prep). The mud around on the shelf and eroded from nearby coastal marshes that could be resuspended and supply sediments to the pit.

Wind forcing, a pivotal contributor to buoyant plumes from the Mississippi and Atchafalaya Rivers, exhibits energetic seasonal patterns, which have been observed during a variety of discharge and wind combinations using satellite imagery (Walker & Hammack, 2000; Walker et al. 2005). A combination of high discharge and strong easterly winds could result in the most extensive hypopycnal plume area to central Louisiana, including the Ship Shoal area (see Fig. 3.6. for an example; Walker et al. 2005). The western portion of the Mississippi River plume can travel up to 1000 km to the west, ultimately joining the Atchafalaya plume (Dinnel & Wiseman, 1986; Murray, 1998) when persistent easterly winds create steady longshore currents

(Murray, 1998). Kobashi et al. (2007) conclude that during fair weather, a dense benthic mud layer originating from the Atchafalaya river is deposited, later resuspended and mixed during winter and spring storm passage. He estimates the consolidated mud layer is between 10 and 15 cm thick (Kobashi et al. 2007). However, coring samples collection by Allison et al. (2000) found no modern sedimentary record near Ship Shoal, indicating that the benthic mud layer is ephemeral and episodic, and too frequently resuspended by the passage of cold fronts to consolidate into hard mud (Allison, et al. 2000; Kobashi et al. 2007).

The sediment infilling Raccoon Island pit is also impacted by the erosion/deposition of the adjacent seafloor sediment triggered by waves and currents. The DODs map of 2013 and 2015 surveys showed erosion in the western wall margin (Fig. 3.2.C). The erodible materials produced by local wall failure could contribute to the sediment infillings. The gradient of the pit wall became gentler from 2013 to 2015 (Fig. 3.4.), which indicated the sediment near the pit margin could be transported into the pit.

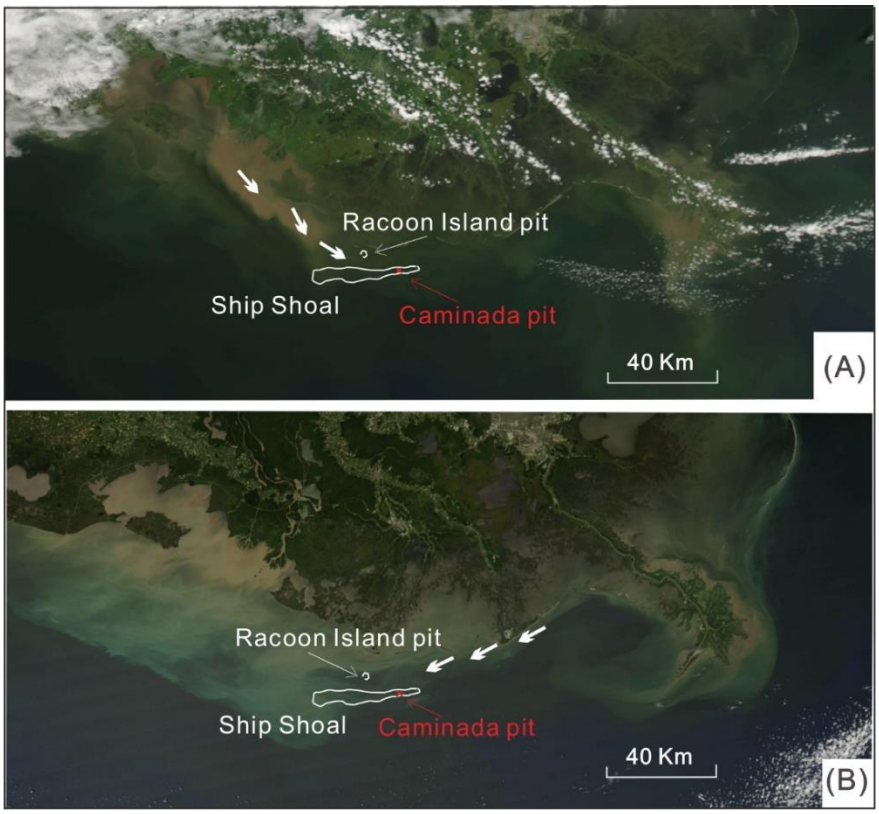

Figure 3.6. Buoyant plumes from the Mississippi and Atchafalaya Rivers to Raccoon Island pit and Caminada pit near Ship Shoal in 2017. (A) July 25, 2017, and (B) Sep 08, 2017.

According to a previous model of pit sedimentation, the sediment infilling process should slow down over a 5-20 year time frame (Nairn, 2005). However, the infilling rate in Raccoon Island pit displayed a surprising trend. The average sediment infilling rate in Raccoon Island pit was 1.1 m/year from 2013 to 2015 but increased to 1.4 m/year from 2015 to 2018 (Fig. 3.2.&3.3.). The rate of 1.4 m/year is a conservative estimate because Raccoon Island pit could have been 100% filled up several months before our survey in 2018. One possible reason is extreme episodic events, such as hurricane and tropical storms affect the sediment infilling rate in Raccoon Island pit. There were three hurricanes and one tropical storm during our study period (2013-2018) passing Raccoon Island pit within a 200 km range: Tropical storm Karen in 2013, as well as hurricanes Nate, Cindy and Harvey in 2017, passed within a distance of 100 - 200 km of Ship Shoal and the dredge pits (Fig. 3.7.). Hurricane Harvey weakened to a tropical

storm when it made landfall near the Texas-Louisiana border. Tropical storm Karen similarly weakened before landfall and became a depression while centered about 140 mi southwest of New Orleans. These episodic extreme events all could move sediments to Raccoon Island pit and contribute to the fast sediment infilling during 2015-2018.

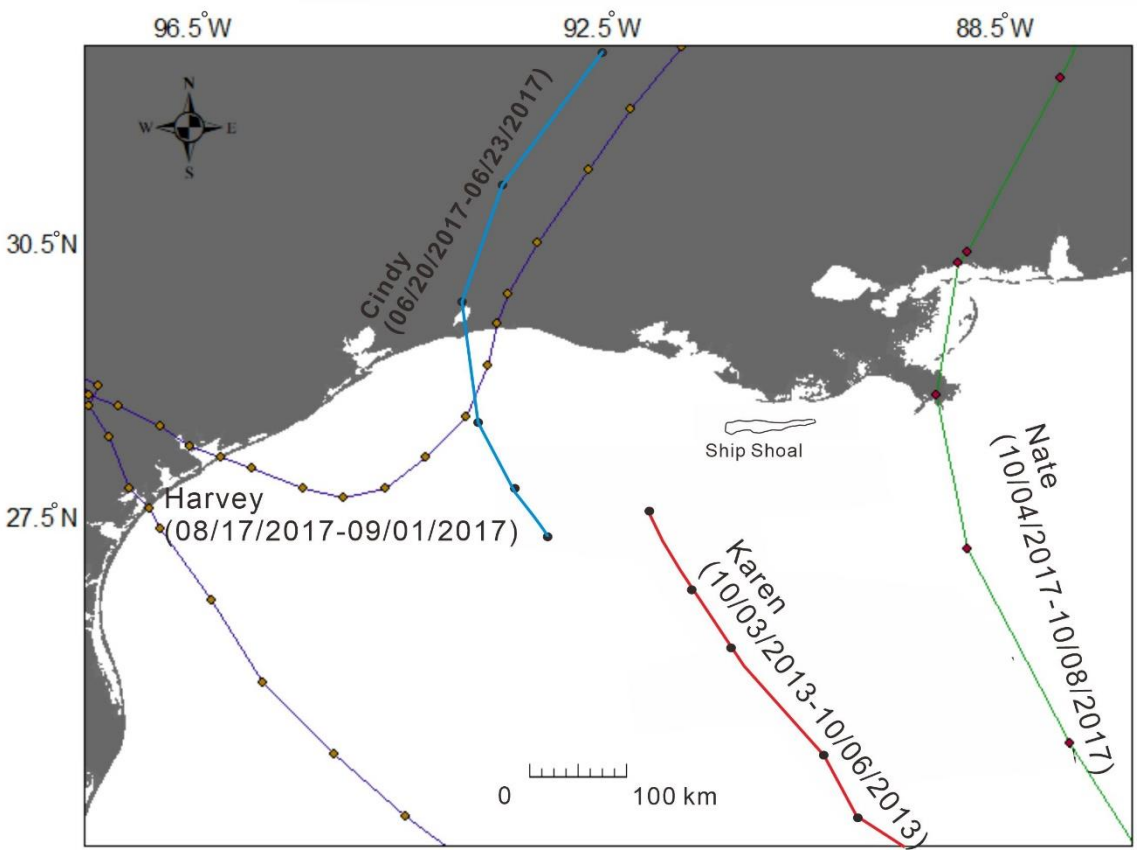

Figure 3.7. Hurricane and tropical storms track from 2013 to 2018 near Ship shoal (within 200 km). Data of tracks of Tropical Storm Karen, and Hurricanes Harvey, Cindy, and Nate downloaded from NOAA national hurricane center(https://www.nhc.noaa.gov/).

3.5.2 Comparison of mud-capped Raccoon Island dredge pit with sandy shoal Caminada dredge pit

Caminada pit can be compared with Raccoon Island pit in geometry, infilling sediment source, and controlling factors (Table 3.1.). Caminada pit was dredged in 2016 with the sand volume of 9.1×10^6 m^3, while the Raccoon Island pit was dredged in 2013 with a much smaller volume of 0.2×10^6 m^3. Caminada pit was dredged in a sandy shoal, where the pit wall was sandy sediment. However, Raccoon Island pit was dredged in a paleo-channel system, where the pit

wall was mainly overburdened mud mixed with sand. The pit wall slope decreased on average 2.3 degrees in Caminada pit within two years, but it dropped averagely 6.8 degrees in Raccoon Island pit within two years. This indicates pit wall erosion and pit wall failure happened in a muddy paleo-channel environment.

Table 3.1. Comparison of Caminada pit with Raccoon Island pit

	Feature	Caminada Pit	Raccoon Island Pit
Study period	Dredging year	2016	2013
	Study period (Month/Year)	07/2017-08/2018	03/2013-08/2018
Pit geometry	Ambient seafloor water depth (m)	12	8
	Sand Volume (10^6 m^3)	9.1	0.2
	Pit margin slope change (degree)	3.3-6.6 (2017) to 1.7-3.6 (2018)	14.2-15(2013) to 7.5-8.2 (2015)
Sediment infilling process	Sediment infilling rate (m/year)	0.15	1.1
	Physical setting	Sandy in sandy shoal	Muddy in paleo-channel
	Infilling material	Mud with few local sand	Mud

Previous studies of Stone et al. (2009) and Kobashi (2009) reported that sediment transport processes on Ship Shoal include contrasting non-cohesive sand and cohesive mud transport. Muds from the Atchafalaya Bay can be delivered to Ship Shoal area and then resuspended and transported elsewhere. As mentioned previously, the transient mud is likely one of the sediment sources to both Raccoon Island pit and Caminada pit (Xue et al. 2017; Liu et al. 2018). Connor (2017) found that ^{7}Be profiles from Raccoon Island accumulation rates exceeded an average of .24 cm/day and that multicores within pit contained almost entirely silt. The sediment infilling rate in these two pits was different, in which Caminada was with a relatively slow rate of 0.15 m/year, but Raccoon island showed a much higher rate of 1.1 m/year. Based on previous coring samples inside two pits, Caminada pit was mainly filled with mud from fluvial sources and

minor quantities of sand from seafloor outside the pit (Xue et al. 2019). However, Raccoon Island pit was filled up only with mud (Connor,2017).

3.5.3 Implication and broader impact

Ribberink (2005) and Nairn (2005) applied the 1D analytical approach and modeled the evolution of a proposed dredge pit near Ship Shoal (see location in Fig. 3.1.B). They included the empirical coefficients, settling velocity of mud, water depth of inside and outside the pit, background concentration, and tidal period. However, these authors did not consider wave resuspension, episodic extreme hurricane, and other tropical events, which this paper is essential in the previous discussion. We applied Nairn's model and compared modeling results with the observed infilling percentages in the first two years after dredging. Narin's modeling infilling percentage (~75%) is much higher than what was observed in Caminada pit (~10%) (Fig. 3.8.). The infilling rate in Raccoon Island pit, however, was over-estimated in the first two years and then under-estimated by Nairn's model (Fig. 3.8.). It is well known that sediment concentration rate and sediment setting velocity can change with the time and evolution of the dredge pit. In future work, the seasonal change of sediment plume from rivers, current, and wind, the episodic extreme events, such as hurricane and tropical storms, should be included when predicting the sediment infilling rate.

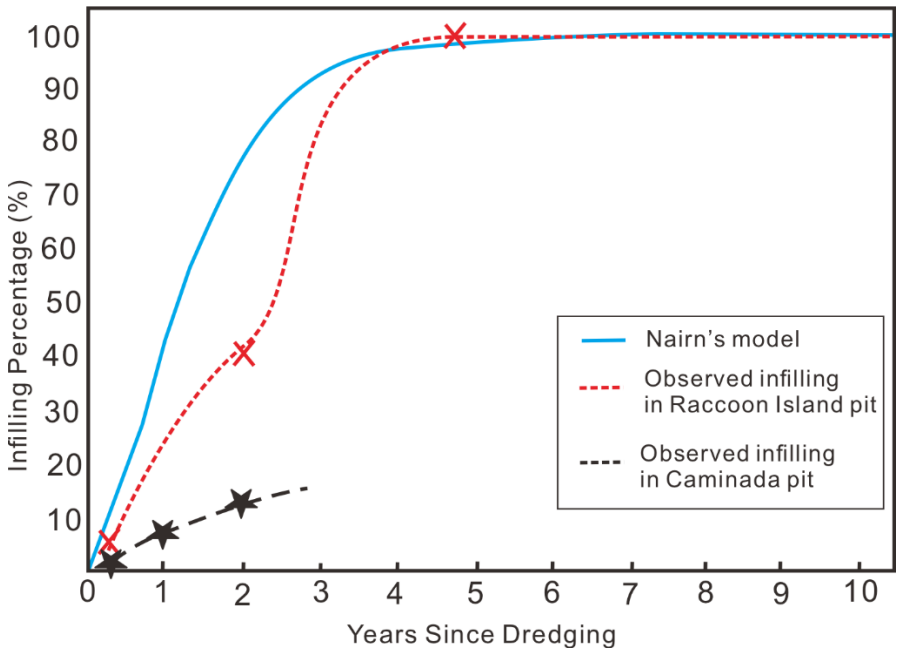

Figure 3.8. Observed infilling volume in Caminada and Raccoon Island pits over time and comparison with Nairn's model in a proposed Block 88 pit. Volumetric calculations for our surveys with uncertainty were made using the Cut-Fill tool in ArcMap. Stars and crosses are observational dada for Caminada and Raccoon Island pits, respectively.

When comparing muddy-capped dredge pits in Louisiana with sandy dredge pits, sandy pits have a relatively low sediment infilling rate in the first five years after dredging (~0.15 m/year at Caminada compared to muddy pits: Raccoon Island (~1.10 m/year), Peveto Channel (≥2.00 m/year; Robichaux, 2020), and Sandy Point (≥0.54 m/year; Obelcz et al. 2018). Proximity to mobile sediment sources appears to be necessary, as all of the muddy pits studied to date are relatively close to major rivers (Obelcz et al. 2018; Robichaux, 2020). The infilling rate between Caminada and Raccoon Island pits showed a noticeable difference (Fig. 3.8.). One possible reason is the topography of seafloor could control the sediment infilling rate. Fig. 1B shows that Caminada is in the east end of Ship Shoal, which is near the eastern shoal crest. The high elevation of eastern shoal crest makes it challenging to transport sandy sediment westward (thus upslope). However, Raccoon Island pit is located within a topographic low between Ship Shoal and Isle Dernieres, where facilitates downslope transport and traps sediments. Thus future

dredging activities may consider choosing topography lows which can facilitate rapid sediment infilling.

Previous studies discussed the geological, physical, and ecological effects of dredging activities on the seafloor and nearby environments. Dredging can change the benthic community drastically, resulting in lower benthic abundance, biomass, and diversity that persists for years (Palmer et al. 2008). Desprez (2000) explored the physical and biological impact of marine aggregate extraction along the French coast of the Eastern English Channel and found the effect of overflowing sands on benthic macrofauna in the surrounding deposition area proved equally significant as in the dredged area. Boyd et al. (2003) found sediments from the southeast coast of England exposed to the highest dredging intensity contained proportionally more sand than other sampled sediments. Multivariate analyses indicated a strong relationship between macrofaunal community structure and dredging intensity at this site. Yozzo et al. (2004) proposed beneficial projects which included the use of dredged material for the construction of artificial reefs, oyster reef restoration, intertidal wetland, and mudflat creation, bathymetric recontouring, filling dead-end canals/basins, creation of bird/wildlife islands, and landfill/brownfields reclamation. Newell et al. (2004) did a survey of benthic macrofauna in the vicinity of a coastal marine aggregate dredging site off the south coast of the UK. They found trailer dredging had no impact on the community composition of macrofauna within the dredge site. Spebroeck et al. (2006) suggested to choose nourishment sands with a sediment composition comparable to the natural sediments and avoid short-term compaction by ploughing immediately after construction due to ecological consideration. Bayraktarov et al. (2016) performed a synthesis of 235 studies with 954 observations from restoration or rehabilitation projects of coral reefs, seagrass, mangroves, saltmarshes, and oyster reefs worldwide. They found coral reefs and seagrass were among the

most expensive ecosystems to restore. Even though Raccoon Island pit is filled up, the low backscatter on the surface of infilling sediment indicates possible finer texture, low porosity, and higher organic matter (Fig. 3.4.). Thus it is likely that the benthic community in Raccoon Island pit has not reached an equilibrium with ambient seafloor yet.

Syed et al. (2018) summarized the availability of sediment resources for the ecosystem restoration of coastal Louisiana. They found the quantity of sediment resources available for critical restoration projects is likely to decrease. Sandy shoals (such as Ship Shoal pits) are prominent and high-quality sand sources off the Louisiana coast. Still, the transportation distance between the dredging pit to the restoration site makes it not cost-effective. Instead, borrowing sand from abandoned paleo-channels (such as Raccoon Island pit) provides an alternative and cost-effective method for sandy shoal dredging. Caminada pit is in a unique depositional environment because of the mixture of local sand with episodic mud bypassing the Ship Shoal. Raccoon Island dredge pit also is in a mixed environment in which the pit was filled with mud. Mud is useful for marsh restoration but is not considered a quality sediment resource for barrier island restoration. Xue et al. (2019) found that the Caminada sandy dredge pit is not a renewable resource for the high-quality sand needed in future barrier island restoration; we similarly find here that muddy dredge pits like Raccoon Island pit are not renewable resources either.

Additionally, the quantity of sand available for restoration is drastically reduced due to safety buffer requirements by regulatory agencies for subsea oil and gas infrastructures and cultural concerns over dredging in these shoals. Relatively small or no dramatic outer migrations (<1 m) of Caminada's and Raccoon Island's walls indicate the current setback buffer distances of ~300 m from planned pipelines are sufficient. However, the degassing of the mud infilling sediment in Raccoon Island pit indicates it is still under the consolidation process (Fig. 3.5.C),

which is not a safe zone for the construction of new oil and gas pipelines. Our results could increase the government's decision-making ability regarding safety and protecting environmental resources and provide for better management of valuable sand resources in the Caminada pit and Raccoon Island pit.

3.6 Conclusion

Raccoon Island dredge pit was excavated from a paleo-river valley north of Ship Shoal for the restoration of Raccoon Island of Louisiana. The integration of repeat bathymetric and side scan surveys in ~5 years following the dredging allowed for a geomorphic analysis of pit evolution and comparison with Caminada pit dredged in a sandy shoal environment. The conclusions are as follows:

(1) DOD maps of three post-dredging surveys (2013, 2015, 2018) revealed that nearly no net new sediment deposited outside pit, but there existed muddy sediments filling in Raccoon Island pit. Three pit-wall-failure zones were found in the western wall of Raccoon Island pit. The average infilling rate in 2013-2015 was about 1.1 m/year. All pit walls lost steepness in the first two years after dredging in Raccoon Island pit, decreasing from 14.2-15 to 7.5-8.2 degrees in 2013-2015.

(2) The infilling rate in Raccoon Island pit (1.10 m/s) was higher than in the Caminada pit (0.15 m/s). Raccoon Island pit was filled up on or before 2018, but Caminada pit is still collecting sediments. Repeat bathymetric surveys showed the pit margin in Raccoon Island and Caminada pits were generally stable with no obvious migration, which indicated the current setback buffer distances of ~300 m from oil and gas pipelines were sufficient.

(3) The sediment infilling process in both Raccoon Island and Caminada pits were likely under the combined influence of wind-driven currents, storm waves, and the dynamic Atchafalaya and Mississippi river dispersal systems.

(4) Sandy shoals (such as Ship Shoal pits) are prominent and high-quality sand sources off the Louisiana coast, but the long transportation distance makes it not cost-effective. Instead, borrowing sand from paleo-channels (such as Raccoon Island pit) provides an alternative and cost-effective method for sandy shoal dredging. Caminada and Raccoon Island pit are not considered as a renewable resource for future restoration due to high mud content. Even after 100% infilling, it will take time for sediment and benthic community to reach a status indistinguishable to ambient seafloor.

CHAPTER 4. SEDIMENT IDENTIFICATION USING MACHINE LEARNING CLASSIFIERS IN A MIXED-TEXTURE DREDGE PIT OF LOUISIANA SHELF FOR COASTAL RESTORATION

4.1. Introduction

Barrier islands protect the wetlands and deltaic plains from meteorological and marine forcings and help stabilize estuarine conditions. Many barrier and deltaic systems, as well as megacities around the world, are under the threat of land loss and rapid relative sea-level rise due to a variety of natural and human activities (Byrnes et al. 2004; Syvitski et al. 2009; Vörösmarty et al. 2009). Dredging has been used in barrier island restoration, beach nourishment, marsh creation, and other coastal protection and restoration projects (Kennedy et al. 2009; CEC,2017; Syed et al. 2018). Sediment has been dredged from multiple types of offshore and onshore borrow sites such as shelves, bays, marshes, river channels, and other sources and delivered to coastal sedimentary environments (CEC, 2017; Syed et al. 2018).

The Louisiana coast has been facing tremendous coastal land loss (~43 km^2 per year since 1985) due to subsidence, levee construction, a shortage of fluvial sediment supply, hurricane landfalls, and other factors (Allison et al. 2014). Although billions of cubic meters of sand are needed for initial and recurring restoration in Louisiana (Stone et al. 2014; Stone et al. 2009; Hanley et al. 2014; Jonah et al. 2015; Brown et al. 2015; Rangel et al. 2015), high-quality sand is largely limited to isolated shoals or paleo river channels on the inner Louisiana shelf. At present, the largest high-quality sand resources on the Louisiana shelf are submarine sandy shoals, such as Ship, Tiger, and Trinity Shoals, and Sabine Bank, as well as some paleochannels (Dubois et al. 2009; Obelcz et al. 2018; Wang et al. 2018; Liu et al. 2017; Xue et al. 2017). These shoals

This chapter was previously published as Liu et al., 2019. Sediment Identification Using Machine Learning Classifiers in a Mixed-Texture Dredge Pit of Louisiana Shelf for Coastal Restoration. Water, 11(6), p.1257.

typically are home to a valuable biological community dominated by a variety of sand, shell, oyster beds, and coral-algal reefs in coastal Louisiana (CEC, 2017; Syed et al. 2018). While the direct physical impacts of dredging are relatively short and spatially restricted to the size of the pits, the impacts of dredging on the ecological function of habitats are not well constrained yet (Pearce et al. 1994; Nairn et al. 2004). The dredging impacts on biological communities in an excavated pit can occur due to the defaunation of sediment, physical changes to the water column caused by stratification, water quality changes such as hypoxia, and changes in sediment characteristics in and around the pits (Nairn et al. 2004; Munnelly et al. 2019). Additionally, the Ship Shoal borrow area (SSBA, Fig. 4.1) is considered the nearest shoal sand resource for barrier restoration along the central Louisiana coast, and tens millions of cubic meters of high-quality sand have been dredged for beach and dune restoration in Port Fourchon and the Grand Isle of Louisiana (CEC, 2017). Previous studies have suggested the existence of a transient mud bypassing Ship Shoal (Stone et al. 2009) and new mud and sand deposition in topographic lows of the bottom of the Caminada pit within two years after dredging (Xue et al. 2017; Liu et al. 2018). Muddy infilling sediments can greatly affect the living quality of benthos (Stone et al. 2009; Liu et al. 2017; Xue et al. 2017), and the identification and prediction of mud distribution inside the dredge pits are critical for the management of valuable sand resources.

Synthesizing historical data and continuously monitoring the pits have been an interest of mineral resource managers and decision-makers (CEC,2017; Stone et al. 2009; Rangel et al. 2015; Liu et al. 2017; Xue et al. 2017; Liu et al. 2018). Traditional methods used to study the pre-dredge, during, and post-dredge processes include geophysical surveys (bathymetric, sub-bottom, and side-scan), corings and grabs, water sampling, time-series observation using optical and acoustic sensors, profiling, vessel-based transects, and other methods (Obelcz et al. 2018;

Wang et al. 2018). Corings and geophysical methods have been widely used to identify the sediment types, but these data can be spatially limited and expensive to obtain. For instance, sediment coring is an effective ground-truthing method. Still, it is time-consuming and labor-intensive, generally occurring once during multiple months or years (e.g., seasonal samplings) (Xu et al. 2014). A multi-beam bathymetric survey is useful to study detailed morphological evolution but is very costly; many dredge pits have been served only once every two to five years. Compared with the narrow swath of multi-beam surveys, the side-scan method uses a relatively wide swath and has been a powerful tool to detect sediment substrates such as hard bottoms, shipwrecks, oyster reefs, sand, and mud (Obelcz et al. 2018; Denny et al. 2007; Freeman et al. 2007).

The growing availability of large geoscience datasets provides an opportunity to use machine learning (ML) to combine observational data with simulations (Diesing et al. 2014; Karpatne et al. 2018). Multi-beam bathymetric and side-scan sonar data are generally collected using acoustic equipment and represent a spatiotemporal field, but their spatial coverages are often limited (Diesing et al. 2014). These bathymetric data can be interpolated in space but can generate uncertainty and sometimes even miss detailed geological features (Stephens et al. 2014). In recent decades, ML methods have been used for identifying seafloor sediment types based on multi-beam backscatter and bathymetry (Diesing et al. 2014; Stephens et al. 2014; Valentine et al. 2016; Lacharite et al. 2018; Blondel et al. 2009), and they provide a statistically optimal estimate by incorporating disparate data and manual interpretation, especially in the locations that cannot be measured directly. However, based on our knowledge, ML methods haven’t been used in the identification of seafloor types and bathymetric terrain analysis in the rapidly changing dredge pits for coastal restoration yet, and our understanding of the

relationships among sediment types, bathymetry, and backscatter data in such a setting is relatively poor. The objective of our study is to apply ML methods to SSBA on the Louisiana continental shelf to identify the sediment deposition and classify the seafloor sediment types. Specifically, we strive to (1) quantify the grain size of sediment within a dredge pit; (2) derive and analyze the features from bathymetry and backscatter data for statistical terrain analysis; (3) compare multiple classification models; and (4) provide recommendations for future sand and mud resource management. How to best utilize the sand resources, predict the mud distribution, and minimize the impact on sensitive seafloor habitats has been an interest of scientists, engineers, stakeholders, mineral resource managers, and decision-makers. We hope that our study will serve as a stepping stone to develop monitoring plans and improve the predictions of pit morphological evolution and ecological response at onshore and offshore dredging environments in many coastal areas around the world.

4.2. Background

Ship Shoal is located off the central Louisiana coast (Fig. 4.1.), which is in the eastern portion of the late Holocene shoreline (Penland et al. 2005). On the inner shelf, which has a depth shallower than 10 m, the gentle southern slopes and steep northern slopes of Ship Shoal indicates an active northward shoal migration. This shoal is approximately 50 km long and varies between 5–7 km in width, as delineated by the 6-m isobaths (Fig. 4.1.). The 6-m isobaths of the shoal are located in a high-energy environment where currents and waves mobilize well-sorted sandy sediment. Sediment on top of this shoal is mainly comprised of clean quartz sand (Stone et al. 2009). It is a high-priority sand resource for the restoration of the Isles Dernieres barrier island chain, Caminada–Moreau headland, and Timbalier Islands, all of which suffered a high rate of land loss in recent decades (Drucker et al. 2004; Khalil et al. 2007; Williams et al. 2012).

The Caminada Headland is a Gulf of Mexico shoreline that spans from Belle Pass on the west to Caminada Pass on the east, which is a distance of 21.4 km (Fig. 4.2.). The Caminada Headland Beach and Dune Restoration Projects were the first ones to use sand resources from the Ship Shoal area for barrier island restoration; these also comprised the costliest restoration effort, and the longest beach and dune restoration project in Louisiana to date (CEC, 2017). The restoration of the Caminada Headland was comprised of two increments: Increment I (BA-45) and Increment II (BA-143). The Increment I Project (in 2014) was the first to utilize the sand resources from Ship Shoal. Subsequently, the Increment II Project (in 2016) for Caminada Headland and the Caillou Lake Headland Restoration ventured into the nearshore continental shelf for sediment resources. The area of the Caminada dredge pit (hereafter abbreviated as 'Caminada') is approximately 6.3 km^2 (1.8 km × 3.5 km), and a total volume of 9.07 million m^3 of sediment was dredged. Post-dredging volumetric analysis indicates that Caminada is presently infilling at an average rate of 0.15 m/year, or 27,480 m^3/year (Liu et al. 2018).

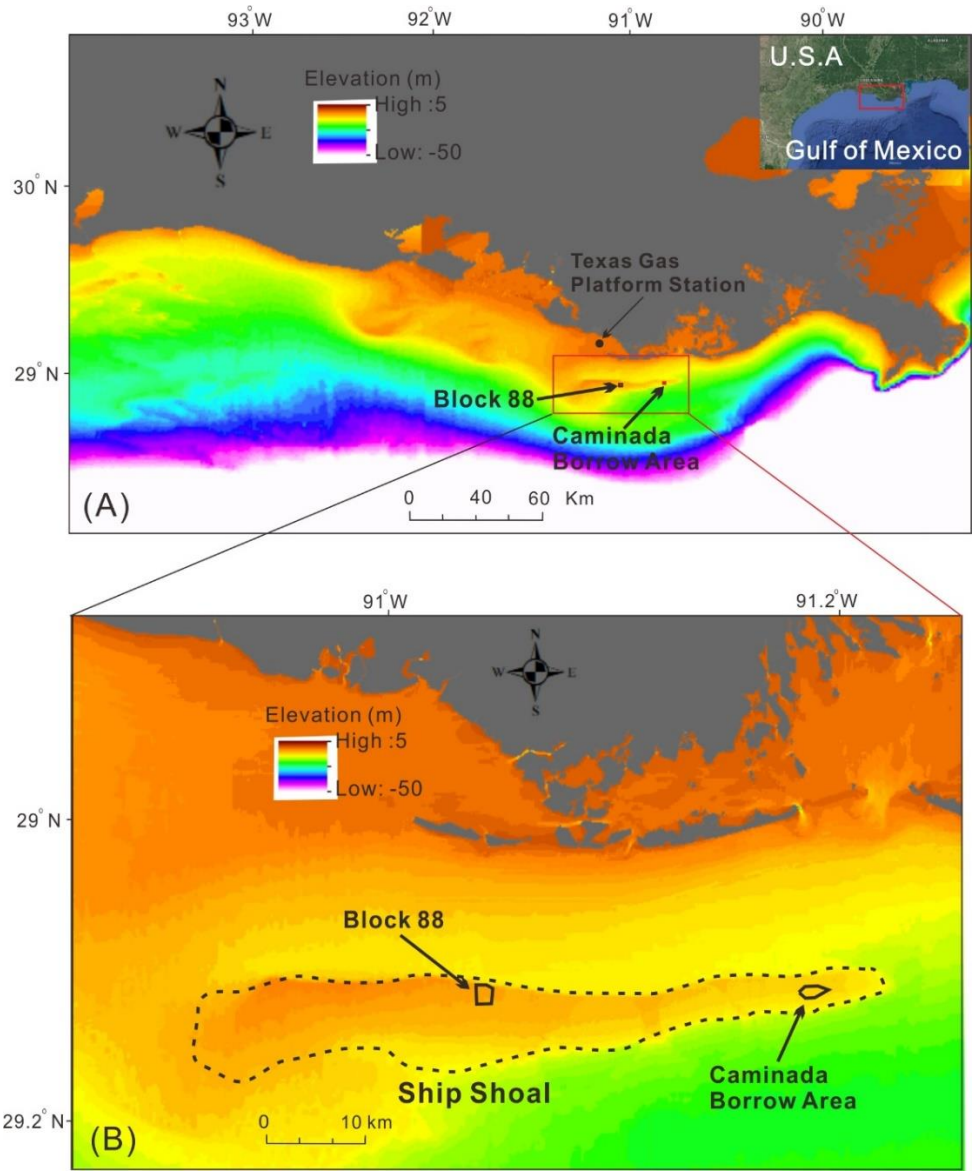

Figure 4.1. (A) A map showing the location of two sandy pits along the Louisiana shelf. The Texas gas platform station is the NOAA (National Oceanic and Atmospheric Administration) tide and current station (ID: 8763535) for tide and bathymetry correction. (B) Two borrow areas in Ship Shoal are Block 88 and Caminada. This study focuses on the Caminada dredge pit.

4.3. Methods

4.3.1. Primary and Secondary Data

Bathymetric and side-scan sonar data were used to quantify the seafloor morphology and topography of the study area. Bathymetric data from a post-dredging survey in August 2018 were processed in CARIS HIPS and SIPS v.11.2 (Teledyne CARIS, Canada) (Fig. 4.2.A). The

bathymetric data were referenced to an NOAA station at the Texas gas platform (Fig. 4.1.A), Caillou Bay, Louisiana (LA). Side-scan mosaics with backscatter values were first generated in CARIS and then exported into ArcMap (Fig. 4.2.B). Details of the processing and analysis of bathymetry and backscatter data can be found in Obelcz et al. (2018) and Liu et al. (2017).

The slope, aspect, curvature, and relative position of features and terrain variability were the derived secondary features of the bathymetry and backscatter datasets (Wilson et al. 2007; Lecours et al. 2016). Some previous studies suggested a range of secondary features that were possibly associated with substrate types from terrain analysis, which includes the bathymetric position index (BPI), roughness, curvature, aspect, Moran's I, and Sobel filter (Stephens et al. 2014; Valentine et al. 2016; Lacharite et al. 2018). BPI is the vertical difference between a cell and the mean of the local neighborhood (Wilson et al. 2007), which is deemed to be significant for sediment transport under the effect of waves and currents. This study used 20-m horizontal resolution as the cell size, which is hereafter defined as 'BPI_20′. Roughness and rugosity are the derived features for terrain variability and refer to the difference between the minimum and maximum of cell and its eight neighbors, which is calculated based on bathymetry and backscatter. Rugosity is a measure of small-scale variations of amplitude in the height of a surface, whereas roughness is the deviations in the direction of the normal vector of a real surface from its ideal form Wilson et al. (2007). In this study, all the derived secondary data were calculated in ArcGIS 10.0 via the BTM (Benthic Terrain Modeler) toolbox (Walbridge et al. 2018). Since sediment samples in this study were collected in the relatively flat seabed with no obvious slope change (Fig. 4.2.C), the slope and aspect feature such as northness and eastness are subsequently removed from the derived features in this model. Then, BPI_20, Roughness_bathymetry (roughness derived from bathymetry), Roughness_backscatter

(roughness derived from backscatter), and Rugosity_backscatter (rugosity derived from backscatter) were selected for further analysis, as described below (Table 4.1.).

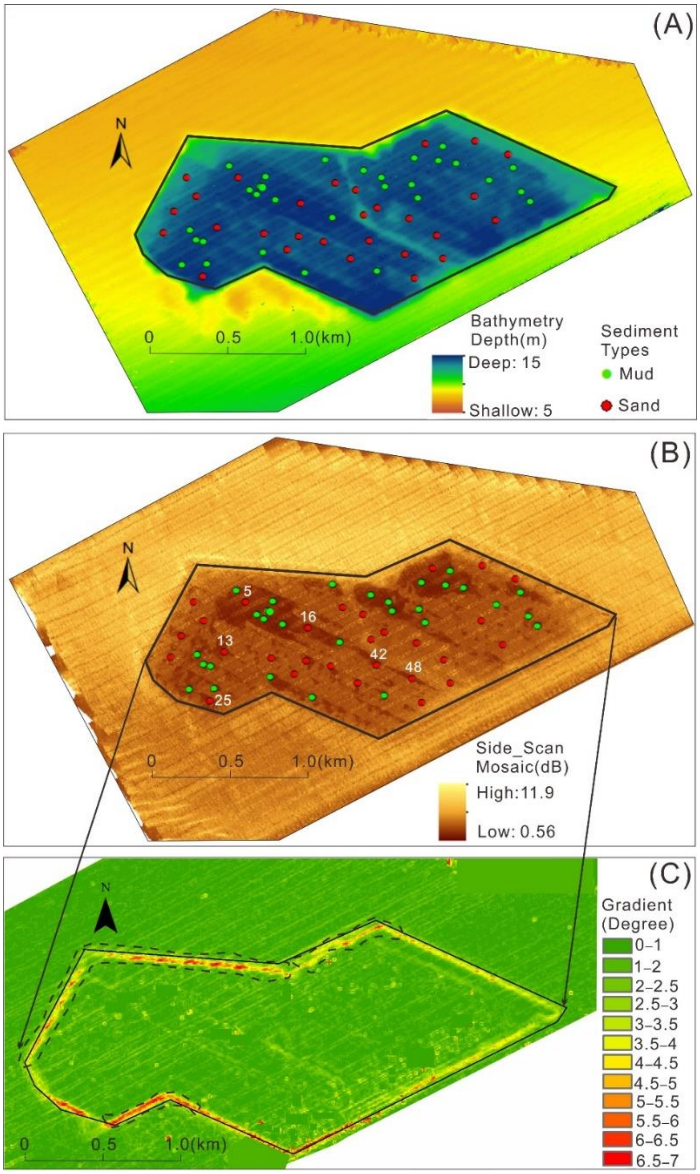

Figure 4.2. (A) Bathymetry map in a survey from August 2018 with 1-m horizontal resolution. The depth value is positive with a unit of meter. (B) Side-scan map of Caminada pit in August 2018 with 10-m resolution. Note that the dark brown indicates the patchy mud with low backscatter values, while the bright yellow is associated with sandy sediment with high backscatter values. (C) Gradient map of the Caminada pit derived from August 2018 bathymetry. Green colors represent flatter surfaces, while red colors indicate steeper ones. The dotted polygons are steep pit walls.

Table 4.1. Secondary acoustic features generated from bathymetry and backscatter

Derivative Features	Variables Names
Seabed curvature	Curvature
Bathymetric position index (BPI)	BPI_20 m
Terrain variability	Backscatter_roughness, Bathymetry_roughness Rugosity_backscatter

4.3.2. Surficial Sediment Data

Surficial sediment samples (n = 58) were collected using a clam-shell grab sampler in the bathymetric survey area in 2018. Grain size analysis was conducted using a Beckmann Coulter laser diffraction particle size analyzer (Model LS 13 320). A subsample from each grab (1 g) was digested with 30% hydrogen peroxide to remove any organic matter. More details of processing and analysis can be found in (Liu et al. 2018; Xu et al. 2014). The sediment types were classified into two basic groups based on grain size analysis of the relative proportions of mud (median grain size $d < 63$ μm) and sand (63 μm$< d < 2000$ μm).

4.3.3. Classification Methods

Decision Tree (Buhl et al. 2009; Ierodiaconou et al. 2011; Gonzalez et al. 2012) and Random Forest learning (Ierodiaconou et al. 2011) were recently used in seabed mapping. Unlike parametric methods, tree-based methods do not have any parametric assumption on the data. Trees can automatically handle the mixed type of data (e.g., categorical and numeric variables) and missing values (Atkinson et al. 2000). The recursive partition algorithm is a popular technique to construct a binary tree, in which each node can have at most two branches. At each splitting node, the tree algorithm finds the “optimal” splitting variable and location through an exhaustive search. The “optimal” here means minimizing some predefined criterion, such as cross-entropy for classification and the sum of squared errors for regression. The splitting process is repeated recursively on the right and left branches derived from the previous

split until some stopping criterion is met (e.g., the minimum sample size to split). Usually, a fully grown tree is highly complicated and overfits the data. To avoid overfitting, the algorithm "prunes" the overfitted tree by collapsing some internal splits and finds the optimal subtree that minimizes the cross-validation error (Atkinson et al. 2000). In this study, the default setting was used to construct and prune the classification trees using the 'rpart' package in R.

The Random Forest algorithm (Breiman, 1996) is one of the most popular ensemble methods in data mining. The fundamental idea of Random Forest is to boost the prediction performance of a single tree by fitting multiple trees and combining their predictions. The Random Forest algorithm uses two ways to make the trees in the forest as diversified as possible. First, each tree is constructed using a random subset of the sample through bootstrapping (i.e., random sampling with replacement). Second, at each split, the optimal splitting variable is chosen from a random subset of variables. The observations not used to construct a tree are called out-of-bag samples. Instead of using cross-validation, the Random Forest algorithm uses the out-of-bag errors to estimate the predictive performance on new samples and stops growing more trees when the out-of-bag error converges. Additionally, regularized logistic regression was a popular classification method by adding a penalty term (e.g., lasso penalty) to the log-likelihood function (Tibshirani et al. 2011), which can be used to pick out the most essential features. The randomForest and 'glmnet' packages with default settings were used in this study to run the Random Forest and regularized logistic regression models, respectively.

In this study, Random Forest, Decision Tree, and Regularized Logistic Regression with Lasso penalty (hereafter abbreviated as Logistic Lasso) were run using randomForest, rpart, and glmnet packages in R, respectively (Fig. 4.3.). The data were randomly split into training (80%) and test (20%) sets. The models were fitted using the training samples only, while the test

samples were used to evaluate the models' predictive performance. The results were based on a total of 250 random splits of the data. The accuracy rate and AUC (Area Under the Curve) score were used to evaluate the model performance (Huang et al. 2005). Accuracy is defined as the proportion of samples that were correctly classified for the test set. AUC, which is based on the Receiver Operating Characteristic (ROC) curve, provides an aggregate measure of performance across all the possible classification thresholds. A model whose predictions are incorrect has an AUC of 0.0; one whose predictions are all correct has an AUC of 1.0. In our models, each sample contained (1) primary features: bathymetry (m) and backscatter data (dB), and (2) derived secondary features: BPI_20, Roughness_bathymetry, Roughness_backscatter, and Rugosity_backscatter. Each classification method in this study was trained three times using different combinations of features: 1) all six features, 2) only primary features (bathymetry and backscatter), and 3) a subset of features chosen by the Random Forest algorithm.

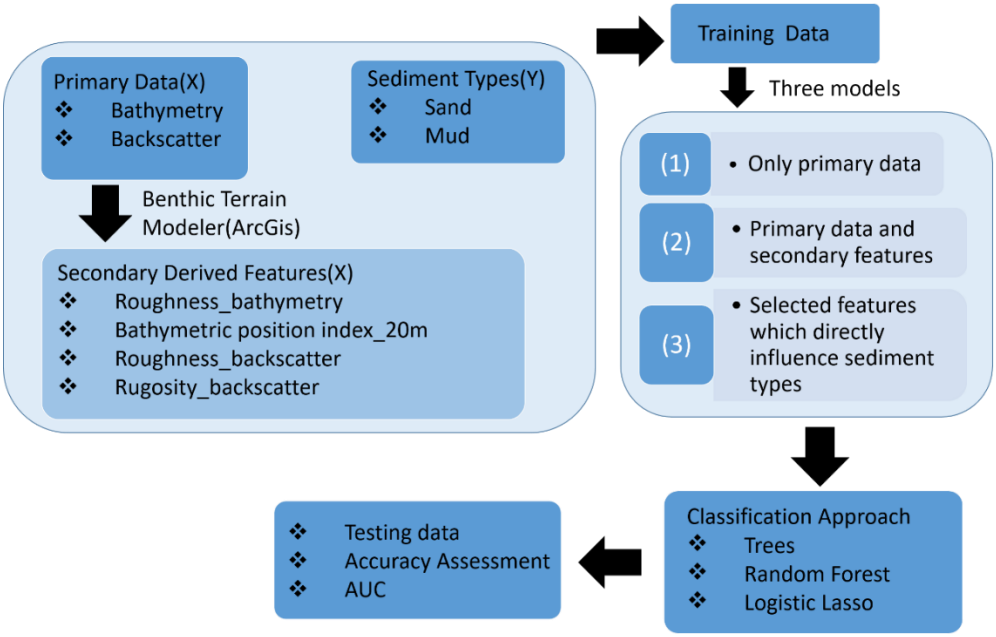

Figure 4.3. Flowchart of models that covers input features, machine learning (ML) methods, and validation methods.

4.4. Results

4.4.1. Grain Sizes

The grain size distributions of a total of 58 samples from Caminada pit are shown in figures 3A & 3B. The majority of the 30 sandy samples within the pit contain about 90% sand and 10% silt, with modes around 100 µm (Fig. 4.4A). However, there are a few sandy samples whose modes are near 63 µm. The grain sizes of the other 28 samples indicate the dominance of silt with modes around 15 µm (Fig. 4.4B). On average, the sand, silt, and clay represent 21%, 75%, and 4%, respectively, with silt being the largest fraction.

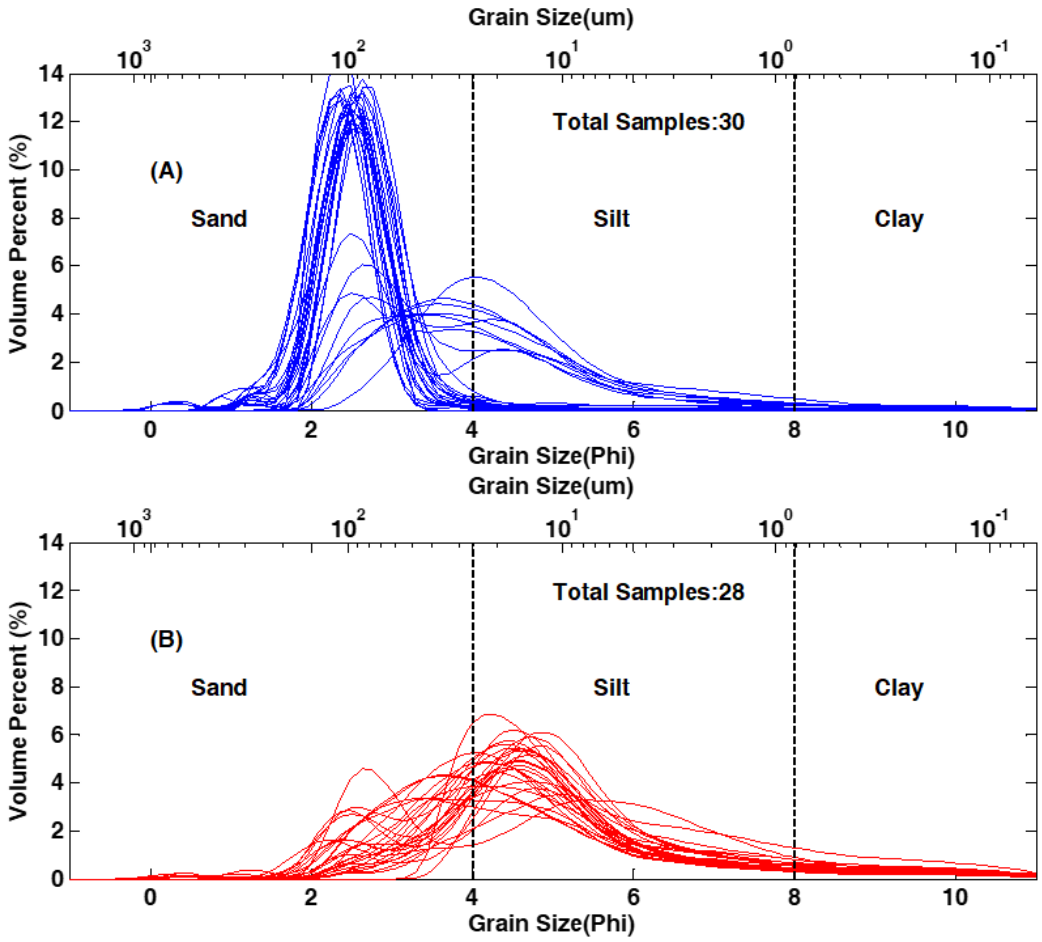

Figure 4.4 Grain size distributions of surficial sediment samples collected inside Caminada pit in August 2018 (see Figure 2B for grab sample locations). (A) Shows the grain size distribution of 30 sandy samples and (B) shows 28 muddy samples.

4.4.2. Data Exploration

The training samples showed that the bathymetry of samples ranges from 9 m to 13.5 m, and most of the data are between 12.0–13.5 m (Fig. 4.5.A). The backscatter data revealed a sampling of values between 0–5 dB (Fig. 4.5.B), with the majority being in the 2–3 dB (Fig. 4.5.B).Further exploration of the sediment types of training data showed that, in general, coarser sediments were associated with higher backscatter and shallower water depths (Fig. 4.5.C, D).

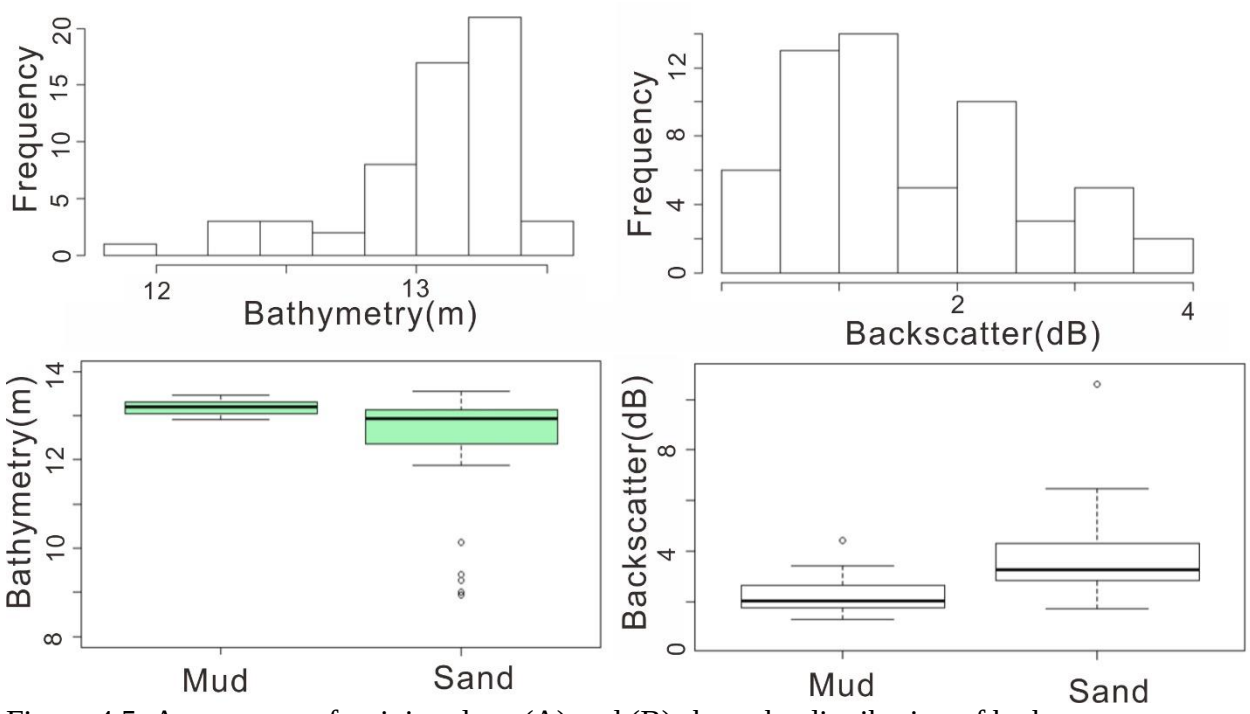

Figure 4.5. A summary of training data. (A) and (B) show the distribution of bathymetry values and backscatter values. (C) and (D) show the distribution of sediment types with bathymetric and backscatter values.

4.4.3. Feature Selection

The correlation matrix shows that backscatter and bathymetry have a strong correlation with sediment types, and the absolute values are both greater than 0.43. Backscatter and all the corresponding derived features indicate a positive relationship with sediment types, whereas bathymetry and BPI_20 have a negative relationship with sediment types (Fig. 4.6.). It shows that a higher backscatter value with shallower water depth is prone to be classified as sand. The

four derived features show autocorrelation with their original primary features. The Random Forest method was applied ten times to calculate the variable importance (Table 4.2.). The results indicate that backscatter, roughness_bathymetry, and rugosity_backscatter bathymetry were the most significant features that were included in the model with a subset of features.

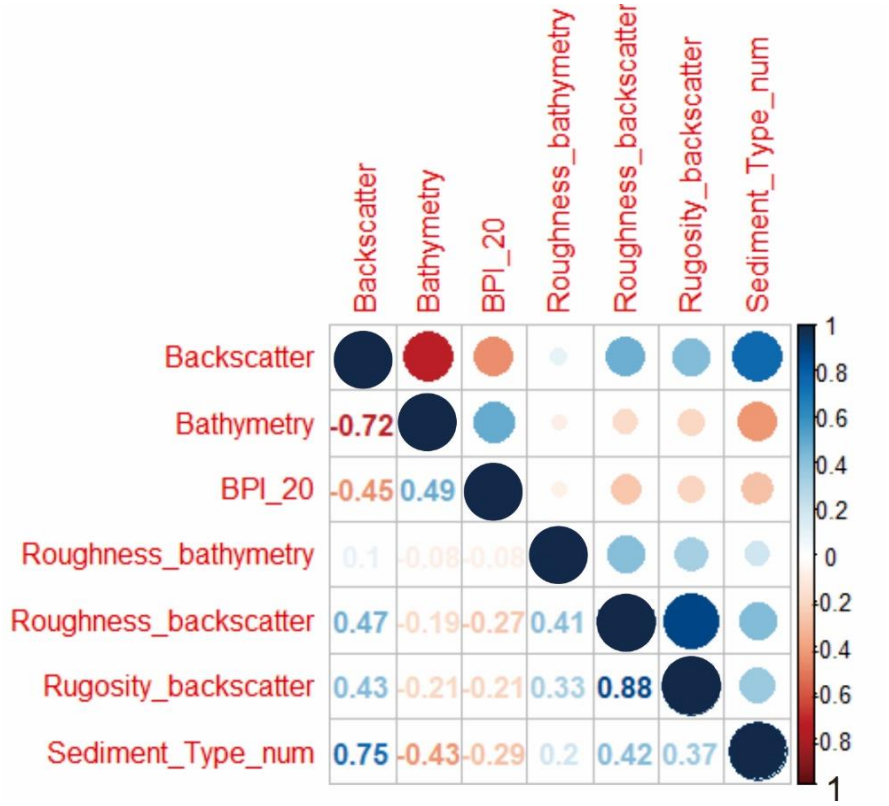

Figure 4.6. The correlation plot is showing the relationship between all the features with sediment types. Blue color means a positive relationship, but the red color indicates a negative connection. Sediment_Type_num: 0 is mud, and 1 is sand.

Table 4.2 Output from Random Forest selection algorithm. The first four bold scores (all greater than the threshold, which we defined as 1.5) are the most important features to identify sediment types.

Feature	Score
Backscatter	16.77
Roughness_bathymetry	2.39
Rugosity_backscatter	2.28
Bathymetry	1.51
Roughness_backscatter	0.76
BPI_20	0.20

4.4.4 Model Performance

Table 4.3. summarizes the test set performance for nine models (the combination of three sets of features and three classification methods) based on 250 random splits of the data. The number refers to three types of models with different input features used in the model. In set 1, all the features were used; in set 2, only the primary features (bathymetry and backscatter) were used; in set 3, a subset of four features chosen by the Random Forest algorithm discussed above was used. For example, DT1 stands for the Decision Tree model using all the features.

Table 4.3. Model performance comparison. The average accuracy rate and Area Under the Curve (AUC) score calculated on the test sets from 250 replications. The model number indicates the input features used in the model. (RF = Random Forest; CT = Classification Tree; Logit_Lasso = Logistic Lasso classification). The number in the parenthesis is the standard deviation of accuracy. The accuracy in bold indicates the best performance in each of the three types of models (RF, CT, and Logit_Lasso).

Model	Accuracy (Standard Deviation)	AUC
RF1	0.82 (0.12)	0.93
CT1	0.84 (0.13)	0.85
Logit_Lasso1	0.83 (0.09)	0.93
RF2	0.85 (0.12)	0.92
CT2	0.84 (0.13)	0.85
Logit_Lasso2	0.84 (0.12)	0.93
RF3	0.90 (0.10)	0.95
CT3	0.87 (0.10)	0.85
Logit_Lasso3	0.84 (0.12)	0.94

As we discussed above, each model was trained by 250 randomly split datasets, and then the average accuracy and standard deviation were recorded in Table 2. In terms of the first-type models, Classification Tree has the best performance with an accuracy of 0.84. However, the AUC only reaches 0.85, which is the smallest among all these three models. Likewise, the classification power increases when the model is only trained with the two primary features, which are the second-type models. The accuracy of the Logit_Lasso models increases from 0.83 to 0.84. Random Forest_2 has the best performance with an accuracy of 0.85 and AUC of 0.92.

The best model of all the 12 is the Random Forest_3, which is trained by only four selected features, and reaches the accuracy of 0.90 and AUC of 0.95. Additionally, Decision Tree and Logistic Lasso classification take the longest time to run among all the 12 models.

4.5. Discussion

4.5.1. Model Evaluation and Comparison with Previous Studies

Previous studies show that the slope, aspect, curvature, and relative position of features and terrain variability were the four different geomorphological relevance in marine-based studies (Table 4.4) (Lecours et al. 2016; Buhl et al. 2009). The slope can be used to evaluate the stability of sediments deposition/acceleration and erosion/movement, which are applied to calculate the basic slope (steepest) and directional slope (Lundblad et al. 2006; Lanier et al. 2007; Micallef et al. 2012; Micallef et al. 2012; Dolan et al. 2014; Ienness et al. 2004). Orientation is related to the direction of dominant geomorphic processes and the orientation of the seabed, i.e., which direction it is facing (Galparsoro et al. 2009). Aspect, Northness, and Eastness are the three terrain attributes of orientation (Wilson et al. 2007). Northness equals the cosine of the aspect, which is the direction of the steepest slope measured in clockwise degrees from north, and eastness refers to the sine of the aspect (Monk et al. 2011). Curvature is useful in the classification of landforms, such as flow and the channeling of sediments/currents (Ienness et al. 2004). Previous studies used Mean Curvature (Dolan et al. 2014), Profile Curvature (Ienness et al. 2004; Guinan et al. 2009), Plan Curvature (Ross et al. 2015), and BPI (Monk et al. 2010; Pirtle et al. 2015) to calculate terrain attributes of curvature. Lastly, the terrain variability and structures that are present reflect dominant geomorphic processes, which contains Rugosity (Dunn et al. 2009), Vector Ruggedness (Tempera et al. 2012), Bathymetric Roughness (Wilson et al. 2007), Relative Relief (Elveness et al. 2013), and Fractal Dimension (Wilson et al. 2007).

In terms of our model, bathymetry and backscatter were identified as two critical features in the model. Our results indicated that bathymetry roughness and backscatter roughness were two important secondary features, which is in line with multiple previous studies (Diesing et al. 2014; Stephens et al. 2014; Lacharite et al. 2018). The BPI was not selected as a significant feature, which was possibly due to the relatively coarse cell size of 20 m when compared with the area of the seabed sampled by the grabs. Additionally, this study limited the number and types of input features to keep the model simulations manageable. A decision was made to limit the secondary features to those that were easily derived with standard GIS software to make this study compared with others. Also, the slope and aspect of the seabed did not change dramatically inside the Caminada dredge pit, and thus northness and eastness were not used.

Table 4.4. Summary of the most commonly used terrain attributes derived from bathymetry and backscatter in marine-based studies

	Slop	Orientation	Curvature	Terrain Variability
Terrain attributes and examples	(1) Basic slope (steepest) (2) Directional slope	(1) Aspect (2) Northness (3) Eastness	(1) Mean curvature (2) Profile curvature) (3) Plan curvature (4) Bathymetric position index (BPI)	(1) Rugosity (2) Vector ruggedness measure (VRM) (3) Bathymetric Roughness (4) Relative relief (5)The fractal dimension

Supervised machine learning techniques that have been applied to seafloor mapping include Maximum Likelihood Estimation (Elvenes et al. 2013; Hasan et al. 2012), k-Nearest Neighbor (Lucieer et al. 2013), Decision Trees (Ierodiaconou et al. 2011; Hasan et al. 2012), Random Forest (Marsh et al. 2009), Artificial Neural Networks (Marsh et al. 2009; Liu et al. 2018), and Support Vector Machines (Hasan et al. 2012; Liu et al. 2018). Many choices of supervised classification methods make it difficult to select the most appropriate method for a specific study site (Stephens et al. 2014). Brown et al. (2008) classified the side-scan sonar mosaics into three

groups and predicted the seabed surface characteristics of observed biological habitats via an unsupervised classification procedure in the United Kingdom with the water depth between 10–60 m. They also found there was a low-to-moderate correlation between the side-scan backscatter and particle size. Blondel et al. (2009) applied the unsupervised classification of the k-means method to a textural analysis of Stanton Banks on Northern Ireland continental shelf with water depths varying from 120 to 160 m and detected different types of seafloor based on multi-beam sonar imagery. Diesing et al. (2017) compared different approaches including manual interpretation, geostatistics, object-based image analysis, and machine learning to test the accuracy of acoustic data interpretation in the western North Sea off the Scottish coast of the United Kingdom based on bathymetry, backscatter, as well as seabed samples in the water depth shallower than 100 m. They found that overall thematic classification accuracy was acceptable, but the difference among statistical methods was not significant. ML methods were also used to compare different supervised or unsupervised classification methods for the prediction of a marine benthic habitat using multi-beam echosounder and grain-size data (Stephens et al. 2014). Liu et al. (2018) applied Decision Tree, Random Forest, Neural Network, and SVM to predict substrate types based on multi-beam sonar imagery in Busszard bay, Massachusetts. They found that Neural Network was a good option classifying sediment types of seafloor with complicated features. In terms of our four ML methods, the Random Forest method achieved the highest accuracy scores, performing significantly better than all the other model runs (Table 4.1.). In terms of three combinations of input features, RF3 had the best classification power with an accuracy rate of 0.9. RF2 included only two primary features but was not as good as RF3, which indicated bathymetry and backscatter data that contained partial information to classify the sediment types. Conversely, RF1 performed worse than all the other model runs according to the

accuracy rates, indicating that the performance of all the features suffered due to the presence of some irrelevant features.

This study focused solely on the prediction performance of the classifiers but did not focus on the tuning and training stages for the classifiers. In general, Random Forest and Logistic Lasso are computationally expensive algorithms compared to Decision Tree, since Random Forest is an ensemble of hundreds of trees, and Logistic Lasso requires choosing the tuning parameter through cross-validation. Additionally, this study focused solely on the classification approach to identify sediment types. Regression methods would be another path to reach a good prediction of variables.

4.5.2. Limitations and Future Work

After evaluating the models, some limitations of our work should be recognized. Firstly, the input features were aggregated to a particular spatial resolution. These were limited by sampling equipment (multi-beam sampling density) and, more significantly, the computing power available for processing the data. The bathymetric and backscatter data were gridded to resolutions of 1 m and 10 m, respectively. However, the variations of sediment types within an area of 6300 m^2 of the Caminada pit seafloor were not at the same scale as the bathymetric and backscatter grids. Future work should investigate the impacts of varying gridding cell sizes when the predictor variables have a coarser resolution than the sampling data.

Secondly, the model was very capable of predicting dominantly sandy or muddy samples, but poor at predicting mud-sand mixture. Grain size analysis indicated the mixed sand and mud environment in the depression zones (Fig. 4.2.B and Fig. 4.4). This study divided the sediment types into two types using 63 μm as the boundary. The mud–sand mixtures were challenging to predict, and they were also the misclassified ones. A partial dependence plot showed that six

sandy samples existed near the classification boundary at 63 μm (Fig. 4.7.). Samples 5, 16, and 48 all have grain size modes near 63 μm (Fig. 4.8.), which was the blind zone of the model for classification. It also showed only sandy samples appeared across the classification boundary, which indicated that the model could better predict mud than sand (Fig. 4.7.).

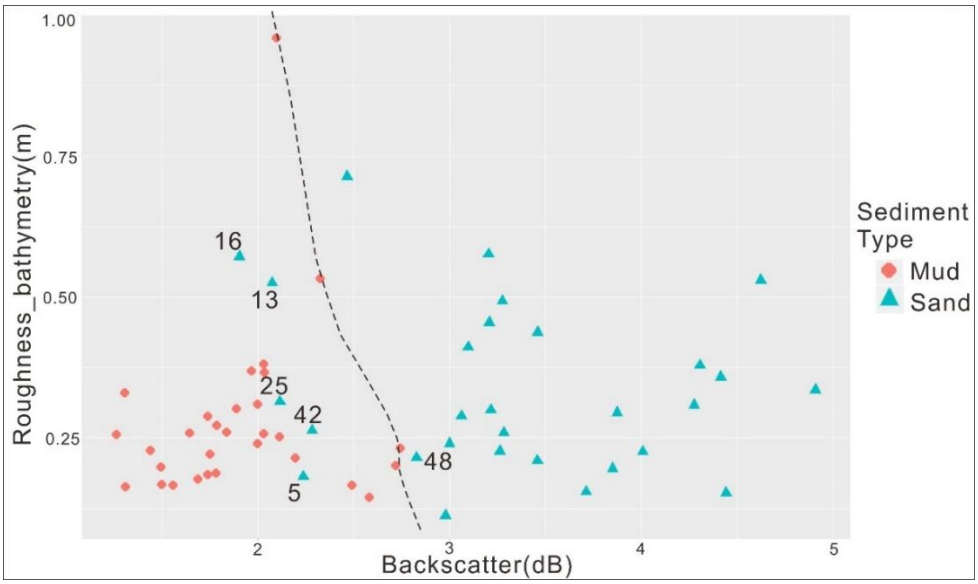

Figure 4.7. Partial dependence plot of backscatter and Roughness_bathymetry. The dotted line is the classification boundary between mud and sand. Backscatter and Roughness_bathymetry are the two most important features to classify the sediment types.

Lastly, positional and sampling accuracy is a challenge in the field. To save time, our sampling boat was not anchored in the field. All 58 samples were collected in one day to save cost, and multiple trials were performed in some sandy sites in which it was hard to penetrate using a clam-shell grab sampler. Strong currents kept moving the boat when sediment samples were collected. It takes 3–5 min to collect one sample using the sampler, but the planned and actual sampling locations can be different. Also, strong currents caused some tilting of the winch cable attached to the grab sampler, leading to some coordinate differences between GPS on top of the boat and actual sampling locations on the pit bottom.

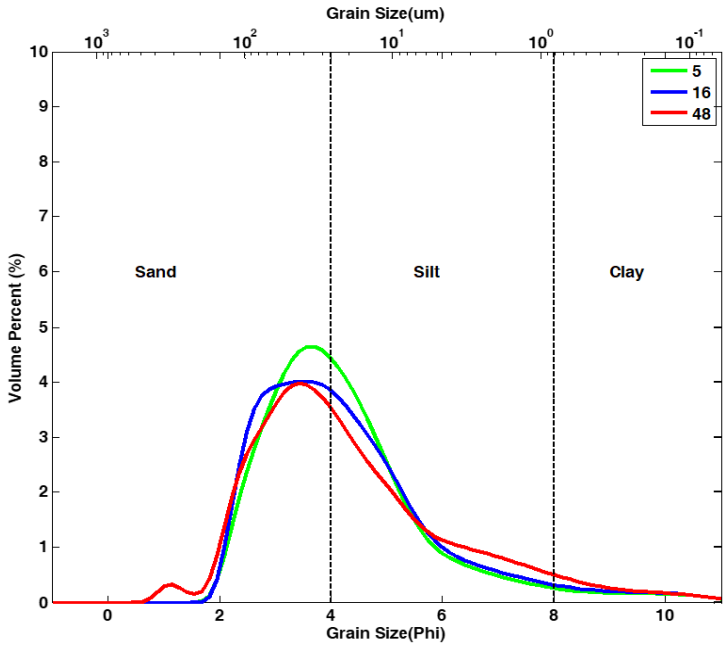

Figure 4.8. Grain size distributions of three sandy samples with the grain size near the classification boundary. Numbers 5, 16, and 48 are sample IDs. See the locations of these samples in Fig. 4.2.B.

Even a small difference between the planned and actual locations of sediment samples can be significant in Caminada pit, because of the mic-topography and patchy sediment distribution (Fig. 4.4.). A partial importance plot shows that samples 13, 25, and 42 are near the classification boundary (Fig. 4.7.). However, these three sandy samples exist in the depression zone (Fig 4.2.B). According to the Random Forest model, these samples should contain high backscatter value, which is predicted as mud. The positional error of these three samples is likely the possible reason for the misclassification.

4.5.3. The implication to Coastal Restoration

It was reported that the majority of Caminada pit infilling is mainly derived from far-field muddy sediments, either the Mississippi River or Atchafalaya River or inner shelf sediments transported by currents and waves (Xue et al. 2017; Liu et al. 2018). Caminada pit is in a unique depositional environment in which the existing sandy sediments are mixed with bypassing mud. Fine-grained bypassing muddy sediments were found inside Caminada and not considered as

reusable resources. The change from sandy to muddy (or even mixed) substrate on Ship Shoal may greatly influence the activities of benthic communities. The deposition and redistribution of muddy inside Caminada would not allow the reuse of infilling sediment for future barrier island restoration. More time series geophysical, hydrodynamic, and sediment data are needed for post-construction management and monitoring in SSBA to evaluate whether the dredging activities in SSBA are cost-effective and sustainable (Stone et al. 2009; Xu et al. 2018).

Sandy shoals such as Tiger Shoal, Trinity Shoal, and Sabine Bank, ebb-tidal deltas such as Barataria Pass, and paleochannels in the Louisianan coastal zone all can potentially have mixed texture environments, similar to the Caminada pit. Block 88 in Ship Shoal was dredged recently in spring 2018 (Fig. 4.1.B) and had a depositional environment similar to the Caminada pit. Future dredging areas in coastal Louisianan zones will be focused on the sandy shoals and paleochannels, which are a sandy environment with possible mud trapping, and our model can be used for sediment identification in such an environment. Furthermore, the dredging pits in East and Gulf Coasts have a similar issue of the muddy sediment infilling in sandy pits. Manasquan Inlet (New Jersey), Mobile Bay (Alabama), and Mobile Quter mound (Alabama) were predicted to exist for more than 100 years due to less sediment supply and transport (Byrnes et al. 2004). Our model provides a new method to predict the change of mixed sediments (mud and sand) distribution inside sandy dredge pits for post-construction management. However, this model may not be applied to a homogenous substrate such as the muddy bay areas where sediment is more uniform; similarly, this model probably would not perform well when new sand fills in a sandy pit. Hard bottoms and oyster reefs are substrate types differing with sand and mud. Our model did not include these substrate types due to the lack of such substrate in Caminada pit, but

our method can be used to predict a variety of contrasting seabed substrate types in future research.

Additionally, dredge pits in Ship Shoal are in inner-shelf shoals offshore Louisiana, where dredging and transporting sediment from offshore is expensive as nearshore sediment sources are being explored and depleted (Syed et al. 2018). Our model provides a cost-saving method to evaluate the seafloor sediments in sand–mud mixed environment. Our results show that backscatter is the single most important feature to predict sediment types (Table 4.2.). When the budget is limited, only collecting backscatter data will be acceptable and cost-effective because of its powerful prediction capability. In other words, after establishing a reliable ML model for dredge pits, sediment samples and multi-beam data can be collected much less frequently than side-scan data. When a monitoring plan is developed, sediment and multi-beam data may be collected once every year, or even every other year, whereas side-scan data can be collected seasonally. Synthesizing observation with modeling would eventually yield the best results for sandy resource management. Our results can also be used to better understand the impacts on biological communities by direct defaunation due to sand excavation and mud accumulation in topographic lows. This study can increase the government's decision-making ability regarding safety and protecting environmental and cultural resources.

4.6. Conclusions

The sand volume of Caminada dredge pit in Ship Shoal is one of the largest in the United States (USA) east and Gulf coasts. The integration of the bathymetric data, backscatter data, and sediment collection in 2018 enabled us to apply ML methods to identify the mud deposition and classify the seafloor sediment types in Caminada dredge pit on the continental shelf offshore Louisiana, USA.

(1) Grain size analysis of the 58 sediment samples inside the dredge pit shows that mud is prone to deposit in trough zones with lower backscatter values, while sand is likely to appear on the flat seabed with higher backscatter values.

(2) The variable importance analysis indicates that backscatter, roughness_bathymetry, rugosity_backscatter, and bathymetry (from high to low) are the four most significant features to classify sediment types. A Random Forest model with these four selected features has the best classification power with the accuracy rate of 0.9 to predict the sediment types inside the dredge pit.

(3) The particular spatial resolution between multi-beam density and the availability of sediment type, a simple mud–sand classification method, and the positional accuracy of the sediment samples collected in the field are the three possible factors that likely lead to differences between the planned and actual locations of sediment samples.

(4) The deposition and redistribution of mud inside the Caminada pit make it unusable for barrier island restoration, but our model provides a new and efficient method to predict the time-series change of sediments (mud and sand) distribution inside the Caminada pit for post-construction management.

CHAPTER 5. SEDIMENT TRANSPORT NEAR SHIP SHOAL FOR COASTAL RESTORATION IN LOUISIANA SHELF: MODEL ESTIMATE OF THE YEAR 2017-2018

5.1 Introduction

In recent decades, new multi-resolution and multidimensional approaches have been used in the studies of coastal sediment modeling and morphological evolution (Chen et al. 2007; Harris et al. 2008; Warner et al. 2010) in the Gulf of Mexico (GoM). The sediment module in DELFT3D, for instance, implements algorithms for up to five different classes, which are specified as either 'mud' or 'sand' (Lesser et al. 2004). A particularity of the approach used in DELFT3D is that the bedload transport rate is related directly to the flow velocities instead of the bed shear stress (Lesser et al. 2004). Additionally, cohesive processes such as flocculation, consolidation, and fluidization are not in the sediment module in DELFT3D (Amoudry, 2008). Caldwell and Edmonds (2014) used DELFT3D to simulate the effect of sediment properties (the median, standard deviation, skewness, and percent cohesive sediment) on deltaic processes and morphology of the Mississippi River.

HYbrid Coordinate Ocean Model (HYCOM) is another modeling approach to develop an eddy-resolving, real-time global and basin-scale ocean hindcast, nowcast, and forecast system (Chassignet, 2007; Chassignet, 2009). Currently, there are three main vertical coordinates in this model. Still, none of them provides all three approaches at every time step, which makes the model a dynamically smooth transition between the coordinate types via the continuity equation (Chassignet, 2007). Prasad & Hogan (2007) employed a 20-layer nested Gulf of Mexico HYCOM to examine the evolving three-dimensional ocean response to Hurricane Ivan during September 2004 and compare it with satellite-altimetry derived sea-surface height. Liu et al. (2009) used HYCOM and satellite data to explore the mechanism that triggers the phytoplankton

bloom after Katrina passage in 2005. Liu et al. (2011) used HYCOM numerical model and satellite remote sensing resources to track the oil spill both at the surface and at depths in the Gulf of Mexico, which guided mitigation efforts and ship surveys. Rudnick et al. (2015) applied the GoM assimilation system in HYCOM to simulate the cyclonic eddies in the Gulf of Mexico, which increased the accuracy of a global hindcast. Additionally, numerical experiments modeling can be used to study on deltas and sediment cohesion focus on their morphology in settings with constant sea level, with some notable exceptions, such as Mississippi River (Armstrong et al. 2014).

Statistical modeling, including machine learning and deep learning, is also becoming popular in the sediment studies, especially in the satellite image analysis and seafloor morphology identification (Diesing et al. 2014; Stephens et al. 2014; Lacharité et al. 2018). Statistical methods provide a statistically optimal estimate by incorporating disparate data and manual interpretation, especially in the locations that cannot be measured directly. Liu et al. (2019) tested multiple machine learning classifiers to identify the sediment types of Caminada dredge pit in the eastern part of the submarine sandy Ship Shoal of Louisiana inner shelf of the USA. In recent decades the regional ocean modeling system (ROMS) has been widely used in the oceanographic community to investigate the dynamics of ocean circulation (Shchepetkin and McWilliams, 2005; Haidvogel et al. 2008). This three-dimensional model implements algorithms for an unlimited number of user-defined sediment classes and the evolution of the bed morphology (Warner et al. 2008). This model has been incorporated in a coastal-circulation model with two-way coupling between a wave model and the sediment transport module (Warner et al. 2010; Kumar et al. 2012). Xu et al. (2016) studied seabed erosion and deposition on the Louisiana shelf in response to Hurricanes Katrina and Rita in the year 2005 via 3-D

sediment models in ROMS and found horizontal erosional patterns are mainly controlled by hurricane tracks, and wave-current combined shear stresses. Moriarty et al. (2018) applied a coupled hydrodynamic sediment transport-biogeochemistry mode in northern GoM. Zang et al. (2019) adapted the coupled ocean-sediment transport model to the northern GoM over a twenty-year period and found decreased river discharge would largely affect sediment concentration in waters around the delta.

In recent decades the Louisiana coast has been facing extensive coastal land loss due to subsidence, shortage of sediment supply from the Mississippi River, occasional hurricane landfalls, frequent passages of winter storms, and human intervention such as dam construction and dredging navigation channels (Allison et al. 2014; Twilley et al. 2016). A major effort to manage coastal land loss is to restore degraded barrier shorelines by dredging sand resources from borrow areas and delivering to the coastal sedimentary environments (Khalil et al. 2010). Although billions of cubic meters of sand are needed for initial and recurring restoration (e.g., Stone, et al. 2004; Hanley et al. 2014; Jonah et al. 2015; Brown et al. 2015; Rangel et al. 2015), high-quality sand is largely limited to isolated submarine shoals or infilled paleo-river channels on the inner shelf. Ship Shoal is estimated to contain 1.2 billion cubic meters of potential high-quality quartz sand (Kobashi et al. 2007). Ship Shoal is considered the closest available sand resource for barrier shorelines in central Louisiana and has been dredged for significant volumes of the high-quality beach and dune restoration in Port Fourchon and Grand Isle of Louisiana (Fig. 5.1). In recent years, several pits were dredged on and near Ship Shoal, including Raccoon Island, Caminada, and Block 88 dredge pits. The Caminada restoration project was the first such project to use sand resources from the Ship Shoal area for barrier island restoration and the largest Louisiana monetary investment in restoration to date (Stone et al. 2004; Dartez et al.

2016; CEC, 2017). A total volume of 9.07×10^6 m^3 of sand was excavated from Caminada pit based on pre- and post-construction surveys (CEC, 2017). However, previous surveys suggest the existence of transient mud bypassing the seabed of Ship Shoal, which could fill borrow areas and affect physical/biological processes and sand quality for future reuse of coastal restoration (Stone et al. 2009; Liu et al. 2017; Xue et al. 2017; Xu et al. 2018; Liu et al. 2018; Liu et al. 2019). Stone et al. (2009) hypothesized that occasional sediment plume shifts from the Atchafalaya Bay to the southeast might result in the accumulation of a thin fluid-mud layer on some portions of Ship Shoal. O'Connor (2017) found that ^{7}Be radioisotope activity in the muddy sediments collected inside Raccoon Island pit indicates a significant portion of the mud was derived from fluvial sources and deposited within ~6 months before core collection. Xue et al. (2018) collected multiple corings in the Caminada pit and found that muddy sediment was deposited within six months from fluvial sources. Liu et al. (2019) found muddy sediments were transported into Caminada pit in Ship Shoal and deposited in heterogeneous patches within two years after dredging. Liu et al. (2018, 2019) applied multiple machine learning classifiers to identify sediment types and found mud was prone to deposit in the trough zones with lower backscatter values in Caminada pit of Ship Shoal. Moran et al. (2019) collected the bathymetry and side-scan data in Block 88 pit on western Ship Shoal and found the steepest slopes were mainly at pit walls and biogenic gas was found above muddy sediment inside that pit. These findings together reveal that transient mud may temporarily blanket the sandy shoal but is later resuspended to fill in pits or transported to deeper water. However, there is very limited knowledge about the source and transport process of suspended muddy sediments near Ship Shoal. Thus, the objective of this study is to apply the ROMS model in Ship Shoal to: 1) quantify sediment transport directions and fluxes near Ship Shoal, (2) compare the relative contribution of

fluvial with estuary and shelf sediments delivered to Ship Shoal; 3) investigate the spatial dispersal pattern of fluvial, estuary and shelf sediments, and (4) apply the model results in the studies of dredges pits for future coastal restoration. Due to limitations on our current model resolution, dredge pits are not included in our model. Rather, modeled 'background' sediment concentrations near the pits will be used to calculated dredge pit infilling rates.

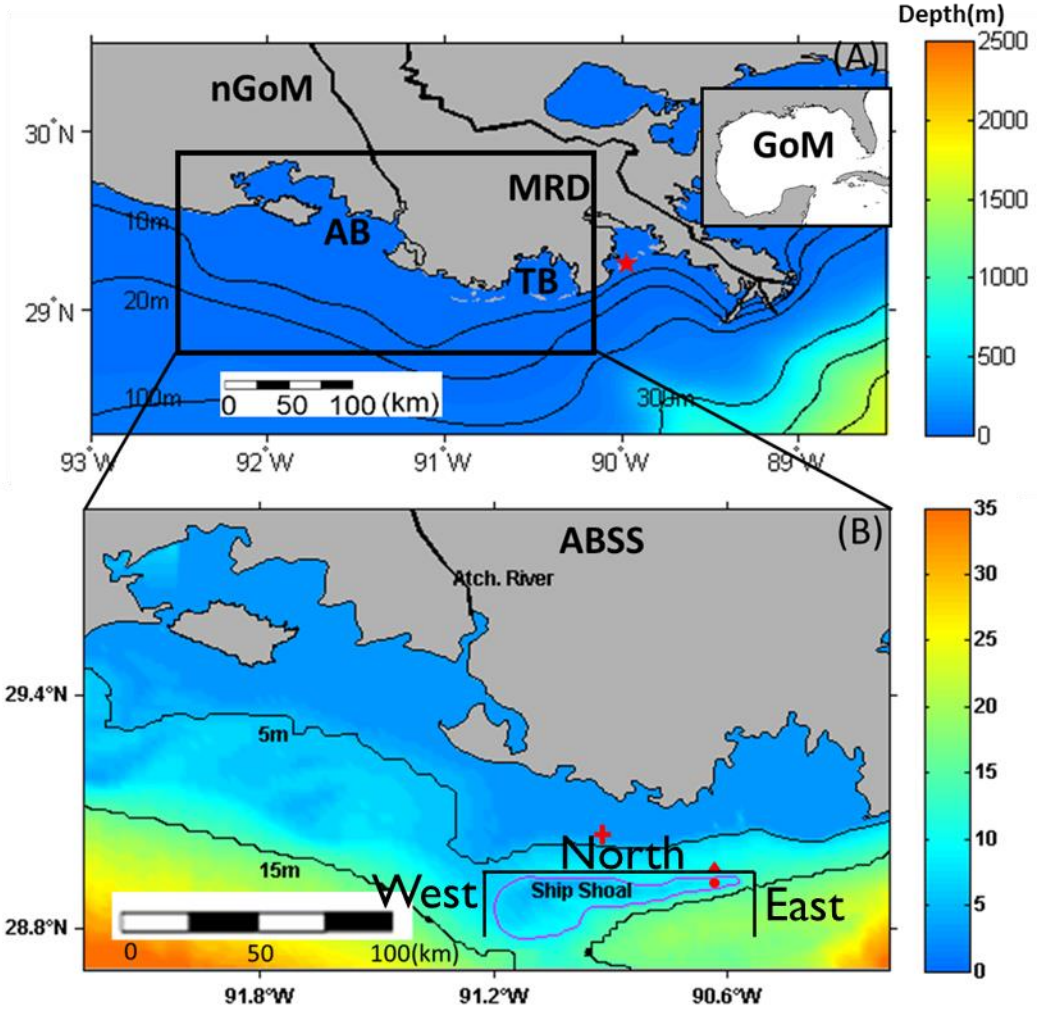

Figure 5.1. (A)(B) The northern Gulf of Mexico (nGoM) and Atchafalaya Bay and Ship Shoal (ABSS) domains used in the Regional Ocean Modeling System (ROMS) overlaid with water depth (color-shading; ETOPO1), Grand Isle (red star), location of tripod observation (red triangle), Caminada pit (red circle), Raccoon Island pit (red cross), and three black transects (north, south, and east of Ship Shoal). (AB: Atchafalaya Bay; TB: Terrebonne Bay; MRD: Mississippi River Delta)

5.2 Model setup

In this study, we run a series of numerical models in the three-dimensional, open-source Regional Ocean Modeling System, ROMS (Haidvogel et al. 2008; http://www.myroms.org/). The Community Sediment Transport Modeling System (CSTMS; http://www.cstms.org/) is incorporated into the ocean model (ROMS) to simulate sediment transport and deposition. Combined wave-current bottom boundary layer (BBL) calculations were based on Styles and Glenn (2000) along with moveable bed routines proposed by Harris and Wiberg (2001). More detailed descriptions of sediment transport calculations are in Warner et al. (2008).

The modeling period was fifteen months from July 01, 2017, to October 01, 2018, which was determined by the field surveying time of two geophysical field trips in Caminada pit for the model validation (Fig. 5.2). Details of geophysical results can be found in Chapter Two. One tripod-attached wave gauge sensor was deployed in August 2017, which was used to calculate wave heights. Our model domain covered the Atchafalaya Bay and Ship Shoal (hereby defined as ABSS domain) and has a 250m horizontal resolution with 16 weighted vertical layers (Fig. 5.1.A). The northern Gulf of Mexico (nGoM) model developed by Zang et al.(2019) was used to generate east, south and west noundary conditions for ABSS domain. Initial conditions of current velocity, sea level, temperature, and salinity were also interpolated from Zang et al. (2019). Monthly average freshwater and suspended sediment inputs from rivers debouching into the GoM were retrieved from the United States Geological Survey (USGS)'s Water Data for the Nation website (http://nwis.waterdata.usgs.gov) and applied as the boundary conditions. The mesh bathymetry was interpolated and smoothed from the ETOPO1 dataset (https://www.ngdc.noaa.gov/mgg/global/). The wave data were generated by Simulating Waves Nearshore model (SWAN, version 41.01) and then fed into ROMS as the wave forcing file.

Model outputs were saved every 12 hours for further analysis. The time step for the ABSS domain was 20s.

Zang et al. (2019) used four cohesive and two non-cohesive sediment classes for river inputs and two cohesive and non-cohesive sediment classes for the seabed. This study focuses on the sediment exchange between areas shallower and deeper than 5-m isobath. Thus, two shallow-sediment and two deep-sediment classes are added for the seafloor based on the 5m water depth contour (Fig. 5.3). Sand content of the seabed is interpolated from the USGS's usSEABED database (Williams et al. 2006), following the method of Xu et al. (2011). We set the initial sediment concentration in the water column as zero on Jan 01, 2017, and then we run the model for six months till July 01, 2017, to reach a relatively stable condition.

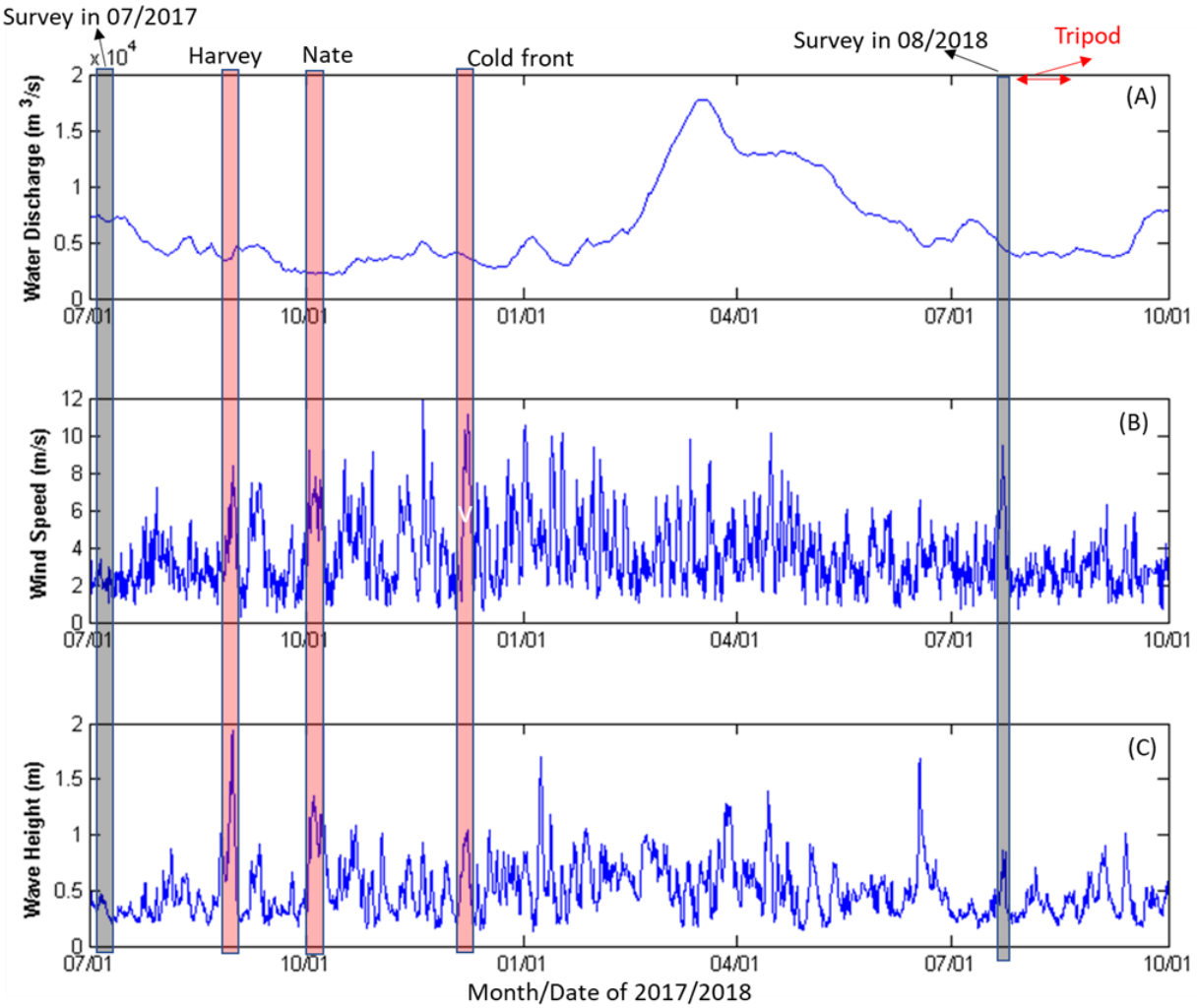

Figure 5.2. Time-series results in the Ship Shoal from 07/01/2017 to 10/01/2018. (A) Daily river discharge at USGS station 07374525 Atchafalaya River in Simmesport, LA. (B) Daily wind speed from NOAA station GISL1-8761724 in Grand Isle, LA. (C) SWAN-modeled wave height calculated at the tripod location (see location in Figure 5.1). Two geophysical surveys were completed in 07/2017 and 08/2018, marked as red blocks, respectively. Hurricanes Harvey (08/17/2017-09/01/2017), Nate (10/04/2017-10/08/2018), and a cold front (12/01/2017) are highlighted in grey blocks.

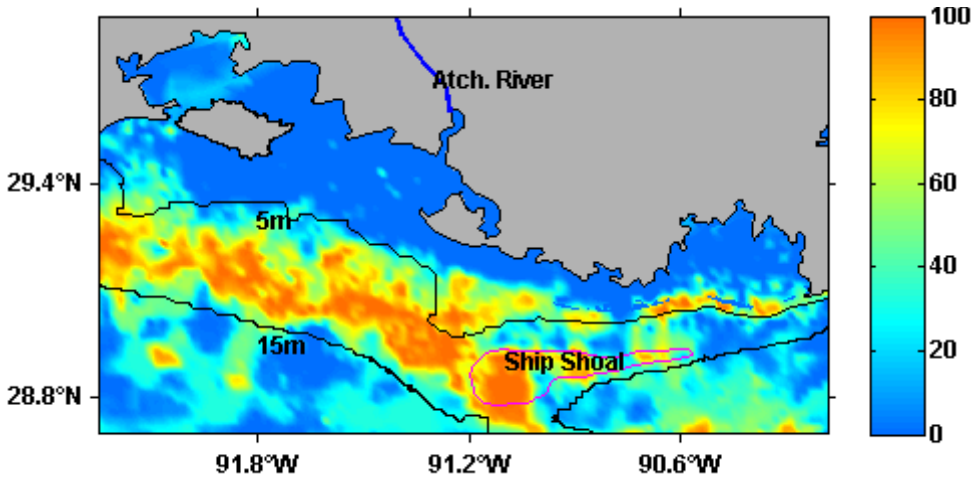

Figure 5.3 Interpolated sand fraction within the model grid based on usSEABED data (Williams et al. 2006), added contours of 5m and 15m. Shallow-sand and deep-sand classes are classified by 5m bathymetry contour. Polygon of Ship Shoal is marked in red and considered as the reference.

To achieve the most reasonable sediment parameterization, we used many parameters from Xu et al. (2011, 2016) and Zang et al. (2019) and compared our simulation results of surface suspended sediment concentration (SSC) against the map derived from Moderate Resolution Imaging Spectroradiometer. In Table 5.1, we list a summary of the sediment model parameterization used in this study. We prescribed four layers of sediment on the seafloor, each with a thickness of 1.0 m. This study added a total of 10 classes of sediment tracers based on Zang et al. (2019). Four classes of mud and two classes of sand from the Mississippi River and Atchafalaya River are added into this model. The seabed is classified into four classes as shallow sediments and deep sediments to explore the sediment exchange betwen shallow and deep water. Seabed erosion–deposition was based on non-cohesive parameterizations (Warner et al. 2008; Sherwood et al. 2018). SSC at the boundaries of the ABSS domain is interpolated from nGoM, and this study applies the gradient and radiation boundary condition to avert unreal artificial sediment plumes along the boundaries.

Table 5.1 Sediment characteristics parameterization

Sediment Type	Grain Diameter (mm)	Settling Velocity (mm/s)	Critical Shear Stress (Pa)	Erosional Rate (10^{-4} kg/m^2/s)
Mud_01(Mississippi River)	0.004	0.1	0.1	5
Mud_02(Mississippi River)	0.03	0.1	0.16	5
Mud_03(Atchafalaya River)	0.004	0.1	0.1	5
Mud_04(Atchafalaya River)	0.03	0.1	0.16	5
Mud_05(Shallow mud)	0.004	0.1	0.1	5
Mud_06(Deep mud)	0.004	0.1	0.1	5
Sand_01(Mississippi River)	0.0625	1	0.2	5
Sand_02(Atchafalaya River)	0.0625	1	0.2	5
Sand_03(Shallow sand)	0.0625	1	0.2	5
Sand_04(Deep sand)	0.0625	1	0.2	5

5.3 Model validation

5.3.1 Hydrodynamics model validation

ABSS domain is interpolated and nested on nGoM domain. Zang et al. (2019) validated the performance of each nGoM model (wave, ocean, and sediment) using available in-situ measurements. For wave, this study gathers daily averaged significant wave height at the tripod station in Ship Shoal (Fig. 5.1.B). The model-data comparison reveals a very good agreement between simulated and observed significant wave height (R^2 = 0.84; Fig. 5.4.). To further evaluate model simulated salinity over a longer period, this study interpolated simulated salinity to the observation sites at corresponding periods and compared it against available measurements from the Southeast Area Monitoring and Assessment Program (http://seamap.gsmfc.org), which has a total of 48 data points from surface, middle and bottom of water colum in 16 stations covering the period from 2017 to 2018 (Fig. 5.5.). The model-observation comparison in Figure 5.5. B indicates that the ocean model is capable of reproducing the pattern of salinity distribution (R^2 = 0.69), with low salinity water embracing Atchafalaya Bay and coastal Louisiana over the inner shelf and high salinity water further offshore.

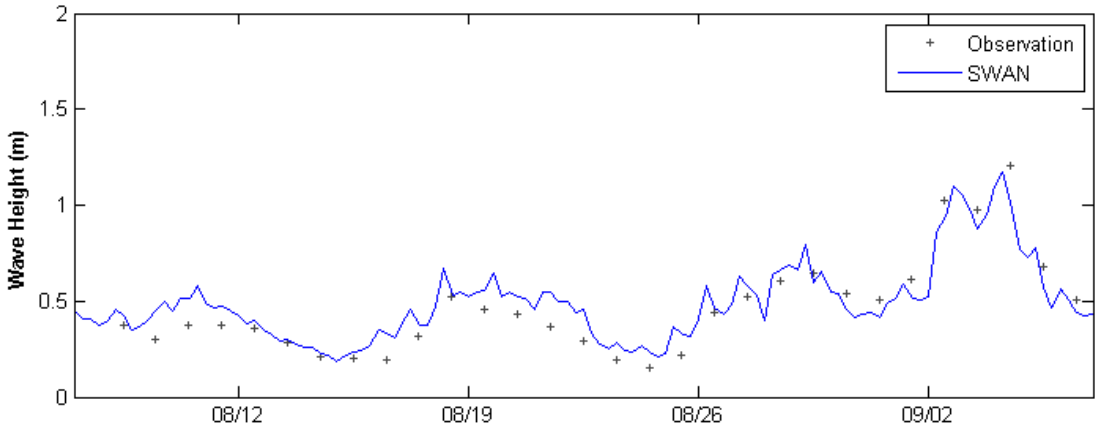

Figure 5.4. Comparison between observed and modeled daily mean significant wave height at tripod station from 07/08/2018 to 09/14/2018. See the location of the tripod in Fig. 5.1.

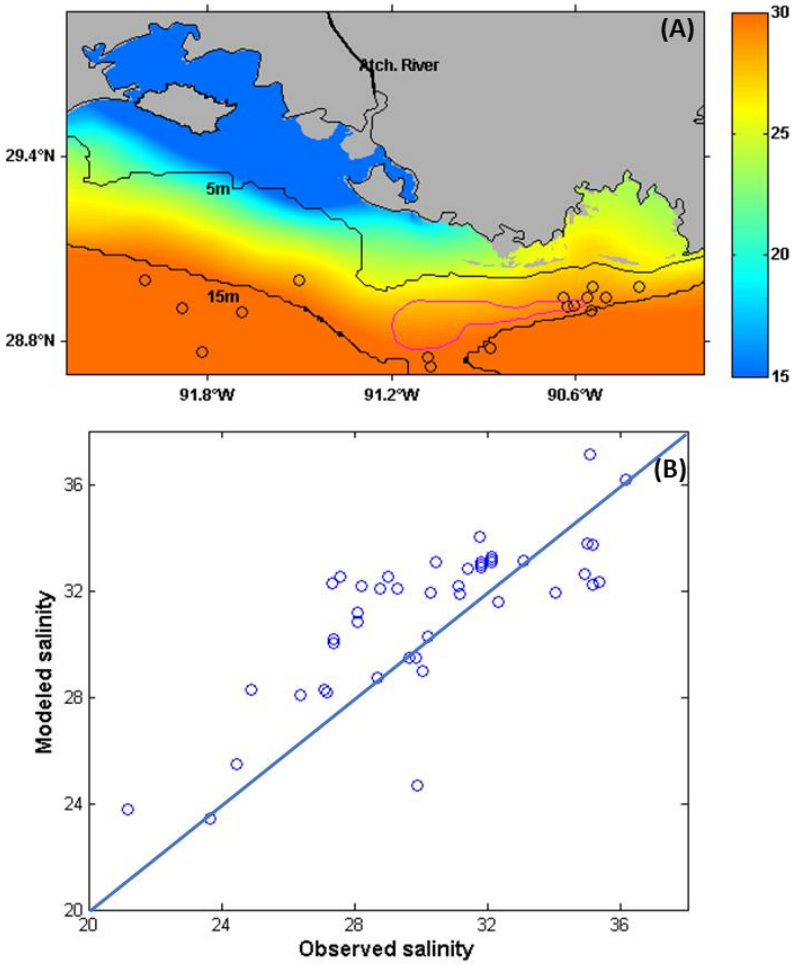

Figure 5.5. Salinity comparison between observations (data source: SEAMAP; http://seamap.gsmfc.org and tripod sensors) and model results of time-averaged surface salinity in the ABSS domain from July 2017 to October 2018. See the stations of salinity observation in A. For each station, we interpolate model results to the locations of the stations to ensure the comparability (R^2=0.69).

5.3.2 Sediment model validation

For the sediment model, we compare the simulated surface SSC against the map derived from the Moderate Resolution Imaging Spectroradiometer (MODIS-aqua; Fig. 5.6.). We select two cloud-free satellite images in September 2017 and April 2018 and apply them to the ABSS domain using the SSC algorithm developed by Miller and McKee (2004). In September 2017, turbid water from the Atchafalaya River dominated the entire Atchafalaya Bay and coastal water (water depth < 15 m). Westward sediment transport could be detected over the coastal Chenier Plain, where the westward alongshore current was strong (Fig. 5.6.A). In April 2018, both SSC and the spatial scale of sediment plume increased dramatically due to high fluvial discharge. The water discharge from the Atchafalaya River reached the highest level in March 2018 (Fig. 5.2.A), which extended sediment plume toward the south (Fig. 5.6.D). The westward transport along the Chenier Plain coast reduced compared with September 2017. During high river discharge, sediment plume from the Atchafalaya River could reach Ship Shoal (Fig.5.6. D). Modeling and satellite data generally agreed well on spatial patterns. The difference between the model result and satellite image in inner bays was likely due to: i) low wave generated inside bay near land, and ii) marsh-edge erosion and exchange are not considered in the model. The missing satellite data inner bay (grey zones inside bay) was due to the presence of dense clouds, sun glint, and water vapor in the coastal region.

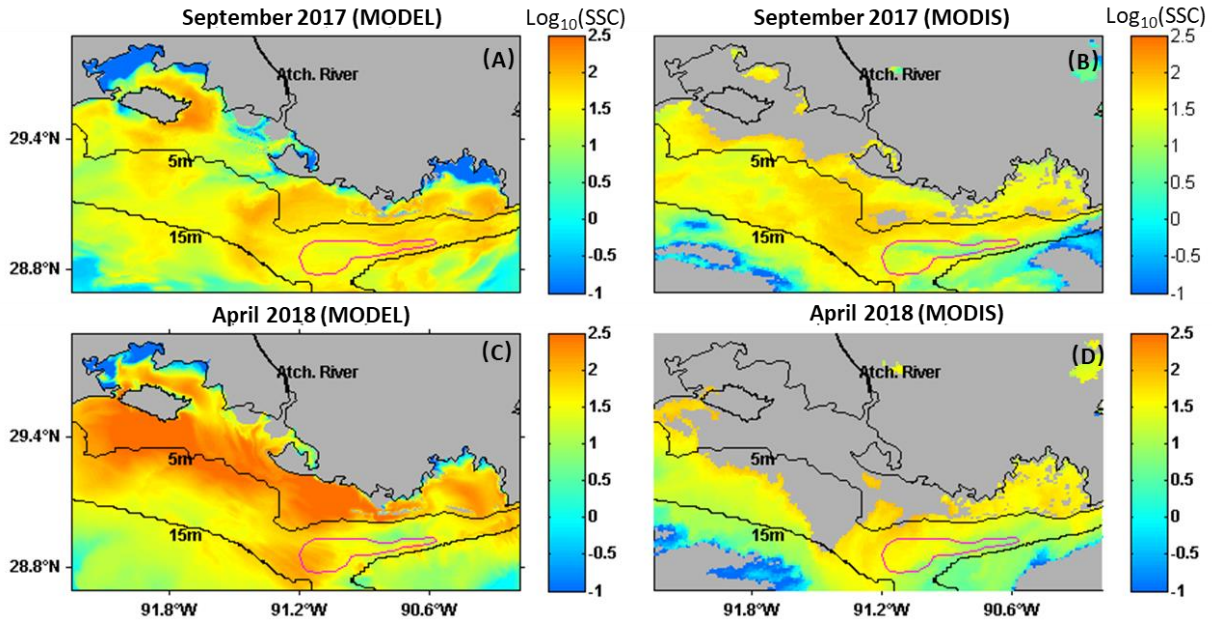

Figure 5.6. Comparison between 8-days averaged model-simulated surface SSC (left panel) and MODIS (aqua)-derived surface SSC (right panel) in September 2017 (09/11/2017-09/19/2017) and April 2018 (04/16/2018-04/24/2018), during which the number of good quality satellite images (no sun glint and cloud-free) is largest. Unit is in $\log_{10}$(mg/l).

5.4 Results

5.4.1 Averages for the year 2017 to 2018

For the period from 07/01/2017 to 10/01/2018, the model estimated that time-averaged surface salinity was low close to the mouth of Atchafalaya River, with a buoyant plume extending southwestward from the freshwater source (Fig. 5.7.A). Depth-averaged currents flowed southwestward at 0.1–0.2 m/s, being relatively strong on the shelf and weakening offshore. Wave orbital velocity was high near Ship Shoal and south of the barrier island near Terrebonne Bay (Fig. 5.7.B). Peak wave height during the entire year increased from about 0.5 m at the 5 m isobath to 1 m at 15 m isobath (Fig. 5.7.C). Shallow water depth and tall waves led to high orbital velocity in these areas. Ship Shoal is located in a region with relatively shallow depth with higher orbital velocity. In the mouth of Terrebonne Bay, the wave magnitude was high compared with the inner and northern part of the bay, which showed as the elongated

narrow yellow bar. Two small tidal inlets inside Terrebonne Bay also showed high orbital velocity (Fig. 5.7.B). Time-averaged and depth-integrated suspended fluvial sediment in the water column was estimated to be high close to the mouths of the Atchafalaya River (Fig. 5.7.D). As shown in Figure 5.7.D, year-average sediment concentration in ABSS varied greatly from 100 mg/l to almost zero. Most Atchafalaya suspended sediment was confined to the inner-most part of the shelf to the west of the bay mouth. Sediments deposited landward of the 5-m isobath, and a small portion of surface sediments can transport to Ship Shoal within 15 m isobaths.

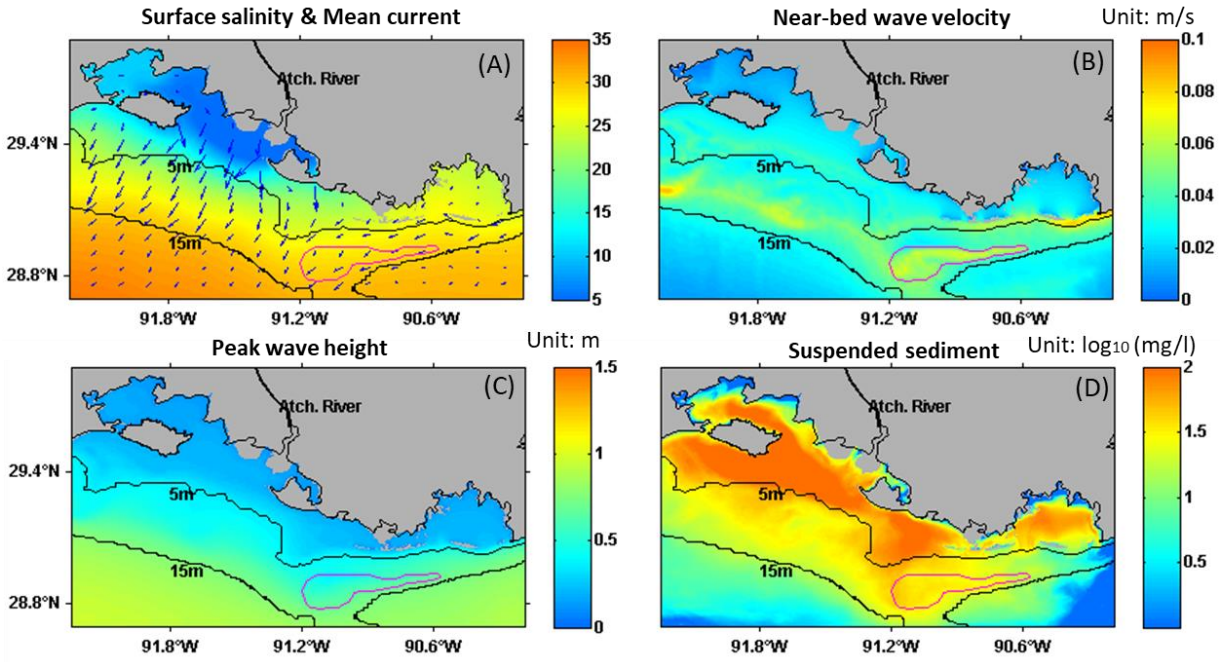

Figure 5.7. (A) Time-averaged surface salinity (color) and mean current (m/s) calculated for the year 2017 and 2018. (B) Near-bed wave orbital velocity (m/s). (C) Peak significant wave height (m) estimated by SWAN. (D) Time-averaged and depth-integrated fluvial suspended sediment (mg/l in logarithmic scale) in the water column calculated for the year 2017 and 2018.

5.4.2 Sediment dispersal

Seabed sediment mass can be determined from thickness, sediment-class distribution, porosity, grain density, and others (Sherwood et al. 2018). This study averaged model-simulated mud mass from 07/01/2017 to 10/01/2018 based on the changes in the sediment mass. Changes of seabed mud mass during this period show the sediment transport from Atchafalaya River to

the bay and then to the inner shelf of coastal Louisiana. As shown in Figure 5.8.A, mud accumulated on seabedwas high near the mouth of the Atchafalaya River and then decreased in the offshore direction to the inner shelf. A large amounts of the Atchafalaya sediments were retained inside the bay. Over the western Louisiana shelf, fluvial sediments were transported westward, crossing 91.2◦ W and deposited over the shelf (Fig. 5.8.A). From 07/01/2017 to 10/01/2018, a limited amount of sediment from the Atchafalaya River moved southeastward, passed Ship Shoal and accumulated southeast of Ship Shoal (green, about 1 kg/m^2). Still, the negligible amount can actually be preserved on top of Ship Shoal (blue, about 0.01 kg/m^2). Previous studies hypothesized that occasional sediment plume shifts from the Atchafalaya Bay to the southeast might result in the accumulation of a thin fluid-mud layer on some portions of the shoal (Stone et al. 2009; Xue et al. 2019; Liu et al. 2019). Our model results verify and prove that sediment bypassing above Ship Shoal is a possibility. Suspended mud may temporarily blanket the shoal or inside Caminada pit but is later transported elsewhere. The sediment transport process between bay and shelf exchange was dynamic in our model domain (Fig. 5.8.B). Suspended mud from the water shallower than 5m could transport to even cross Ship Shoal, which is also considered as the primary sediment source infilling Caminada dredge pit (Fig. 5.8.B). Over the simulation period, our model shows minimal fluvial sediment was deposited in waters deeper than 10 m, indicating limited cross-shelf suspended sediment transport.

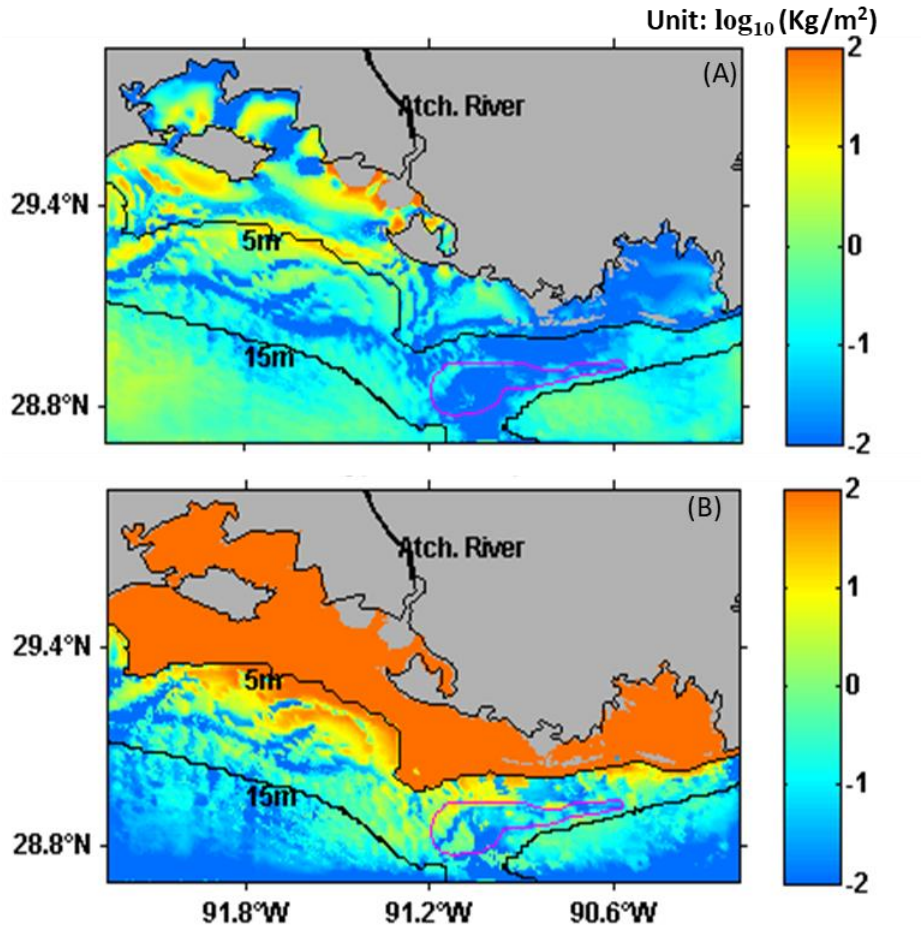

Figure 5.8. Change of seabed mud mass in ABSS domain from 07/01/2017 to 10/01/2018. (A) Sum of mud_03 and mud_04 in $\log_{10}$ scale from the Atchafalaya River (B) mud_05 in $\log_{10}$ scale from the bay and inner shelf shallower than 5m. Mud_03 are mud_04 are two sediment tracers from Atchafalaya river. Mud_05 is the shallow mud tracer showing in table 5.1. The unit is $\log_{10}$ (Kg/m^2).

5.5 Discussion

5.5.1 Sediment transport flux near Ship Shoal

Sediment transport fluxes were calculated along three transects (see locations in Fig. 5.1.B) north, east, and west of Ship Shoal, respectively. The magnitudes of east and west sediment fluxes of all ten sediment tracers generally exceeded those of northward fluxes (Fig. 5.9.B & 5.9.C). Negative magnitude in north transect indicated southward sediment flux from shallow areas in bay and inner shelf to Ship Shoal (Fig. 5.9.A). Though sediment flux in west

and east transects was generally westward (Fig. 5.9C), at times, winds reversed, creating some eastward flux (Fig 5.9B). During Hurricane Harvey (08/17/2017-09/01/2017) in 2017, for example, the high eastward flux of 5 kg/m/s occurred during periods of wind (8 m/s) and high wave height (2 m) (Fig. 5.2.B & 5.2.C). Eastward fluxes resumed once winds relaxed and reversed, leading to eastward sediment transport for the storm. After that, Hurricane Nate (10/04/2017-10/08/2017) and a cold front (12/01/2017) led to increased westward flux. It is well known that the hurricanes are counter-clockwise in the northern hemisphere. Since Ship Shoal was ~300 km east of the track line of Hurricane Harvey, its sediment transport was eastward. However, Ship Shoal was ~200 km west of the track line of Hurricane Nate, and its sediment transport was westward (Fig. 5.10.). This indicates hurricanes could bring sediments to infill dredge pits in Ship Shoal. However, the contributions from hurricanes are highly depending on the distance between hurricane track lines and dredge pits, the orientations, and the categoty of hurricanes.

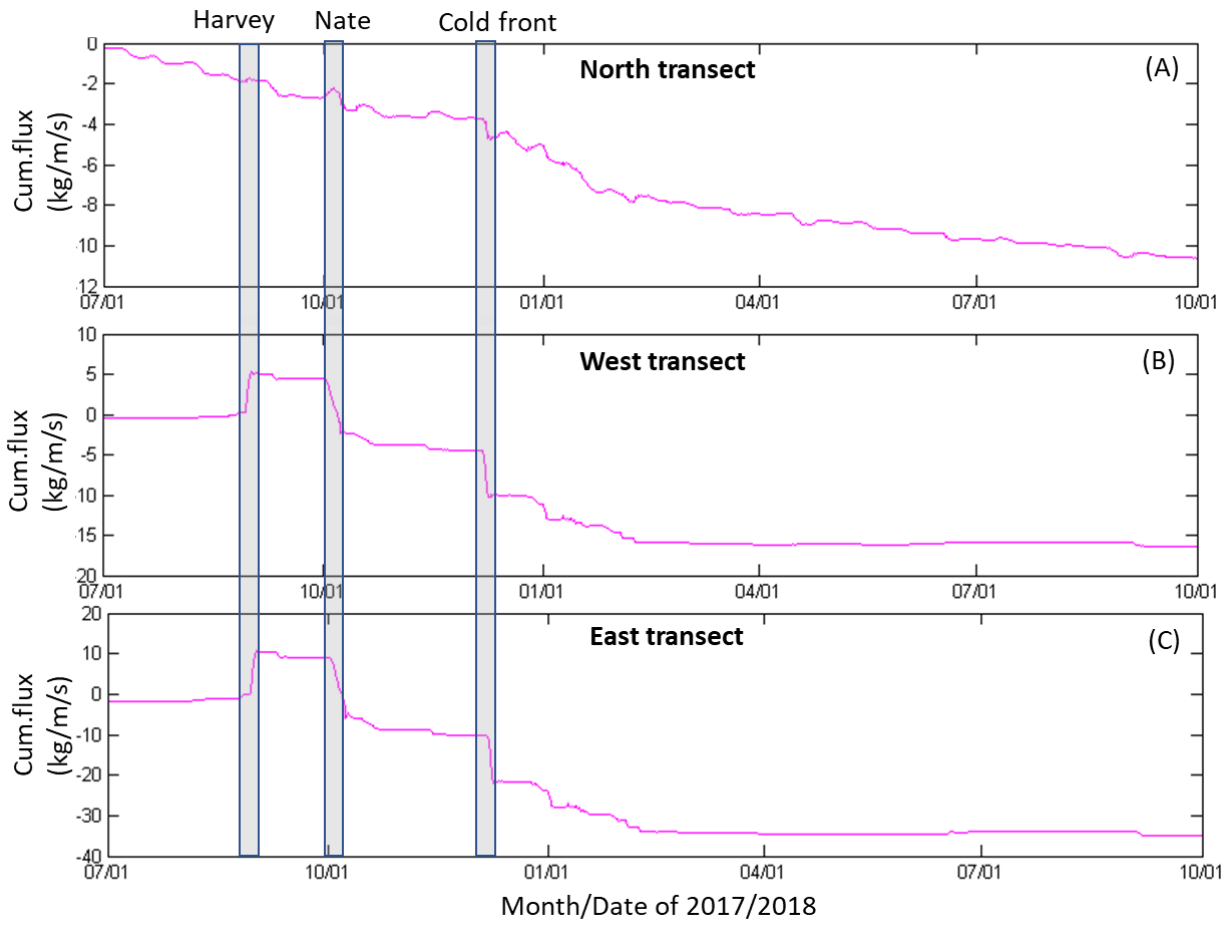

Figure 5.9. Cumulative sediment fluxes (in kg/m/s) near north(A), west(B), and east(C) transects. See locations of transects in Fig. 5.1.B.

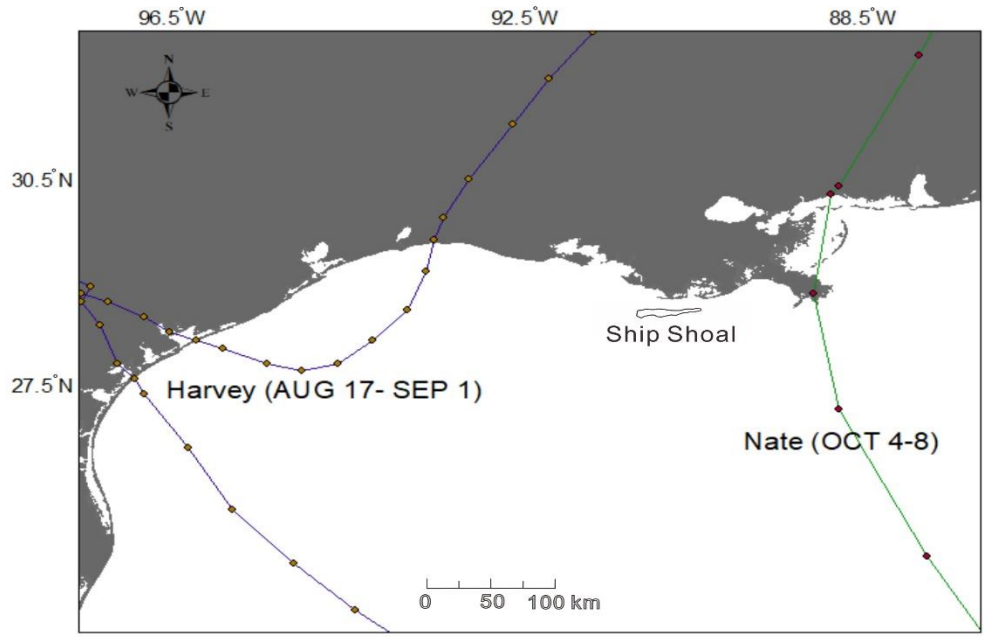

Figure 5.10. Hurricane and tropical storms track from 2017 to 2018 near Ship shoal. Data on tracks of Hurricanes Harvey and Nate downloaded from NOAA national hurricane center(https://www.nhc.noaa.gov/).

5.5.2 Application to dredging studies for coastal restoration

In the recent years, several pits were dredged in the ABSS domain, including Raccoon Island, Caminada, and Block 88 dredge pits (Fig. 5.3.). Calculation of sediment thickness infilling dredge pits is critical for future dredging activities. Ribberink and Nairn (2005) applied the 1D analytical approach and modeled the evolution of a proposed dredge pit in Block 88 (see location in Fig. 5.1.B), which is 31 km west of Caminada pit. Their equation included the empirical coefficients, settling velocity of mud, water depth of inside and outside the pit, background concentration outside, and tidal period but lacked consideration of wave resuspension, episodic extreme hurricane and other tropical events. It should be noted that they used a constant value for sediment concentration. Due to proximity, it is assumed that Caminada and Raccoon Island pits have a depositional environment similar with Block 88 pit. Due to the model grid horizontal resolution of 250 m, our ABSS model domain did not include Caminada and Raccoon Island pits in which sediments can be trapped (Fig. 5.8.). Instead of using one

constant in Nairn model in mnay previous studies, we derived a time series of bottom sediment concentrations (C_0) inside Caminada and Raccoon Island pit based on the ABSS model output from 07/01/2017 to 10/01/2018 and kept the other parameters the same (Nairn et al. 2005).

$$\Delta Z_b = k_1 C_0 \omega_s T \frac{1}{\rho_{dry}} \left[1 - \left(\frac{h_0}{h_1} \right)^3 \right] \quad (1)$$

Where ΔZ_b is total siltation thickness per tide (m), K1 is empirical coefficients. C_0 is background concentration outside the pit, which is generally determined by using the tide-mean and depth-averaged sediment concentration for the surrounding area (kg/m^3 or mg/l). ω_s is settling velocity of mud (m/s). T is a tidal period (s). ρ_{dry} is dry bulk density (kg/m^3). h_0 is water depth outside the pit (m). h_1 is water depth inside the pit (m).

From our calculations, the sediment concentration inside Caminada pit was very low (near 0 mg/l) in most of the days during the modeling period (Fig. 5.10A). However, the sediment thickness per day infilling Caminada pit increased to 0.005 m and even 0.017 m during the hurricanes or cold front that occurred during our modeling period (Fig. 5.10B). In contrast, sediment concentration inside the Racoon Island pit was much higher than in Caminada (0.05 mg/l), and sediment infilling in Raccoon Island pit was modelled to be dynamic and episodically increased with storm events (Fig. 5.10C). These findings of sediment infilling rate from modeling matched previous results from sediment coring and geophysical observation in Caminada pit and Raccoon Island pit. Xue et al. (2019), for instance, analyzed ^{7}Be penetration depths in repeat multi-coring study in Caminada pit and found seasonal sedimentation rates ranging between 7.3 cm/year and 55.0 cm/year in 2017. Liu et al. (2020) found the sediment infilling rate in Caminada pit of 15.00 cm/year calculated by a repeat bathymetric survey in 2017-2018. Similarly, O'Connor (2016) found that ^{7}Be profiles from Raccoon Island pit

accumulation rates exceeded an average of 0.24 cm/day and that multicores within pit contained almost entirely silt. Liu et al. (2020) also found sediment infilling rate in Raccoon Island showed a much higher rate of 1.1 m/year. Our model also captured similar patterns, in which bottom sediment concentration in Raccoon Island pit was generally higher than over Caminada during the same time period. The total calculated sediment thickness in Raccoon Island pit from July 2017-Oct 2018 (~2.1 m) was more significant than in Caminada pit (~0.25 m) in the ABSS model domain (Fig. 5.11).

Our modeling results show that hurricanes Harvey and Nate and one cold front in 2017 suspended sediment which can possibly contribute to infilling of dredge pits (Fig. 5.11), but they accounted for less than 10% of sediments infilling in both Caminada and Raccoon Island dredge pits from July 2017-Oct 2018. Xu et al. (2016) reported that the region to the east of tracks of hurricanes Katrina and Rita had stronger winds, taller waves and deeper erosions at centimeter to meter levels. The relatively low contribution of 10% should be mainly due to very-far distances (> 100s km) from dredge pits to hurricanes Harvey and Nate. If eyes of hurricanes had passed pits within a few kilometers, their contribution would be presumably much higher. In addition, hurricanes can generate very tall waves which trigger landslides and mass wasting of pit walls which is not in our model. Moreover, hurricanes contributions of 10% should be used with cautions because of the following simiplications and assumptions: (1) the interaction between dredge pits and hydrodynamic condition (including waves and currents) is negeleted; (2) the wind input for our ROMS model may not be highly enough to fully resolve hurricanes Harvey and Nate when dealing with high spatial resoltuon; and (3) as now our ROMS model only included suspended sediment load but did not include any bed load or fluid mud processes which can be significant contributors to pit infilling.

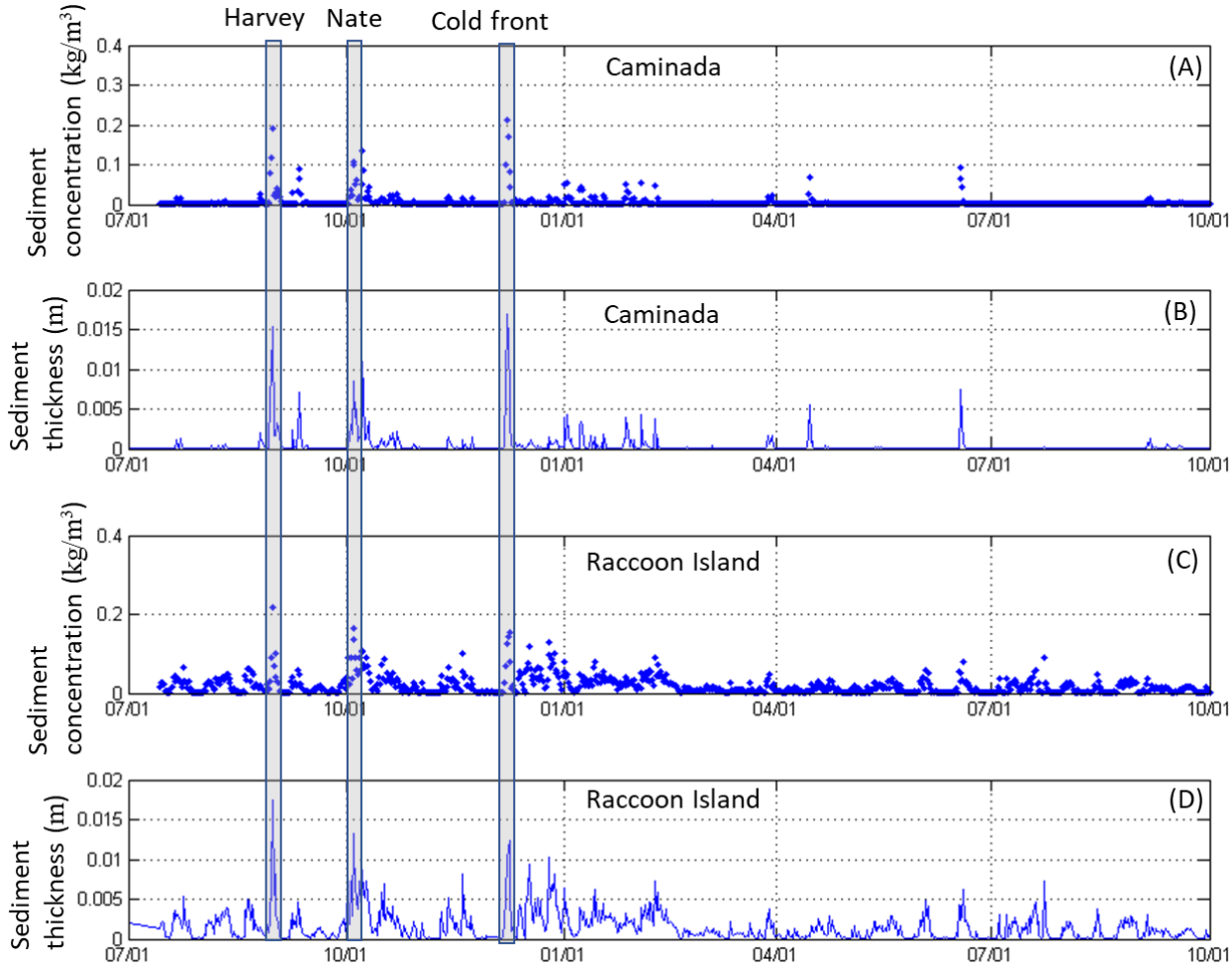

Figure 5.11. Time series change of sediment thickness in Caminada pit (A and B) and Raccoon Island pit (C and D) from 07/07/2017 to 10/01/2018. Two tropical events and one cold front were marked in grey blocks.

Xue et al. (2019) found laminations from sediment coring were related to Hurricane Harvey induced deposition in 2017. The depth-average bottom concentration from our model correlated well with the occurrence of Hurricane Harvey, Nate, and cold front in 2017 (Fig. 5.11.). It indicated hurricanes or tropical storms were potential sources infilling Caminada and Raccoon Island pits. However, Nairn's model showing above was not included in this factor. Also, Nairn's model applied a constant sediment concentration when calculating the infilling process. Still, our modeling result indicated sediment concentration was temporally dynamic

inside Caminada pit and Raccoon Island pit (Fig. 5.11.). Future modeling work of the infilling process should consider these factors.

Regarding the sediment budgets for coastal restoration in Louisiana, the longshore transport in our model domain drived sediment coming from the river, inner shelf, and bay westward to Texas (Fig. 5.8.). It will lead to decreasing/losing sediment, especially during the strong long-shore current. Suspended mud sediment from rivers, inner shelf, and bay can bypass or transport and deposit in Caminada pit, which indicated Caminada pit and Raccoon Island pits would not be considered as a renewable pit for future sand dredging activities for coastal restoration.

5.5.3 Limitation and future work

This simulation reproduced the overall pattern of sediment dispersal and bay shelf exchange in the ABSS. However, it is noteworthy that a few critical sediment transport mechanisms were not included in our model. First, sand and mud transport in a different way, and for the future study comparison of these two will be tested. Secondly, this study does not consider wave-supported fluid mud in the ABSS domain. Previous studies (Sheremet et al. 2011; Traykovski et al. 2015) found wave-supported fluid mud movement is another important mechanism in terms of fluvial sediment across-shelf transport over the muddy Atchafalaya Shelf. Lastly, marsh edge sediment inside bays is not considered into this model. It is likely to lead to the low sediment concentration near marsh edge. For future modeling work, the ABSS domain can be subdivided into a small domain with high-resolution grid nested dredge pits inside. It can better to test and compare the sediment infilling process inside pits and outside pits. This study only uses the sediment module in ROMS with waves feeding as the input file, and future studies can be focused on the coupling of SWAN and ROMS.

5.6 Conclusion

This study adapted the sediment transport model to the ABSS to investigate sediment dynamics and exchange from riverine/bay/inner shelf to Ship Shoal. Our model simulation shows that:

(1) Suspended fluvial sediment in the water column accumulated close to the mouths of Atchafalaya River, and most of the suspended sediment was confined to the inner-most part of the continental shelf to the west of the bay mouth. Only a small portion of sediments can transport to Ship Shoal within 15 m isobaths. The coastal current carried some Atchafalaya sediment westward.

(2) Suspended mud from the Atchafalaya river can transport and bypass above Ship Shoal. The sediment transport process between bay and shelf exchange was dynamic in ABSS. Suspended mud from the inner shelf could also be transported to even cross Ship Shoal and generated a thin mud layer, which was also considered as the primary sediment source infilling the Caminada dredge pit.

(3) Since Ship Shoal was ~300 km east of the track line of Hurricane Harvey, its sediment transport was eastward. Ship Shoal was ~200 km west of the track line of Hurricane Nate, and its sediment transport was westward. The magnitudes of sediment fluxes from east and west of Ship Shoal exceeded those of north fluxes offshore of both sediment sources. Two hurricanes and one cold front changed the direction of sediment flux near Ship Shoal, even the distance between hurricanes and Ship Shoal was more than 200 km. This indicated hurricanes could bring a proportion of sediments infilling pits in Ship Shoal. However, hurricanes contributed less than 10% of sediments infilling in both Caminada and Raccoon

Island dredge pits from July 2017-Oct 2018 due to far distances. This percentage can change dramatically for other hurricanes during other periods.

(4) Our model also captured that bottom sediment concentration in Raccoon Island pit was relatively higher than the one in Caminada in the same period. The total sediment thickness in Raccoon Island pit (~2.3 m) was greater than in the Caminada pit (~0.25 m) in the ABSS model domain. Suspended mud sediment from the river, inner shelf, and bay can bypass or transport and deposit in Caminada pit and Racoon Island pit, which showed Caminada pit and Raccoon Island pits would not be considered as a renewable pit for future sand dredging activities for coastal restoration.

CHAPTER 6. SUMMARY

This dissertation focuses on the study of sediment transport and geomorphological evolution in the transgressive Ship Shoal using three different approaches, including geophysics, ROMS modeling, and supervised machine learning.

Chapters two and three explored two case studies of Caminada dredge pit and Raccoon Island pit near Ship Shoal using geophysical methods. The topography of seafloor inside Caminada pit has a direct relationship with the patchy mud distribution. Sidescan mosaic maps showed topographic lows, or troughs, inside Caminada pit infilled with mud within two years after dredging. Repeat bathymetric surveys showed the pit margin in Raccoon Island and Caminada pits were generally stable, with no obvious outward migration, which indicated the current setback buffer distances of ~300 m from oil and gas pipelines were sufficient. However, the integration of repeat bathymetric and backscatter surveys showed that the infilling rate in Raccoon Island pit (1.10 m/s) was much higher than in the Caminada pit (0.15 m/s). Raccoon Island pit was filled up on or before 2018, but Caminada pit is still collecting sediments slowly. The pit wall slope change rate in Raccoon Island pit is also higher than in Caminada pit. Caminada and Raccoon Island pit are not considered as a renewable resource for future restoration due to high mud content.

Chapter four trains multiply machine learning models to identify the mud deposition and classify the seafloor sediment types inside Caminada pit. Grain size analysis of 58 sediment samples inside Caminada pit shows mud is prone to deposit in the deeper trough zones with lower backscatter values, while sand is likely to appear on the flat seabed with higher backscatter values. The variable importance analysis indicates that backscatter, roughness_bathymetry, and rugosity_backscatter, and bathymetry (from high to low) are four most significant features to

classify sediment types. Random Forest model with these four selected features has the best classification power with the accuracy rate of 0.9 to predict the sediment types inside Caminada pit.

Chapter five uses the sediment transport model to the ABSS domain to investigate sediment dynamics from riverine/bay/inner shelf to Ship Shoal. This model simulation reveals that suspended fluvial sediment accumulated close to the mouth of Atchafalaya River, and most of the suspended sediment was confined to the inner-most part of the shelf to the west of the bay mouth. Only a small portion of suspended mud from the Atchafalaya River can be transported southward and bypass Ship Shoal. Mud from the inner shelf could be transported to Ship Shoal and was considered as the major sediment source infilling Caminada and Raccoon Island pits. Two hurricanes and one tropical event impacted the direction of sediment transport flux near Ship Shoal, even the distance between hurricanes and Ship Shoal was more than 200 km. This indicated hurricanes could bring a proportion of sediments infilling pits in Ship Shoal. However, hurricanes could contribute less than 10% of sediments infilling in both Caminada and Raccoon Island dredge pits.

Sandy shoals (such as Ship Shoal pits) are prominent and high-quality sand sources off the Louisiana coast, but the long transportation distance makes it not cost-effective. Instead, borrowing sand from paleo-channels (such as Raccoon Island pit) provides an alternative and cost-effective method for sandy shoal dredging. However, both geophysical and modeling methods improve that suspended mud sediment from the river, inner shelf and bay can bypass or transport and deposit in Caminada, and Racoon Island pits, which shows both pits would not be considered as a renewable pit for future sand dredging activities for coastal restoration due to high mud content.

APPENDIX A. CHAPTER 2 SUPPLEMENTAL MATERIALS

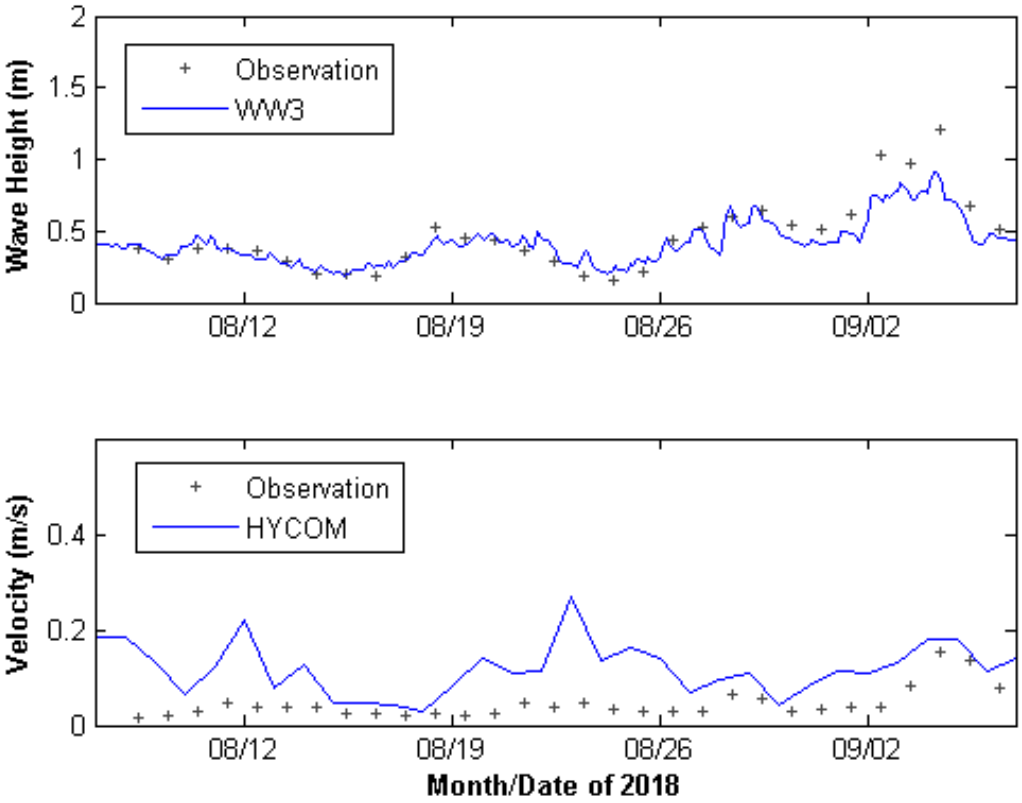

Figure A1. Daily wave height and horizontal current velocity from the tripod near Caminada dredge pit with the comparison with NOAA WAVEWATCH III and HYCOM from 07/08/2018 to 09/14/2018.

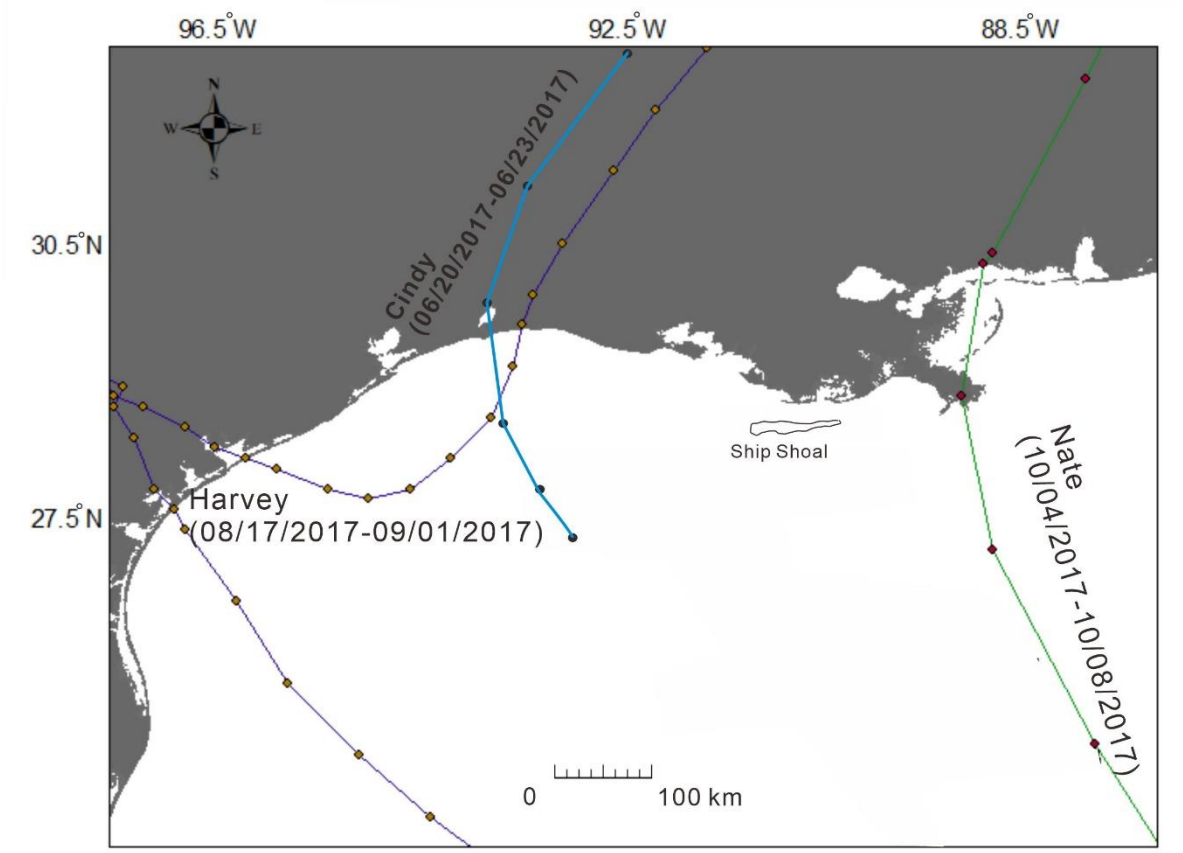

Figure A2. Hurricane and tropical storms tracks in 2017 near Ship Shoal. Track map of Hurricanes Harvey and Nate is from NOAA national hurricane center.

APPENDIX B. COPYRIGHT INFORMATION

Re: Published paper copyright question

MM Ms. Madeline Zhang/MDPI <madeline.zhang@mdpi.com>
To Haoran Liu
Cc water@mdpi.com

Reply | Reply All | Forward | ...
Sun 5/24/2020 7:52 PM

We removed extra line breaks from this message.

Dear Dr. Liu,

Thank you very much for your message. Actually, no special permission is required to reuse all or part of article published by MDPI, including figures and tables. For articles published under an open access Creative Common CC BY license, any part of the article may be reused without permission provided that the original article is clearly cited.

You can find more detail by these two links:
https://nam04.safelinks.protection.outlook.com/?url=https%3A%2F%2Fwww.mdpi.com%2Fabout%2Fopenaccess&data=02%7C01%7Chliu39%40lsu.edu%7C2176bf76922644536df508d800569aed%7C2d4dad3f50ae47d983a09ae2b1f466f8%7C0%7C0%7C637259719252070062&sdata=PeVmAMTmeZ5WdHGzow0WndDNQUhtNz9EBijNS46Mf%2B4%3D&reserved=0
https://nam04.safelinks.protection.outlook.com/?url=https%3A%2F%2Fcreativecommons.org%2Flicenses%2Fby%2F4.0%2F&data=02%7C01%7Chliu39%40lsu.edu%7C2176bf76922644536df508d800569aed%7C2d4dad3f50ae47d983a09ae2b1f466f8%7C0%7C0%7C637259719252070062&sdata=8NDEK1wvVv%2BVLPS7HQlYZLD4vvChFmWk7Zfln4I5sCE%3D&reserved=0

If you have any other questions, please feel free to contact us directly.

Kind regards,

Ms. Madeline Zhang
Assistant Editor
E-Mail: madeline.zhang@mdpi.com
Water (https://nam04.safelinks.protection.outlook.com/?url=http%3A%2F%2Fwww.mdpi.com%2Fjournal%2Fwater&data=02%7C01%7Chliu39%40lsu.edu%7C2176bf76922644536df508d800569aed%7C2d4dad3f50ae47d983a09ae2b1f466f8%7C0%7C0%7C637259719252080060&sdata=QYraRcuaL8ruXa%2BXaFJgQe9DaQx%2FZk6NZ65gnMzTktk%3D&reserved=0)
We invite you to follow us on Twitter @Water_MDPI

On 2020/5/24 4:22, Haoran Liu wrote:
> Dear Ms. Madeline,
>
> I published one article in WATER in 2019. Please see the details below.
>
> Sediment identification using machine-learning classifiers in a
> mixed-texture dredge pit of Louisiana shelf for coastal restoration.
>
> I would like to include this article in my Ph.D. dissertation and need
> to get your permission before I submit to my graduation office.
>
> Thank you for your help.
>
> Best,
>

REFERENCES

Ajdukiewicz, JM, PH Nicholson, and WL Esch. 2010. 'Prediction of deep reservoir quality using early diagenetic process models in the Jurassic Norphlet Formation, Gulf of Mexico', AAPG bulletin, 94: 1189-227.

Alleway, Heidi K, and Sean D Connell. 2015. 'Loss of an ecological baseline through the eradication of oyster reefs from coastal ecosystems and human memory', Conservation Biology, 29: 795-804.

Allison, Mead A, Gail C Kineke, Elizabeth S Gordon, and Miguel A Goni. 2000. 'Development and reworking of a seasonal flood deposit on the inner continental shelf off the Atchafalaya River', Continental Shelf Research, 20: 2267-94.

Allison, Mead A, Michael T Ramirez, and Ehab A Meselhe. 2014. 'Diversion of Mississippi River water downstream of New Orleans, Louisiana, USA to maximize sediment capture and ameliorate coastal land loss', Water resources management, 28: 4113-26.

Alzaga-Ruiz, Humberto, Didier Granjeon, Michel Lopez, Michel Seranne, and François Roure. 2009. 'Gravitational collapse and Neogene sediment transfer across the western margin of the Gulf of Mexico: Insights from numerical models', Tectonophysics, 470: 21-41.

Amoudry, Laurent. 2008. 'A review on coastal sediment transport modelling'.

Armstrong, Christopher, David Mohrig, Thomas Hess, Terra George, and Kyle M Straub. 2014. 'Influence of growth faults on coastal fluvial systems: examples from the late Miocene to Recent Mississippi River Delta', Sedimentary Geology, 301: 120-32.

Atkinson, Elizabeth J, and Terry M Therneau. 2000. 'An introduction to recursive partitioning using the RPART routines', Rochester: Mayo Foundation.

Bayraktarov, Elisa, Megan I Saunders, Sabah Abdullah, Morena Mills, Jutta Beher, Hugh P Possingham, Peter J Mumby, and Catherine E Lovelock. 2016. 'The cost and feasibility of marine coastal restoration', Ecological applications, 26: 1055-74.

Benedet, L., and J. H. List. 2008. 'Evaluation of the physical process controlling beach changes adjacent to nearshore dredge pits', Coastal Engineering, 55: 1224-36.

Blondel, Ph, and O Gómez Sichi. 2009. 'Textural analyses of multibeam sonar imagery from Stanton Banks, Northern Ireland continental shelf', Applied Acoustics, 70: 1288-97.

Bolaños, Rodolfo, Jennifer M Brown, and Alejandro J Souza. 2014. 'Wave–current interactions in a tide dominated estuary', Continental Shelf Research, 87: 109-23.

Boyd, SE, DS Limpenny, HL Rees, KM Cooper, and S Campbell. 2003. 'Preliminary observations of the effects of dredging intensity on the re-colonisation of dredged

sediments off the southeast coast of England (Area 222)', Estuarine, Coastal and Shelf Science, 57: 209-23.

Breiman, Leo. 1996. 'Bagging predictors', Machine learning, 24: 123-40.

Brown, Craig J, and Jenny S Collier. 2008. 'Mapping benthic habitat in regions of gradational substrata: an automated approach utilising geophysical, geological, and biological relationships', Estuarine, Coastal and Shelf Science, 78: 203-14.

Brown, Jennifer M, Laurent O Amoudry, Alejandro J Souza, and Jon Rees. 2015. 'Fate and pathways of dredged estuarine sediment spoil in response to variable sediment size and baroclinic coastal circulation', Journal of environmental management, 149: 209-21.

Buhl-Mortensen, Pål, Margaret Dolan, and Lene Buhl-Mortensen. 2009. 'Prediction of benthic biotopes on a Norwegian offshore bank using a combination of multivariate analysis and GIS classification', ICES Journal of Marine Science, 66: 2026-32.

Byrnes, Mark R, Richard M Hammer, Tim D Thibaut, and David B Snyder. 2004. 'Physical and biological effects of sand mining offshore Alabama, USA', Journal of Coastal Research: 6-24.

Caldwell, Rebecca L, and Douglas A Edmonds. 2014. 'The effects of sediment properties on deltaic processes and morphologies: A numerical modeling study', Journal of Geophysical Research: Earth Surface, 119: 961-82.

Calvert, Jay, James Asa Strong, Matthew Service, Chris McGonigle, and Rory Quinn. 2014. 'An evaluation of supervised and unsupervised classification techniques for marine benthic habitat mapping using multibeam echosounder data', ICES Journal of Marine Science, 72: 1498-513.

Chassignet, Eric P, Harley E Hurlburt, E Joseph Metzger, Ole Martin Smedstad, James A Cummings, George R Halliwell, Rainer Bleck, Remy Baraille, Alan J Wallcraft, and Carlos Lozano. 2009. 'US GODAE: global ocean prediction with the HYbrid Coordinate Ocean Model (HYCOM)', Oceanography, 22: 64-75.

Chassignet, Eric P, Harley E Hurlburt, Ole Martin Smedstad, George R Halliwell, Patrick J Hogan, Alan J Wallcraft, Remy Baraille, and Rainer Bleck. 2007. 'The HYCOM (hybrid coordinate ocean model) data assimilative system', Journal of Marine Systems, 65: 60-83.

Chen, Changsheng, Haosheng Huang, Robert C Beardsley, Hedong Liu, Qichun Xu, and Geoffrey Cowles. 2007. 'A finite volume numerical approach for coastal ocean circulation studies: Comparisons with finite difference models', Journal of Geophysical Research: Oceans, 112.

Coastal Engineering Consultants Inc. 2017. 'NRDA Caminada Headland Beach and Dune Restoration, Increment II (BA-143) Completion Report', Prepared for Coastal Protection and Restoration Authority: Baton Rouge, LA, 63p. + 23 appendice

Couvillion, Brady R, John A Barras, Gregory D Steyer, William Sleavin, Michelle Fischer, Holly Beck, Nadine Trahan, Brad Griffin, and David Heckman. 2011. 'Land area change in coastal Louisiana from 1932 to 2010'.

Couvillion, Brady R, Holly Beck, Donald Schoolmaster, and Michelle Fischer. 2017. "Land area change in coastal Louisiana (1932 to 2016)." In.: US Geological Survey.

Dartez, J.S. 2016. "“The Biggest, The Baddest, and The Bestest – Coastal Restoration Cajun Style” Proceedings of the Twenty', First World Dredging Congress, WODCON XXI, Miami, Florida, USA.

Day, John W, Donald F Boesch, Ellis J Clairain, G Paul Kemp, Shirley B Laska, William J Mitsch, Kenneth Orth, Hassan Mashriqui, Denise J Reed, and Leonard Shabman. 2007. 'Restoration of the Mississippi Delta: lessons from hurricanes Katrina and Rita', science, 315: 1679-84.

Deng, Hang, Lesli Wood, Irina Overeem, and Eric Hutton. 2016. "The Influence of Topography on Subaqueous Sediment Gravity Flows and the Resultant Deposits: Examples from Deep-water Systems in Offshore Morocco and Offshore Trinidad." In AGU Fall Meeting Abstracts.

Denny, JF, WE Baldwin, WC Schwab, PT Gayes, R Morton, and NW Driscoll. 2007. "Morphology and texture of modern sediments on the inner shelf of South Carolina's Long Bay from Little River Inlet to Winyah Bay." In.: US Geological Survey.

Desprez, Michel. 2000. 'Physical and biological impact of marine aggregate extraction along the French coast of the Eastern English Channel: short-and long-term post-dredging restoration', ICES Journal of Marine Science, 57: 1428-38.

Diesing, Markus, Sophie L Green, David Stephens, R Murray Lark, Heather A Stewart, and Dayton Dove. 2014. 'Mapping seabed sediments: Comparison of manual, geostatistical, object-based image analysis and machine learning approaches', Continental Shelf Research, 84: 107-19.

Dinnel, Scott Page, and Wm J Wiseman Jr. 1986. 'Fresh water on the Louisiana and Texas shelf', Continental Shelf Research, 6: 765-84.

Dolan, Margaret FJ, and Vanessa L Lucieer. 2014. 'Variation and uncertainty in bathymetric slope calculations using geographic information systems', Marine Geodesy, 37: 187-219.

Drucker, Barry S, William Waskes, and Mark R Byrnes. 2004. 'The US minerals management service outer continental shelf sand and gravel program: environmental studies to assess

the potential effects of offshore dredging operations in federal waters', Journal of Coastal Research: 1-5.

Du Preez, Cherisse. 2015. 'A new arc–chord ratio (ACR) rugosity index for quantifying three-dimensional landscape structural complexity', Landscape ecology, 30: 181-92.

Dubois, Stanislas, Carey G Gelpi, Richard E Condrey, Mark A Grippo, and John W Fleeger. 2009. 'Diversity and composition of macrobenthic community associated with sandy shoals of the Louisiana continental shelf', Biodiversity and Conservation, 18: 3759-84.

Dunn, Daniel C, and Patrick N Halpin. 2009. 'Rugosity-based regional modeling of hard-bottom habitat', Marine Ecology Progress Series, 377: 1-11.

Elvenes, Sigrid, Margaret FJ Dolan, Pål Buhl-Mortensen, and Valérie K Bellec. 2013. 'An evaluation of compiled single-beam bathymetry data as a basis for regional sediment and biotope mapping', ICES Journal of Marine Science, 71: 867-81.

Freeman, Angelina M, Harry H Roberts, and Patrick D Banks. 2007. 'Hurricane impact analysis of a Louisiana shallow coastal bay bottom and its shallow subsurface geology'.

Galparsoro, Ibon, Ángel Borja, Juan Bald, Pedro Liria, and Guillem Chust. 2009. 'Predicting suitable habitat for the European lobster (Homarus gammarus), on the Basque continental shelf (Bay of Biscay), using Ecological-Niche Factor Analysis', Ecological modelling, 220: 556-67.

Gonzalez-Mirelis, Genoveva, and Mats Lindegarth. 2012. 'Predicting the distribution of out-of-reach biotopes with decision trees in a Swedish marine protected area', Ecological applications, 22: 2248-64.

Grant, William D, and Ole Secher Madsen. 1979. 'Combined wave and current interaction with a rough bottom', Journal of Geophysical Research: Oceans, 84: 1797-808.

Guinan, Janine, Colin Brown, Margaret FJ Dolan, and Anthony J Grehan. 2009. 'Ecological niche modelling of the distribution of cold-water coral habitat using underwater remote sensing data', Ecological Informatics, 4: 83-92.

Haidvogel, Dale B, Hernan Arango, W Paul Budgell, Bruce D Cornuelle, Enrique Curchitser, Emanuele Di Lorenzo, Katja Fennel, W Rockwell Geyer, Albert J Hermann, and Lyon Lanerolle. 2008. 'Ocean forecasting in terrain-following coordinates: Formulation and skill assessment of the Regional Ocean Modeling System', Journal of Computational Physics, 227: 3595-624.

Hanley, ME, SPG Hoggart, DJ Simmonds, A Bichot, MA Colangelo, F Bozzeda, H Heurtefeux, B Ondiviela, R Ostrowski, and M Recio. 2014. 'Shifting sands? Coastal protection by sand banks, beaches and dunes', Coastal Engineering, 87: 136-46.

Harris, Courtney K, Christopher R Sherwood, Richard P Signell, Aaron J Bever, and John C Warner. 2008. 'Sediment dispersal in the northwestern Adriatic Sea', Journal of Geophysical Research: Oceans, 113.

Hasan, Rozaimi Che, Daniel Ierodiaconou, and Laurie Laurenson. 2012. 'Combining angular response classification and backscatter imagery segmentation for benthic biological habitat mapping', Estuarine, Coastal and Shelf Science, 97: 1-9.

Hasan, Rozaimi, Daniel Ierodiaconou, and Jacquomo Monk. 2012. 'Evaluation of four supervised learning methods for benthic habitat mapping using backscatter from multi-beam sonar', Remote Sensing, 4: 3427-43.

Huang, Haosheng, Dubravko Justic, Robert R Lane, John W Day, and Jaye E Cable. 2011. 'Hydrodynamic response of the Breton Sound estuary to pulsed Mississippi River inputs', Estuarine, Coastal and Shelf Science, 95: 216-31.

Huang, Jin, and Charles X Ling. 2005. 'Using AUC and accuracy in evaluating learning algorithms', IEEE Transactions on Knowledge and Data Engineering, 17: 299-310.

Ierodiaconou, D, J Monk, A Rattray, L Laurenson, and VL Versace. 2011. 'Comparison of automated classification techniques for predicting benthic biological communities using hydroacoustics and video observations', Continental Shelf Research, 31: S28-S38.

Jenness, Jeff S. 2004. 'Calculating landscape surface area from digital elevation models', Wildlife Society Bulletin, 32: 829-40.

Jonah, Fredrick Ekow, Daniel Adjei-Boateng, Nelson Winston Agbo, Emmanuel Abeashi Mensah, and Regina Esi Edziyie. 2015. 'Assessment of sand and stone mining along the coastline of Cape Coast, Ghana', Annals of GIS, 21: 223-31.

Karimpour, Arash, and Qin Chen. 2017. 'Wind wave analysis in depth limited water using OCEANLYZ, A MATLAB toolbox', Computers & Geosciences, 106: 181-89.

Karpatne, Anuj, Imme Ebert-Uphoff, Sai Ravela, Hassan Ali Babaie, and Vipin Kumar. 2018. 'Machine learning for the geosciences: Challenges and opportunities', IEEE Transactions on Knowledge and Data Engineering.

Kennedy, Andrew B, K Clint Slatton, Michael Starek, Kittipat Kampa, and Hyun-Chong Cho. 2009. 'Hurricane response of nearshore borrow pits from airborne bathymetric lidar', Journal of Waterway, Port, Coastal, and Ocean Engineering, 136: 46-58.

Khalil, Syed M, Charles W Finkl, Jeff Andrews, and Christopher P Knotts. 2007. 'Restoration-quality sand from Ship Shoal, Louisiana: geotechnical investigation for sand on a drowned barrier island.' in, Coastal Sediments' 07.

Khalil, Syed M, Angelina M Freeman, and Richard C Raynie. 2018. 'Sediment management for sustainable ecosystem restoration of coastal Louisiana', Shore & Beach, 86: 17.

Khalil, Syed M., Charles W. Finkl, Harry H. Roberts, and Richard C. Raynie. 2010. 'New Approaches to Sediment Management on the Inner Continental Shelf Offshore Coastal Louisiana', Journal of Coastal Research: 591-604.

Kim, Booyong. 2004. 'Seismic sequence stratigraphy of Pliocene-Pleistocene turbidite systems, Ship Shoal South Addition, Northwestern Gulf of Mexico', Texas A&M University.

Kobashi, F. Jose, and G. W. Stone. 2007. 'Impacts of Fluvial Fine Sediments and Winter Storms on a Transgressive Shoal, off South-Central Louisiana, U.S.A', Journal of Coastal Research: 858-62.

Kobashi, Daijiro. 2009. 'Bottom boundary layer physics and sediment transport along a transgressive sand body, Ship Shoal, south-central Louisiana: implications for fluvial sediments and winter storms'.

Kulp, Mark, Shea Penland, S Jeffress Williams, Chris Jenkins, Jim Flocks, and Jack Kindinger. 2005. 'Geologic framework, evolution, and sediment resources for restoration of the Louisiana coastal zone', Journal of Coastal Research: 56-71.

Kumar, Nirnimesh, George Voulgaris, John C Warner, and Maitane Olabarrieta. 2012. 'Implementation of the vortex force formalism in the coupled ocean-atmosphere-wave-sediment transport (COAWST) modeling system for inner shelf and surf zone applications', Ocean modelling, 47: 65-95.

Lacharité, Myriam, Craig J Brown, and Vicki Gazzola. 2017. 'Multisource multibeam backscatter data: developing a strategy for the production of benthic habitat maps using semi-automated seafloor classification methods', Marine Geophysical Research: 1-16.
. 2018. 'Multisource multibeam backscatter data: developing a strategy for the production of benthic habitat maps using semi-automated seafloor classification methods', Marine Geophysical Research, 39: 307-22.

Lanier, Andrew, Chris Romsos, and Chris Goldfinger. 2007. 'Seafloor habitat mapping on the Oregon continental margin: A spatially nested GIS approach to mapping scale, mapping methods, and accuracy quantification', Marine Geodesy, 30: 51-76.

Lecours, Vincent, Margaret FJ Dolan, Aaron Micallef, and Vanessa L Lucieer. 2016. 'A review of marine geomorphometry, the quantitative study of the seafloor', Hydrology and Earth System Sciences, 20: 3207.

Lesser, Giles R, JA v Roelvink, JATM Van Kester, and GS Stelling. 2004. 'Development and validation of a three-dimensional morphological model', Coastal Engineering, 51: 883-915.

Liu, H, K Xu, SJ Bentley, C Li, MD Miner, C Wilson, and Z Xue. 2017. "Sediment Transport and Slope Stability of Ship Shoal Borrow Areas for Coastal Restoration of Louisiana." In AGU Fall Meeting Abstracts.

Liu, H, Z Zheng, J WANG, and S He. 2018. "A comparison of supervised classification methods for prediction and mapping of sediment types with multibeam bathymetry and backscatter data in Buzzards Bay, Massachusetts." In AGU Fall Meeting Abstracts.

Liu, Haoran, K Xu, SJ Bentley, C Wilson, Z Xue, and MD Miner. 2018a. "Sediment transport and geomorphologic response in multiple dredge pits near Ship Shoal of coastal Louisiana." In AGU Fall Meeting Abstracts.

Liu, Haoran, Kehui Xu, Samuel J Bentley, Carol Wilson, Zehao Xue, and MD Miner. 2018b. "Sediment transport and geomorphologic response in multiple dredge pits near Ship Shoal of coastal Louisiana." In AGU Fall Meeting Abstracts.

Liu, Haoran, Kehui Xu, Bin Li, Ya Han, and Guandong Li. 2019. 'Sediment Identification Using Machine Learning Classifiers in a Mixed-Texture Dredge Pit of Louisiana Shelf for Coastal Restoration', Water, 11: 1257.

Liu, Xiaoming, Menghua Wang, and Wei Shi. 2009. 'A study of a Hurricane Katrina–induced phytoplankton bloom using satellite observations and model simulations', Journal of Geophysical Research: Oceans, 114.

Liu, Yonggang, Robert H Weisberg, Chuanmin Hu, and Lianyuan Zheng. 2011. 'Tracking the Deepwater Horizon oil spill: A modeling perspective', Eos, Transactions American Geophysical Union, 92: 45-46.

Lu, Qimiao, and Robert B Nairn. 2011. 'Prediction on morphological response of dredged sand-borrow pits', Coastal Engineering Proceedings, 1: 74.

Lucieer, Vanessa, Nicole A Hill, Neville S Barrett, and Scott Nichol. 2013. 'Do marine substrates ‘look’and ‘sound’the same? Supervised classification of multibeam acoustic data using autonomous underwater vehicle images', Estuarine, Coastal and Shelf Science, 117: 94-106.

Lundblad, Emily R, Dawn J Wright, Joyce Miller, Emily M Larkin, Ronald Rinehart, David F Naar, Brian T Donahue, S Miles Anderson, and Tim Battista. 2006. 'A benthic terrain classification scheme for American Samoa', Marine Geodesy, 29: 89-111.

Marsh, Ivor, and Colin Brown. 2009. 'Neural network classification of multibeam backscatter and bathymetry data from Stanton Bank (Area IV)', Applied Acoustics, 70: 1269-76.

Micallef, Aaron, Timothy P Le Bas, Veerle AI Huvenne, Philippe Blondel, Veit Hühnerbach, and Alan Deidun. 2012. 'A multi-method approach for benthic habitat mapping of

shallow coastal areas with high-resolution multibeam data', Continental Shelf Research, 39: 14-26.

Micallef, Aaron, Joshu J Mountjoy, Miquel Canals, and Galderic Lastras. 2012. 'Deep-seated bedrock landslides and submarine canyon evolution in an active tectonic margin: Cook Strait, New Zealand.' in, Submarine mass movements and their consequences (Springer).

Monk, J, D Ierodiaconou, A Bellgrove, Euan Harvey, and L Laurenson. 2011. 'Remotely sensed hydroacoustics and observation data for predicting fish habitat suitability', Continental Shelf Research, 31: S17-S27.

Monk, Jacquomo, Daniel Ierodiaconou, Vincent L Versace, Alecia Bellgrove, Euan Harvey, Alex Rattray, Laurie Laurenson, and Gerry P Quinn. 2010. 'Habitat suitability for marine fishes using presence-only modelling and multibeam sonar', Marine Ecology Progress Series, 420: 157-74.

Moriarty, Julia, Courtney K Harris, Marjorie AM Friedrichs, Katja Fennel, and Kehui Xu. 2018. 'A Model Archive for a Coupled Hydrodynamic-Sediment Transport-Biogeochemistry Model for the Northern Gulf of Mexico, USA'.

Morton, Robert A. 2008. National assessment of shoreline change: Part 1: Historical shoreline changes and associated coastal land loss along the US Gulf of Mexico (Diane Publishing).

Munnelly, Ryan T, David B Reeves, Edward J Chesney, and Donald M Baltz. 2019. 'Summertime hydrography of the nearshore Louisiana Continental Shelf: Effects of riverine outflow, shelf morphology, and the presence of sand shoals on water quality', Continental Shelf Research.

Murray, Stephen P. 1998. 'An observational study of the Mississippi-Atchafalaya coastal plume'.

Nairn, R, S Langendyk, and J Michel. 2004. 'Preliminary Infrastructure Stability Study, Offshore Louisiana. Prepared by Baird & Associates and Research Planning, Inc. Submitted to US Department of the Interior, Minerals Management Service', contract: 31051.

Nairn, RB, Q Lu, and SK Langendyk. 2005. 'A study to address the issue of seafloor stability and the Impact on Oil and Gas infrastructure in the Gulf of Mexico', US Dept. of the Interior, MMS, Gulf of Mexico OCS Region, New Orleans, LA OCS Study MMS, 43: 179.

Nairn, Rob, Jay A Johnson, Dane Hardin, and Jacqueline Michel. 2004. 'A biological and physical monitoring program to evaluate long-term impacts from sand dredging operations in the United States outer continental shelf', Journal of Coastal Research: 126-37.

Neumeier, Urs, Christian Ferrarin, Carl L. Amos, Georg Umgiesser, and Michael Z. Li. 2008. 'Sedtrans05: An improved sediment-transport model for continental shelves and coastal

waters with a new algorithm for cohesive sediments', Computers & Geosciences, 34: 1223-42.

Newell, RC, LJ Seiderer, NM Simpson, and JE Robinson. 2004. 'Impacts of marine aggregate dredging on benthic macrofauna off the south coast of the United Kingdom', Journal of Coastal Research: 115-25.

Nittrouer, Jeffrey A, Mead A Allison, and Richard Campanella. 2008. 'Bedform transport rates for the lowermost Mississippi River', Journal of Geophysical Research: Earth Surface, 113.

O'Connor, Meg Cathlin, SJ Bentley, K Xu, J Obelcz, C Li, and MD Miner. 2016. "Sediment infilling of Louisiana continental-shelf dredge pits: a record of sedimentary processes in the Northern Gulf of Mexico." In American Geophysical Union, Ocean Sciences Meeting 2016, abstract# EC34C-1206.

Obelcz, Jeffrey, Kehui Xu, Samuel J. Bentley, Meg O'Connor, and Michael D. Miner. 2018. 'Mud-capped dredge pits: An experiment of opportunity for characterizing cohesive sediment transport and slope stability in the northern Gulf of Mexico', Estuarine, Coastal and Shelf Science, 208: 161-69.

Oertel, George F. 1972. 'Sediment transport of estuary entrance shoals and the formation of swash platforms', Journal of Sedimentary Research, 42: 858-63.

Palmer, Terence A, Paul A Montagna, and Robert B Nairn. 2008. 'The effects of a dredge excavation pit on benthic macrofauna in offshore Louisiana', Environmental management, 41: 573-83.

Pearce, David William. 1994. Valuing the environment: past practice, future prospect (Citeseer).

Penland, Shea, Paul F Connor Jr, Andrew Beall, Sarah Fearnley, and S Jeffress Williams. 2005. 'Changes in Louisiana's shoreline: 1855–2002', Journal of Coastal Research: 7-39.

Penland, Shea, John R Suter, and Thomas F Moslow. 1986. 'Inner-shelf shoal sedimentary facies and sequences: Ship Shoal, northern Gulf of Mexico'.

Pirtle, Jodi L, Thomas C Weber, Christopher D Wilson, and Christopher N Rooper. 2015. 'Assessment of trawlable and untrawlable seafloor using multibeam-derived metrics', Methods in Oceanography, 12: 18-35.

Prasad, TG, and Patrick J Hogan. 2007. 'Upper‐ocean response to Hurricane Ivan in a 1/25 nested Gulf of Mexico HYCOM', Journal of Geophysical Research: Oceans, 112.

Protection, Coastal, and Restoration Authority. 2017. "Louisiana’s comprehensive master plan for a sustainable coast. State of Louisiana. Baton Rouge (LA)." In.

Rangel-Buitrago, Nelson Guillermo, Giorgio Anfuso, and Allan Thomas Williams. 2015. 'Coastal erosion along the Caribbean coast of Colombia: magnitudes, causes and management', Ocean & Coastal Management, 114: 129-44.

Reichstein, Markus, Gustau Camps-Valls, Bjorn Stevens, Martin Jung, Joachim Denzler, and Nuno Carvalhais. 2019. 'Deep learning and process understanding for data-driven Earth system science', Nature, 566: 195.

Restreppo, Giancarlo A, Samuel J Bentley, Jiaze Wang, and Kehui Xu. 2019. 'Riverine Sediment Contribution to Distal Deltaic Wetlands: Fourleague Bay, LA', Estuaries and Coasts, 42: 55-67.

Ribberink, Jan S. 2005. 'Migration and infill of trenches in the marine environment: An analytical and numerical engineering model.' in, Sandpit. Sand transport and morphology of offshore sand mining pits. Process knowledge and guidlines for coastal management. End document EC frameswork V projec EVK3-2001-00056. (Aqua publications).

Robichaux, Patrick. 2017. 'How Dredge Pits Evolve Over Time: A Look At Their Geomorphologic Evolution and Infilling Processes'.

Robichaux, Patrick, Kehui Xu, Samuel J Bentley, Michael Miner, and Z George Xue. 2020. 'Morphological evolution of a mud-capped dredge pit on the Louisiana shelf: Nonlinear infilling and continuing consolidation', Geomorphology: 107030.

Roos, Pieter C. 2004. 'Seabed pattern dynamics and offshore sand extraction'.

Ross, Lauren K, Rebecca E Ross, Heather A Stewart, and Kerry L Howell. 2015. 'The influence of data resolution on predicted distribution and estimates of extent of current protection of three 'listed'deep-sea habitats', PloS one, 10: e0140061.

Rudnick, Daniel L, Ganesh Gopalakrishnan, and Bruce D Cornuelle. 2015. 'Cyclonic eddies in the Gulf of Mexico: Observations by underwater gliders and simulations by numerical model', Journal of Physical Oceanography, 45: 313-26.

Schimel, Alexandre CG, Daniel Ierodiaconou, Lachlan Hulands, and David M Kennedy. 2015. 'Accounting for uncertainty in volumes of seabed change measured with repeat multibeam sonar surveys', Continental Shelf Research, 111: 52-68.

Shchepetkin, Alexander F, and James C McWilliams. 2005. 'The regional oceanic modeling system (ROMS): a split-explicit, free-surface, topography-following-coordinate oceanic model', Ocean modelling, 9: 347-404.

Speybroeck, Jeroen, Dries Bonte, Wouter Courtens, Tom Gheskiere, Patrick Grootaert, Jean-Pierre Maelfait, Mieke Mathys, Sam Provoost, Koen Sabbe, and Eric WM Stienen. 2006. 'Beach nourishment: an ecologically sound coastal defence alternative? A review', Aquatic conservation: Marine and Freshwater ecosystems, 16: 419-35.

Staneva, Joanna, Kathrin Wahle, Heinz Günther, and Emil Stanev. 2016. 'Coupling of wave and circulation models in coastal–ocean predicting systems: a case study for the German Bight', Ocean Science, 12: 797-806.

Stephens, David, and Markus Diesing. 2014. 'A comparison of supervised classification methods for the prediction of substrate type using multibeam acoustic and legacy grain-size data', PloS one, 9: e93950.

Stone, Gregory W., David A. Pepper, Jingping Xu, and Xiongping Zhang. 2004. 'Ship Shoal as a Prospective Borrow Site for Barrier Island Restoration, Coastal South-Central Louisiana, USA: Numerical Wave Modeling and Field Measurements of Hydrodynamics and Sediment Transport', Journal of Coastal Research, 201: 70-88.

Stone, GW, RE Condrey, JW Fleeger, SM Khalil, D Kobashi, F Jose, E Evers, S Dubois, B Liu, and S Arndt. 2009. 'Environmental investigation of long-term use of Ship Shoal sand resources for large scale beach and coastal restoration in Louisiana', US Dept. of the Interior, Minerals Management Service, Gulf of Mexico OCS Region, New Orleans, LA. OCS Study MMS, 24: 278.

Syed Khalil, Angelina Freeman, Richard C.Raynie. 2018. 'Sediment management for sustainable ecosystem restoration of coastal Louisiana', shore and beach, 86: 17-27.

Syvitski, James PM, Albert J Kettner, Irina Overeem, Eric WH Hutton, Mark T Hannon, G Robert Brakenridge, John Day, Charles Vörösmarty, Yoshiki Saito, and Liviu Giosan. 2009. 'Sinking deltas due to human activities', Nature Geoscience, 2: 681.

Tempera, Fernando, Eva Giacomello, Neil C Mitchell, Aldino S Campos, Andreia Braga Henriques, Igor Bashmachnikov, Ana Martins, Ana Mendonça, Telmo Morato, and Ana Colaço. 2012. 'Mapping Condor seamount seafloor environment and associated biological assemblages (Azores, NE Atlantic).' in, Seafloor Geomorphology as Benthic Habitat (Elsevier).

Tibshirani, Robert. 2011. 'Regression shrinkage and selection via the lasso: a retrospective', Journal of the Royal Statistical Society: Series B (Statistical Methodology), 73: 273-82.

Twilley, Robert R, Samuel J Bentley, Qin Chen, Douglas A Edmonds, Scott C Hagen, Nina S-N Lam, Clinton S Willson, Kehui Xu, DeWitt Braud, and R Hampton Peele. 2016. 'Co-evolution of wetland landscapes, flooding, and human settlement in the Mississippi River Delta Plain', Sustainability Science, 11: 711-31.

Valentine, AP, and LM Kalnins. 2016. 'An introduction to learning algorithms and potential applications in geomorphometry and earth surface dynamics', Earth surface dynamics., 4: 445-60.

Viles, Heather, and Tom Spencer. 2014. Coastal problems: geomorphology, ecology and society at the coast (Routledge).

Vörösmarty, Charles J, James Syvitski, John Day, Alex De Sherbinin, Liviu Giosan, and Chris Paola. 2009. 'Battling to save the world's river deltas', Bulletin of the Atomic Scientists, 65: 31-43.

Walbridge, Shaun, Noah Slocum, Marjean Pobuda, and Dawn Wright. 2018. 'Unified geomorphological analysis workflows with benthic terrain modeler', Geosciences, 8: 94.

Walker, Nan D, and Adele B Hammack. 2000. 'Impacts of winter storms on circulation and sediment transport: Atchafalaya-Vermilion Bay region, Louisiana, USA', Journal of Coastal Research: 996-1010.

Walker, Nan D, William J Wiseman Jr, Lawrence J Rouse Jr, and Adele Babin. 2005. 'Effects of river discharge, wind stress, and slope eddies on circulation and the satellite-observed structure of the Mississippi River plume', Journal of Coastal Research: 1228-44.

Wang, Jiaze, Kehui Xu, Samuel J Bentley, Crawford White, Xukai Zhang, and Haoran Liu. 2019. 'Degradation of the plaquemines sub-delta and relative sea-level in eastern Mississippi deltaic coast during late holocene', Estuarine, Coastal and Shelf Science, 227: 106344.

Wang, Jiaze, Kehui Xu, Chunyan Li, and Jeffrey Obelcz. 2018. 'Forces Driving the Morphological Evolution of a Mud-Capped Dredge Pit, Northern Gulf of Mexico', Water, 10: 1001.

Warner, John C, Brandy Armstrong, Ruoying He, and Joseph B Zambon. 2010. 'Development of a coupled ocean–atmosphere–wave–sediment transport (COAWST) modeling system', Ocean modelling, 35: 230-44.

Warner, John C., Christopher R. Sherwood, Richard P. Signell, Courtney K. Harris, and Hernan G. Arango. 2008. 'Development of a three-dimensional, regional, coupled wave, current, and sediment-transport model', Computers & Geosciences, 34: 1284-306.

Waye-Barker, Georgia A, Paul McIlwaine, Sophie Lozach, and Keith M Cooper. 2015. 'The effects of marine sand and gravel extraction on the sediment composition and macrofaunal community of a commercial dredging site (15 years post-dredging)', Marine pollution bulletin, 99: 207-15.

Wiberg, Patricia L, and Christopher R Sherwood. 2008. 'Calculating wave-generated bottom orbital velocities from surface-wave parameters', Computers & Geosciences, 34: 1243-62.

Wiegman, Adrian RH, Jeffrey S Rutherford, and John W Day. 2018. 'The Costs and Sustainability of Ongoing Efforts to Restore and Protect Louisiana's Coast.' in, Mississippi Delta Restoration (Springer).

Williams, S Jeffress, James Flocks, Chris Jenkins, Syed Khalil, and Juan Moya. 2012. 'Offshore sediment character and sand resource assessment of the northern Gulf of Mexico, Florida to Texas', Journal of Coastal Research: 30-44.

Wilson, Carol A, and Mead A Allison. 2008. 'An equilibrium profile model for retreating marsh shorelines in southeast Louisiana', Estuarine, Coastal and Shelf Science, 80: 483-94.

Wilson, Margaret FJ, Brian O'Connell, Colin Brown, Janine C Guinan, and Anthony J Grehan. 2007. 'Multiscale terrain analysis of multibeam bathymetry data for habitat mapping on the continental slope', Marine Geodesy, 30: 3-35.

Work, Paul A., Fairlight Fehrenbacher, and George Voulgaris. 2004. 'Nearshore Impacts of Dredging for Beach Nourishment', Journal of Waterway, Port, Coastal, and Ocean Engineering, 130: 303-11.

Xu, K, DR Corbett, JP Walsh, D Young, KB Briggs, GM Cartwright, CT Friedrichs, CK Harris, RC Mickey, and S Mitra. 2014. 'Seabed erodibility variations on the Louisiana continental shelf before and after the 2011 Mississippi River flood', Estuarine, Coastal and Shelf Science, 149: 283-93.

Xu, K, MD Miner, SJ Bentley, C Li, J Obelcz, and MC O'Connor. 2016. "Assessment of Mud-Capped Dredge Pit Evolution Offshore Louisiana: Implications to Sand Excavation and Coastal Restoration." In American Geophysical Union, Ocean Sciences Meeting 2016, abstract# EC31B-07.

Xu, Kehui, Sibel Bargu, Samuel J Bentley, Bridgette Duplantis, Chunyan Li, Kanchan Maiti, Michael D Miner, John R White, Carol Wilson, and Z George Xue. 2018. "Sediment Transport and Water Quality of a Dredge Pit on Louisiana Shelf for Coastal Restoration." In AGU Fall Meeting Abstracts.

Xu, Kehui, Samuel J Bentley, Patrick Robichaux, Xiaoyu Sha, and Haifei Yang. 2016. 'Implications of texture and erodibility for sediment retention in receiving basins of coastal Louisiana diversions', Water, 8: 26.

Xu, Kehui, Courtney K Harris, Robert D Hetland, and James M Kaihatu. 2011. 'Dispersal of Mississippi and Atchafalaya sediment on the Texas–Louisiana shelf: Model estimates for the year 1993', Continental Shelf Research, 31: 1558-75.

Xu, Kehui, Rangley C Mickey, Qin Chen, Courtney K Harris, Robert D Hetland, Kelin Hu, and Jiaze Wang. 2016. 'Shelf sediment transport during hurricanes Katrina and Rita', Computers & Geosciences, 90: 24-39.

Xue, Zehao. 2019. 'Sandy Dredge Pit Sedimentation–Characteristics and Processes in Caminada Borrow Area, Ship Shoal, Louisiana Shelf, USA'.

Xue, Zehao, Carol Wilson, Samuel J Bentley, Kehui Xu, Haoran Liu, Chunyan Li, and Michael D Miner. 2017. "Quantifying Sediment Characteristics and Infilling Rate within a Ship Shoal Dredge Borrow Area, Offshore Louisiana." In AGU Fall Meeting Abstracts.

Yozzo, David J, Pace Wilber, and Robert J Will. 2004. 'Beneficial use of dredged material for habitat creation, enhancement, and restoration in New York–New Jersey Harbor', Journal of environmental management, 73: 39-52.

Zang, Zhengchen, Z George Xue, Kehui Xu, Samuel J Bentley, Qin Chen, Eurico J D'Sa, and Qian Ge. 2019. 'A Two Decadal (1993–2012) Numerical Assessment of Sediment Dynamics in the Northern Gulf of Mexico', Water, 11: 938.

VITA

Haoran Liu was born in Nanyang, China. He enrolled at China University of Geosciences (Wuhan) and earned a BS and an MS in petroleum geology and geophysics. After graduation, he moved to Baton Rouge, Louisiana, to pursue his Ph.D. degree under the supervision of Dr. Kehui Xu in the Department of Oceanography and Coastal Sciences and an MS degree under the supervision of Dr. Bin Li in Department of Experimental Statistics of Louisiana State University. Following expected graduation in August 2020, Haoran will focus future studies on the combination of geosciences with applied statistics at an institution.